

Stability and performance guarantees for misspecified multivariate score-driven filters

SIMON DONKER VAN HEEL^{a,c,*}, RUTGER-JAN LANGE^{a,c},
 BRAM VAN OS^b, and DICK VAN DIJK^{a,c}

August 19, 2025

^a*Econometric Institute, Erasmus University Rotterdam, The Netherlands*

^b*Econometrics and Data Science Department, Vrije Universiteit Amsterdam, The Netherlands*

^c*Tinbergen Institute, The Netherlands*

Abstract

Can stochastic gradient methods track a moving target? We address the problem of tracking multivariate time-varying parameters under noisy observations and potential model misspecification. Specifically, we examine implicit and explicit score-driven (ISD and ESD) filters, which update parameter predictions using the gradient of the logarithmic postulated observation density (commonly referred to as the score). For both filter types, we derive novel sufficient conditions that ensure the exponential stability of the filtered parameter path and the existence of a finite mean squared error (MSE) bound relative to the pseudo-true parameter path. Our (non-)asymptotic MSE bounds rely on mild moment conditions on the data-generating process, while our stability results are agnostic about the true process. For the ISD filter, concavity of the postulated log density combined with simple parameter restrictions is sufficient to guarantee stability. In contrast, the ESD filter additionally requires the score to be Lipschitz continuous and the learning rate to be sufficiently small. We validate our theoretical findings through simulation studies, showing that ISD filters outperform ESD filters in terms of accuracy and stability.

Keywords: Explicit and implicit-gradient methods; error bounds; pseudo-true parameters

*Corresponding author.

E-mail addresses: donkervanheel@ese.eur.nl (S.W. Donker van Heel), lange@ese.eur.nl (R-J. Lange), b.van.os2@vu.nl (B. van Os), djvandijk@ese.eur.nl (D.J. van Dijk).

1 Introduction

In a wide range of disciplines, from economics and finance to engineering and climate science, variables exhibit characteristics that change over time. These fluctuations can be captured through unobserved states or parameters, tracked using filtering techniques that alternate between prediction and update steps. These steps generate state or parameter estimates based on lagged and contemporaneous information sets, respectively, as in Kalman's (1960) approach and its successors in the state-space literature (e.g., Durbin and Koopman, 2012).

In this paper, we consider score-driven (SD) filters for tracking (vectors of) unobserved parameters. These filters update the parameter estimates by moving them in the direction of the score; that is, the gradient of the logarithmic observation density. Importantly, these filters may be misspecified in that the true parameter dynamics may be unknown and the postulated observation density incorrect. Following Lange et al. (2024), we differentiate between *explicit* and *implicit* score-driven (ESD and ISD) filters, which use the score evaluated in the researcher's predicted or updated parameters, respectively.

Our theoretical contribution is twofold. First, we present new sufficient conditions for the exponential stability of both SD filter types (Theorem 1). Exponential stability means that the distance between any two filtered paths originating from different starting points but based on identical data converges to zero exponentially fast over time. Our conditions relate only to the postulated density; hence, they are verifiable in practice. Moreover, they are easily interpretable and hard to relax if the data-generating process (DGP) is unknown. Second, for both filter types, we combine stability with mild conditions on the DGP to derive performance guarantees by upper-bounding the (non-)asymptotic mean squared errors (MSEs) of the filtered and predicted paths relative to the pseudo-true parameter path (Theorem 2).

Our approach departs in several ways from the extensive literature on SD models (e.g.,

Artemova et al., 2022; Harvey, 2022), which are also known as dynamic conditional score (DCS; Harvey, 2013) models and generalized autoregressive score (GAS; Creal et al., 2013) models. First, we do not assume that the true time-varying parameters follow SD dynamics. Rather, we adopt the more cautious perspective that our SD filters may be (severely) misspecified. Second, unlike standard SD approaches (but in line with the state-space literature), we distinguish between prediction and update steps. This distinction is not only conceptually useful but also instrumental to our theory development. Third, while all SD filters in the literature are of the explicit type, we also consider the implicit version recently introduced by Lange et al. (2024). The stability and performance guarantees derived here turn out to be substantially more favorable for ISD than ESD filters.

Theorem 1 establishes the exponential stability of both SD filters, which is critical to ensure the consistency and asymptotic normality of the maximum-likelihood estimator (MLE; Straumann and Mikosch, 2006) for the static (hyper-)parameters of the filter. While ESD filters are commonly estimated using the MLE, existing stability results are often restricted to the case of a single (i.e., scalar) time-varying parameter (e.g., Harvey and Lange, 2018; Blasques et al., 2022). In the multivariate setting, analytical conditions tend to be overly restrictive (see Pötscher and Prucha, 1997, sec. 6.4; Artemova, 2023, pp. 11–2). For ISD filters, the stability result in Lange et al. (2024) relies on the (assumed) concavity of the postulated logarithmic observation density. In contrast, Theorem 1 provides two novel, verifiable sufficient conditions for multivariate SD filter stability; one each for the ESD and the ISD filter. These conditions do not require concavity and ensure the stability of the SD filtered path uniformly for *any* data sequence, meaning that we can remain entirely agnostic about the DGP. In the correctly specified case, in which both the filter and the DGP are score driven, while also sharing the same static parameters, exponential stability implies that the true time-varying parameter can be perfectly recovered in the limit. This property no longer holds under *misspecification*, which motivates our second contribution.

Theorem 2 provides formal theoretical guarantees on the tracking accuracy of SD filters, even when misspecified. The analysis of misspecified stochastic gradient methods is a key concern in statistics (e.g., Liang and Su, 2019) and machine learning (e.g., Cutler et al., 2023). It has also recently gained traction in the time-series literature (e.g., Brownlees and Llorens-Terrazas, 2024; Lange, 2024), although it remains relatively underexplored. For example, Koopman et al. (2016) perform a simulation-based analysis for misspecified ESD filters but do not provide formal guarantees. Under model misspecification, the most we can hope for is to track the *pseudo*-true state, as espoused by Beutner et al. (2023). This necessitates some mild assumptions on the DGP, such as the existence of a pseudo-true state with finite-variance increments. For both SD filter types, Theorem 2 establishes (non-)asymptotic performance guarantees by deriving upper bounds on the MSE of the filtered and predicted parameter paths relative to the pseudo-true path. The asymptotic MSE bounds can be minimized, often analytically, with respect to tuning parameters such as the learning rate. In a special case related to the Kalman filter, this minimized bound is tight (i.e., cannot be improved).

A key insight from this paper, evident from both Theorems 1 and 2, is that ESD filters require substantially stronger conditions than ISD filters. In particular, theoretical guarantees for misspecified ESD filters are available only when the score is Lipschitz continuous with respect to the parameter of interest. Assuming twice differentiability, this condition implies that the Hessian of the postulated logarithmic density must be bounded. While this Lipschitz condition is well-established in the optimization literature (e.g., Nesterov, 2018), it is often overlooked in the literature on SD filters (e.g., it is rarely mentioned in the ~ 400 papers listed on gasmodel.com). Unfortunately, it is frequently violated in practice, even in relatively simple settings (e.g., for a Poisson distribution with a logarithmic intensity parameter). Although our theoretical results identify this Lipschitz condition as a sufficient condition for ESD filter invertibility, our simulation studies suggest that in the misspecified

case it is also (near) necessary. When it does not hold and the true state exhibits sufficient volatility, ESD filters can become unstable or even diverge, whereas ISD filters continue to perform robustly.

In three Monte Carlo experiments, we assess the performance of SD filters in terms of stability, theoretical MSE bounds, and empirical MSEs. First, we consider a linear setting with high-dimensional states as in Cutler et al. (2023), where the Lipschitz condition is satisfied and performance guarantees exist for both SD filters. Comparing the SD filters to three recent alternatives, we find that the ISD filter consistently achieves the lowest MSE bounds and empirical MSEs across all time steps, state dimensions, and observation dimensions. It is also the only filter whose performance improves as the Lipschitz constant increases. Notably, our MSE bounds are up to three orders of magnitude lower than those in Cutler et al. (2023). Second, we examine nine non-linear settings investigated by Koopman et al. (2016). Finite MSE bounds are available for all DGPs when using the ISD filter. For the ESD filter, however, such guarantees hold only in the two cases where the score is Lipschitz continuous. For the remaining seven DGPs, when the true state is sufficiently volatile, the ESD filter becomes unstable and, in some cases, diverges. This result adds nuance to Koopman et al.'s (2016) conclusion that misspecified ESD filters are accurate in tracking unobserved states, which appears to hold only when the score is Lipschitz continuous or the state volatility low. Third, we analyze the widely used time-varying Poisson count distribution, where the Lipschitz condition is violated. In this case, all examined variants of the ESD filter diverge, while the ISD filter remains stable throughout.

The remainder of this article is organized as follows. Section 2 introduces ISD and ESD filters. Sections 3 and 4 present our stability and performance guarantees. Sections 5 contains our simulation studies, while Section 6 provides a brief conclusion. The online supplement contains proofs of our main results (Appendix A), additional theoretical results (Appendix B), and further numerical results and detailed discussion (Appendix C).

2 Implicit and explicit score-driven filters

2.1 Problem setting

The $n \times 1$ observation \mathbf{y}_t at times $t = 1, \dots, T$ is drawn from a true conditional observation density $p^0(\mathbf{y}_t | \boldsymbol{\vartheta}_t, \boldsymbol{\psi}^0, \mathcal{F}_{t-1})$. Here, $\boldsymbol{\vartheta}_t$ is a time-varying parameter vector that takes values in some parameter space $\boldsymbol{\Theta}^0$, $\boldsymbol{\psi}^0$ is a vector of static shape parameters, and \mathcal{F}_{t-1} denotes the information set at time $t-1$. The inclusion of \mathcal{F}_{t-1} allows the observation density to depend on exogenous variables and/or lags of \mathbf{y}_t . For brevity, we suppress the dependence on $\boldsymbol{\psi}^0$ and \mathcal{F}_{t-1} . In the case of discrete observations, $p^0(\mathbf{y}_t | \boldsymbol{\vartheta}_t)$ is interpreted as a probability rather than a density. The researcher-postulated density, which is typically misspecified, is denoted by $p(\mathbf{y}_t | \boldsymbol{\theta}_t)$, where $\boldsymbol{\theta}_t \in \boldsymbol{\Theta}$ is a vector of parameters in a (non-empty) convex parameter space $\boldsymbol{\Theta} \subseteq \mathbb{R}^k$ (e.g., $\boldsymbol{\Theta}$ could represent the positive quadrant). Additional dependence of $p(\cdot | \boldsymbol{\theta}_t)$ on a static (shape) parameter $\boldsymbol{\psi}$ and/or \mathcal{F}_{t-1} is permitted but suppressed for brevity.

2.2 Filtering algorithm

Similar to Kalman's (1960) filter, our SD filters alternate between update and prediction steps. The updated and predicted states reflect the researcher's estimates of the time-varying parameter at time t , based on the contemporaneous information set \mathcal{F}_t and the lagged information set \mathcal{F}_{t-1} , respectively. The updated (or "filtered") states are denoted by $\{\boldsymbol{\theta}_{t|t}^j\}$, where the superscript $j \in \{\text{im}, \text{ex}\}$ indicates whether we are using *implicit* (ISD) or *explicit* (ESD) score-driven filters. Sequences of predicted states are denoted by $\{\boldsymbol{\theta}_{t|t-1}^j\}$, again with $j \in \{\text{im}, \text{ex}\}$. The primary distinction between ISD and ESD filters lies in their update steps, which for all $t = 1, \dots, T$ read

$$\text{ISD update: } \boldsymbol{\theta}_{t|t}^{\text{im}} = \boldsymbol{\theta}_{t|t-1}^{\text{im}} + \mathbf{H}_t \nabla \ell(\mathbf{y}_t | \boldsymbol{\theta}_{t|t}^{\text{im}}), \quad (1)$$

$$\text{ESD update: } \boldsymbol{\theta}_{t|t}^{\text{ex}} = \boldsymbol{\theta}_{t|t-1}^{\text{ex}} + \mathbf{H}_t \nabla \ell(\mathbf{y}_t | \boldsymbol{\theta}_{t|t-1}^{\text{ex}}), \quad (2)$$

where $\mathbf{H}_t \in \mathbb{R}^{k \times k}$ is the \mathcal{F}_{t-1} -measurable learning-rate matrix, assumed to be positive definite (i.e., $\mathbf{H}_t \succ \mathbf{O}_k$, meaning $\mathbf{v}'\mathbf{H}_t\mathbf{v} > 0$ for all $\mathbf{v} \neq \mathbf{0}_k$), $\nabla := \text{d}/\text{d}\boldsymbol{\theta}$ is the gradient operator acting on the second argument of $\ell(\mathbf{y}|\boldsymbol{\theta})$, and $\ell(\mathbf{y}|\boldsymbol{\theta}) := \log p(\mathbf{y}|\boldsymbol{\theta})$. Therefore, $\nabla\ell(\mathbf{y}|\boldsymbol{\theta})$ represents the score, which explains part of the nomenclature. While the learning-rate matrix \mathbf{H}_t need not be identical for both methods (i.e., we allow \mathbf{H}_t^j with $j \in \{\text{im}, \text{ex}\}$), its superscript is often suppressed for simplicity. Note that the score on the right-hand side of (1) is evaluated at the update $\boldsymbol{\theta}_{t|t}^{\text{im}}$, which also appears on the left-hand side, making this method *implicit*. In contrast, (2) is immediately computable, as the score is evaluated at the prediction $\boldsymbol{\theta}_{t|t-1}^{\text{ex}}$. We will see in Section 2.3 that the implicit update (1) should be understood as a first-order condition for an optimization problem, while the explicit update (2) solves a linearized version of the same problem. Interestingly, Kalman's (1960) update can be written as an ISD or ESD update, albeit with different learning rates; for a detailed derivation, see Appendix B.1.

Turning to the prediction step, both filters employ a linear first-order specification:

$$\text{prediction step: } \boldsymbol{\theta}_{t|t-1}^j = (\mathbf{I}_k - \boldsymbol{\Phi}) \boldsymbol{\omega} + \boldsymbol{\Phi} \boldsymbol{\theta}_{t-1|t-1}^j, \quad j \in \{\text{im}, \text{ex}\}, \quad (3)$$

for $t = 1, \dots, T$. Here, $\boldsymbol{\omega}$ is a $k \times 1$ vector, $\boldsymbol{\Phi}$ is a $k \times k$ matrix, and \mathbf{I}_k is the $k \times k$ identity. While $\boldsymbol{\omega}$ and $\boldsymbol{\Phi}$ need not be identical for both filters (i.e., we allow $\boldsymbol{\omega}^j$ and $\boldsymbol{\Phi}^j$ with $j \in \{\text{im}, \text{ex}\}$), their superscripts are suppressed when convenient. Setting $\boldsymbol{\Phi}^j = \mathbf{I}_k$ would imply $\boldsymbol{\theta}_{t|t-1}^j = \boldsymbol{\theta}_{t-1|t-1}^j$. Initializations $\boldsymbol{\theta}_{0|0}^j \in \boldsymbol{\Theta} \subseteq \mathbb{R}^k$ with $j \in \{\text{im}, \text{ex}\}$ are considered given. Throughout, we assume that the prediction step maps the parameter space $\boldsymbol{\Theta}$ to itself. If $\boldsymbol{\Theta} \neq \mathbb{R}^k$, we can often ensure this by restricting $\boldsymbol{\omega}$ and $\boldsymbol{\Phi}$. For example, if $\boldsymbol{\Theta}$ is the positive quadrant, taking $\boldsymbol{\omega} \in \boldsymbol{\Theta}$, $\boldsymbol{\Phi}$ diagonal, and $\mathbf{O}_k \preceq \boldsymbol{\Phi} \preceq \mathbf{I}_k$ suffices. While the prediction step (3) could be generalized to accommodate nonlinear and/or higher-order dynamics, this would complicate the theory; hence, we do not pursue this here.

2.3 Reformulation as optimization-based filters

We reformulate the ISD update (1) as a multivariate optimization problem:

$$\text{ISD update: } \boldsymbol{\theta}_{t|t}^{\text{im}} = \underset{\boldsymbol{\theta} \in \boldsymbol{\Theta}}{\text{argmax}} \left\{ \ell(\mathbf{y}_t | \boldsymbol{\theta}) - \frac{1}{2} \left\| \boldsymbol{\theta} - \boldsymbol{\theta}_{t|t-1}^{\text{im}} \right\|_{\mathbf{P}_t}^2 \right\}, \quad (4)$$

where $\mathbf{P}_t \in \mathbb{R}^{k \times k} \succ \mathbf{O}_k$ is the penalty matrix and $\|\mathbf{v}\|_{\mathbf{P}_t}^2 = \mathbf{v}' \mathbf{P}_t \mathbf{v}$ denotes a squared (weighted) norm. The first-order condition associated with (4) reads $\mathbf{0}_k = \nabla \ell(\mathbf{y}_t | \boldsymbol{\theta}_{t|t}^{\text{im}}) - \mathbf{P}_t(\boldsymbol{\theta}_{t|t}^{\text{im}} - \boldsymbol{\theta}_{t|t-1}^{\text{im}})$. This can be rearranged as $\boldsymbol{\theta}_{t|t}^{\text{im}} = \boldsymbol{\theta}_{t|t-1}^{\text{im}} + \mathbf{P}_t^{-1} \nabla \ell(\mathbf{y}_t | \boldsymbol{\theta}_{t|t}^{\text{im}})$, thus recovering equation (1), provided the penalty matrix \mathbf{P}_t is set to the inverse of the learning-rate matrix. Hence, we set $\mathbf{P}_t := \mathbf{H}_t^{-1} \succ \mathbf{O}_k$ throughout. (Moreover, in Sections 3–4 both are static.)

Parameter update (1) can be interpreted as shorthand for optimization (4), which clarifies that the ISD update maximizes the most recent log-likelihood contribution, subject to a weighted quadratic penalty centered at the one-step-ahead prediction. In principle, the objective function in (4) may possess multiple stationary points, while the global maximizer may not fulfill the first-order condition (e.g., when it lies on the boundary of the parameter space). To eliminate this possibility, Assumption 1 in Section 3 ensures the existence of a unique interior maximizer, which coincides with the unique solution to the first-order condition (1). Under Assumption 1, therefore, formulations (1) and (4) are equivalent.

In optimization (4), we may suppose $\boldsymbol{\Theta} = \mathbb{R}^k$ (to rule out boundary solutions) and linearly approximate $\ell(\mathbf{y}_t | \boldsymbol{\theta})$ around the prediction to obtain the ESD update (2):

$$\boldsymbol{\theta}_{t|t}^{\text{ex}} = \underset{\boldsymbol{\theta} \in \mathbb{R}^k}{\text{argmax}} \left\{ \underbrace{\ell(\mathbf{y}_t | \boldsymbol{\theta}_{t|t-1}^{\text{ex}}) + (\boldsymbol{\theta} - \boldsymbol{\theta}_{t|t-1}^{\text{ex}})' \nabla \ell(\mathbf{y}_t | \boldsymbol{\theta}_{t|t-1}^{\text{ex}})}_{\text{linear approximation of } \ell(\mathbf{y}_t | \boldsymbol{\theta}) \text{ at } \boldsymbol{\theta} = \boldsymbol{\theta}_{t|t-1}^{\text{ex}}} - \frac{1}{2} \left\| \boldsymbol{\theta} - \boldsymbol{\theta}_{t|t-1}^{\text{ex}} \right\|_{\mathbf{P}_t}^2 \right\}. \quad (5)$$

The corresponding first-order condition, $\mathbf{0}_k = \nabla \ell(\mathbf{y}_t | \boldsymbol{\theta}_{t|t-1}^{\text{ex}}) - \mathbf{P}_t(\boldsymbol{\theta}_{t|t}^{\text{ex}} - \boldsymbol{\theta}_{t|t-1}^{\text{ex}})$ can be rearranged as $\boldsymbol{\theta}_{t|t}^{\text{ex}} = \boldsymbol{\theta}_{t|t-1}^{\text{ex}} + \mathbf{P}_t^{-1} \nabla \ell(\mathbf{y}_t | \boldsymbol{\theta}_{t|t-1}^{\text{ex}})$, thus recovering equation (2) with $\mathbf{P}_t^{-1} = \mathbf{H}_t$.

The full optimization (4) offers several advantages over its linearized counterpart (5).

First, optimization (4) ensures $\ell(\mathbf{y}_t | \boldsymbol{\theta}_{t|t}^{\text{im}}) \geq \ell(\mathbf{y}_t | \boldsymbol{\theta}_{t|t-1}^{\text{im}})$; that is, the implicit update cannot worsen the fit of the postulated logarithmic density. The explicit update (2) does not have this guarantee; for details, see Appendix C.1. Second, linearization (5) implies that no boundaries can be imposed on the parameter space $\boldsymbol{\Theta}$; $\boldsymbol{\theta}_{t|t}^{\text{ex}}$ must be allowed to take values in the entire space \mathbb{R}^k . Thus we have no choice but to assume, throughout, that the ESD filter applies with $\boldsymbol{\Theta}^{\text{ex}} = \mathbb{R}^k$. For variables with intrinsic bounds (e.g., volatility or correlation), ESD filters are often applied with link functions mapping $\boldsymbol{\theta} \in \mathbb{R}^k$ to the desired space. This introduces an additional source of nonlinearity, which may complicate the filter's theoretical properties. For the ISD filter, our theory development will accommodate a general state space $\boldsymbol{\Theta}^{\text{im}} \subseteq \mathbb{R}^k$, meaning we do not require (but may still use) link functions.

2.4 Static (hyper-)parameter estimation

The static (hyper-)parameters of both filters must be estimated. Suppose we use a static learning-rate matrix (i.e., $\mathbf{H}_t^j = \mathbf{H}^j = (\mathbf{P}^j)^{-1} \succ \mathbf{O}_k$ for all t and $j \in \{\text{im}, \text{ex}\}$) and collect all static parameters into a column vector $\mathbf{v}^j := (\text{vech}(\mathbf{H}^j)', \boldsymbol{\omega}^{j'}, \text{vec}(\boldsymbol{\Phi}^j)', \boldsymbol{\psi}^{j'})'$ with $j \in \{\text{im}, \text{ex}\}$, where $\text{vech}(\cdot)$ and $\text{vec}(\cdot)$ denote the half-vectorization and vectorization matrix operations, respectively. Following Creal et al. (2013), the static parameters can then be estimated as

$$\hat{\mathbf{v}}^j := \underset{\mathbf{v}^j \in \boldsymbol{\Upsilon}}{\text{argmax}} \sum_{t=1}^T \ell \left(\mathbf{y}_t \mid \boldsymbol{\theta}_{t|t-1}^j, \boldsymbol{\psi}^j, \mathcal{F}_{t-1} \right), \quad j \in \{\text{im}, \text{ex}\}. \quad (6)$$

Here, $\boldsymbol{\Upsilon}$ is the subset of the static-parameter space for which $\mathbf{H}^j \succ \mathbf{O}_k$ and $\boldsymbol{\psi}^j$ lies within its permissible domain. While the logarithmic density $\ell(\cdot | \cdot) := \log p(\cdot | \cdot)$ in (6) typically matches that in the filter (1) or (2), they can also be allowed to differ as suggested in Blasques et al. (2023); this is analogous to quasi-maximum likelihood (QML) estimation. In this case, the density used in the filter is a critical ingredient in our theory development.

3 Stability of score-driven filters

For both SD filter types, we investigate their exponential stability (e.g., Guo and Ljung, 1995) and the closely related concept of invertibility (e.g., Straumann and Mikosch, 2006). These properties are important not only in their own right but also as a prerequisite for the maximum-likelihood estimation of static parameters (e.g., Blasques et al., 2022). Exponential filter stability ensures that, given identical data, filtered paths originating from different starting points converge exponentially fast over time. We focus on a particularly strong kind of exponential stability, which holds uniformly for all data sequences, as required in the context of (possibly severe) filter misspecification.

Definition 1 (Exponential filter stability). *Consider two starting points, $\boldsymbol{\theta}_{0|0}$ and $\tilde{\boldsymbol{\theta}}_{0|0}$, and corresponding filtered paths, $\{\boldsymbol{\theta}_{t|t}\}$ and $\{\tilde{\boldsymbol{\theta}}_{t|t}\}$, respectively, based on the same data $\{\mathbf{y}_t\}$ and the same filter (i.e., with identical static parameters). For a given set of static parameters, the filter is said to be exponentially stable if there exists a weight matrix $\mathbf{W} \succ \mathbf{O}_k$ and contraction coefficient $\tau < 1$ such that, uniformly for all $\boldsymbol{\theta}_{0|0}, \tilde{\boldsymbol{\theta}}_{0|0} \in \Theta$ and all data $\{\mathbf{y}_t\}$,*

$$\|\boldsymbol{\theta}_{t|t} - \tilde{\boldsymbol{\theta}}_{t|t}\|_{\mathbf{W}}^2 \leq \tau^t \|\boldsymbol{\theta}_{0|0} - \tilde{\boldsymbol{\theta}}_{0|0}\|_{\mathbf{W}}^2, \quad \forall t \geq 0. \quad (7)$$

Exponential stability implies that the distance between any two filtered paths shrinks to zero; hence, there exists a unique limiting path. A given filter may be exponentially stable for some sets of static parameters (e.g., $\boldsymbol{\omega}$, $\boldsymbol{\Phi}$, and \mathbf{P}), but not others. As our filters may be misspecified, the unique limiting path of an exponentially stable filter need not be the true parameter path. Moreover, this limiting path need not be stationary and ergodic if the data are not. Our concept of exponential stability in Definition 1 therefore relates only to the filter, not the DGP. Requirement (7) is stronger than most in the literature (e.g., Straumann and Mikosch, 2006; Blasques et al., 2018) in that it contains a “sure” rather than “expected” contraction of the distance between any two paths.

Assumption 1(a) below denotes the Hessian matrix (with respect to $\boldsymbol{\theta}$) of the postulated logarithmic density as $\mathcal{H}(\mathbf{y}, \boldsymbol{\theta}) := \nabla^2 \ell(\mathbf{y} \mid \boldsymbol{\theta})$. We assume $\mathcal{H}(\mathbf{y}, \boldsymbol{\theta})$ to be well defined, meaning that the logarithmic density is twice differentiable, although perhaps not continuously so. Parts (b)-(c) are needed to analyze the complete optimization problem (4), but not its linearized version (5). This is because the linearized optimization problem is already strictly concave (as $\mathbf{P} \succ \mathbf{O}_k$) and always has interior solutions (as $\boldsymbol{\Theta}^{\text{ex}} = \mathbb{R}^k$ is unbounded).

Assumption 1 (Regularity conditions). *Let the penalty matrix $\mathbf{P} = \mathbf{H}^{-1} \succ \mathbf{O}_k$ be static.*

- a. *The Hessian $\mathcal{H}(\mathbf{y}, \boldsymbol{\theta})$ is well defined and satisfies $\alpha \mathbf{I}_k \preceq -\mathcal{H}(\mathbf{y}, \boldsymbol{\theta}) \preceq \beta \mathbf{I}_k$ for all $\boldsymbol{\theta} \in \boldsymbol{\Theta}, \mathbf{y} \in \mathbb{R}^n$ and some $\alpha \in (-\infty, \beta]$, while $\beta \in (0, \infty]$ may be unbounded; and*
- b. *Optimization (4) is strictly concave, implying $\lambda_{\min}(\mathbf{P}^{\text{im}}) > \alpha^- := \max\{0, -\alpha\}$; and*
- c. *Optimization (4) allows an interior solution $\boldsymbol{\theta}_{t|t}^{\text{im}} \in \boldsymbol{\Theta}_{t|t}^{\text{im}}$ for all t .*

Part (a) posits a Hessian bound, as is customary in the analysis of stochastic gradient methods (e.g., Chen et al., 2020, Ass. 3.1). We adopt a one-sided version of this condition (allowing $\beta = \infty$), applying it uniformly for all $\mathbf{y} \in \mathbb{R}^n$ rather than in expectation, which is convenient as the DGP is unspecified. Under concavity, the negative Hessian is positive semi-definite, such that $\alpha \geq 0$. If positive, $\alpha > 0$ is the parameter of strong concavity. If the postulated logarithmic density (locally) fails to be concave, we have $\alpha < 0$. We can write $\alpha = \alpha^+ - \alpha^-$, where $\alpha^+ := \max\{0, \alpha\}$ and $\alpha^- := \max\{0, -\alpha\}$. Then α^- is the maximum *violation* of concavity, which in part (a) is assumed to be bounded (i.e., $\alpha^- < \infty$). If the gradient is Lipschitz continuous, the negative Hessian is bounded above by $\beta < \infty$, in which case the Lipschitz constant $L := \max\{\alpha^-, \beta\}$ is bounded.

Part (b) restricts the penalty matrix \mathbf{P}^{im} , requiring its smallest eigenvalue to exceed α^- , ensuring that the objective function in optimization (4) is strictly concave. As $\mathbf{P}^{\text{im}} = (\mathbf{H}^{\text{im}})^{-1}$, this is equivalent to requiring $\lambda_{\max}(\mathbf{H}^{\text{im}}) < 1/\alpha^-$, which collapses to

the trivial requirement $\lambda_{\max}(\mathbf{H}^{\text{im}}) < \infty$ under concavity. Part (c) is critical in analyzing optimization (4) using its first-order condition (1).

Our first main result, Theorem 1, contains a weighted matrix norm written as $\|\mathbf{A}\|_{\mathbf{W}} = \|\mathbf{W}^{1/2} \mathbf{A} \mathbf{W}^{-1/2}\|$ for any positive-definite matrix \mathbf{W} and square real matrix \mathbf{A} of equal dimension (e.g., Jungers, 2009, p. 39). Here $\|\mathbf{A}\| = \sqrt{\lambda_{\max}(\mathbf{A}' \mathbf{A})}$ denotes the spectral norm of \mathbf{A} , and $\mathbf{W}^{1/2}$ denotes the (unique) positive-definite square root of \mathbf{W} .

Theorem 1 (Stability of misspecified SD filters). *Let Assumption 1 hold. Then ISD and ESD filters are exponentially stable (see Definition 1) with weight matrix $\mathbf{W} = \mathbf{P} = \mathbf{H}^{-1}$ if the static parameters imply $\tau_{\text{im}} < 1$ and $\tau_{\text{ex}} < 1$, respectively, where*

$$\tau_{\text{im}} := \|\mathbf{\Phi}\|_{\mathbf{P}}^2 \left(1 - \frac{\alpha^+}{\lambda_{\max}(\mathbf{P}) + \alpha^+} + \frac{\alpha^-}{\lambda_{\min}(\mathbf{P}) - \alpha^-} \right)^2, \quad (8)$$

$$\tau_{\text{ex}} := \|\mathbf{\Phi}\|_{\mathbf{P}}^2 \left(1 - \min \left\{ \frac{\alpha^+}{\lambda_{\max}(\mathbf{P})} - \frac{\alpha^-}{\lambda_{\min}(\mathbf{P})}, 2 - \frac{\beta}{\lambda_{\min}(\mathbf{P})} \right\} \right)^2. \quad (9)$$

Remark 1 (Interpretable conditions.). *If the intuitive conditions (i) $\alpha \geq 0$ and (ii) $\|\mathbf{\Phi}\|_{\mathbf{P}} \leq 1$ hold, with at least one of these conditions holding strictly, then $\tau_{\text{im}} < 1$: hence, the ISD filter is exponentially stable. To achieve the same result for the ESD filter, we additionally need $\lambda_{\max}(\mathbf{H}) \leq 2/\beta$.*

In Appendices A.1–A.4, we present several preliminary results culminating in the proof of Theorem 1. Intuitively, conditions $\tau_{\text{im}} < 1$ and $\tau_{\text{ex}} < 1$ define subsets of the static-parameter space for which the exponential stability of ISD and ESD filters is guaranteed. (The requirement $\tau_{\text{ex}} < 1$ is potentially more stringent, as discussed in more detail below.) Theorem 1 thus offers a new multivariate stability result that is both easily verifiable and agnostic with respect to the DGP. Specifically, it is verifiable because the contraction conditions $\tau_{\text{im}} < 1$ and $\tau_{\text{ex}} < 1$ contain only parameters involved in the filter (i.e., $\alpha, \beta, \mathbf{P}$, and $\mathbf{\Phi}$), and agnostic because it imposes no restrictions on the DGP. Under these conditions, Theorem 1 yields the existence of a unique limiting path to which all filtered paths converge.

Generally, our filters are score driven and the DGP is unknown; here, we highlight a consequence of Theorem 1 for the special case in which the filter is correctly specified.

Remark 2 (Correct specification). *If the contraction conditions $\tau_{\text{im}}, \tau_{\text{ex}} < 1$ in Theorem 1 hold and the data sequence $\{\mathbf{y}_t\}$ is stationary and ergodic (SE), then the limiting filtered path is also SE provided its dependence on the previous data remains measurable (for details, see Krengel, 1985, Prop. 4.3; Brandt, 1986, Thm. 1; Bougerol, 1993, Thm. 3.1). Moreover, if both the filter and the DGP are score driven, while sharing the same observation density and the same static parameters (e.g., $\boldsymbol{\omega}$, $\boldsymbol{\Phi}$, and \mathbf{P}), then $\|\boldsymbol{\theta}_{t|t-1}^j - \boldsymbol{\vartheta}_t\| \rightarrow 0$ exponentially fast (as $t \rightarrow \infty$) uniformly for all data $\{\mathbf{y}_t\}$ and any starting point $\boldsymbol{\theta}_{0|0}^j \in \boldsymbol{\Theta}$, with $j \in \{\text{im}, \text{ex}\}$. In this case, the true path can be perfectly recovered in the limit. The above “sure” (rather than “almost-sure”) convergence to zero is stronger than the results typically reported in the literature (e.g., Blasques et al., 2018, Rem. 3.1).*

We now discuss the contraction conditions $\tau_{\text{im}}, \tau_{\text{ex}} < 1$ in more detail. As highlighted in Remark 1, the postulated logarithmic density $\ell(\mathbf{y}|\boldsymbol{\theta})$ being (strictly) concave in $\boldsymbol{\theta}$ (i.e., $\alpha \geq 0$), along with simple parameter restrictions on $\boldsymbol{\Phi}$ and \mathbf{P} , is sufficient to ensure exponential stability of the ISD filter. By the same logic, $\alpha < 0$ or $\|\boldsymbol{\Phi}\|_{\mathbf{P}} > 1$ may be permitted if $\tau_{\text{im}} < 1$. The case $\beta = \infty$ poses no issue, since τ_{im} is unaffected by β .

For the ESD filter, however, large values of β are potentially problematic. The second argument of $\min\{\cdot, \cdot\}$ in equation (9) reads $2 - \beta/\lambda_{\min}(\mathbf{P})$, which should be nonnegative to ensure stability. Using $1/\lambda_{\min}(\mathbf{P}) = \lambda_{\max}(\mathbf{H})$, this additional requirement can be succinctly denoted as $\lambda_{\max}(\mathbf{H}) \leq 2/\beta$. Leading textbooks on optimization impose a similar condition on explicit gradient methods; see the discussions in Boyd and Vandenberghe (2004) (around Eq. 9.17) and Nesterov (2018) (around Eqns. 1.2.18–22). This condition is also well known in machine learning (e.g, Wu and Su, 2023). For ESD filters, therefore, the surprise is *not* that a learning-rate restriction is needed *per se*, but rather that a simple, easily interpretable condition guarantees stability even in our dynamic and stochastic context.

A notable implication of this condition (i.e., $\lambda_{\max}(\mathbf{H}) \leq 2/\beta$) is that the learning rate must shrink to zero as $\beta \rightarrow \infty$. In Section 5, we find that misspecified ESD filters with $\beta = \infty$ and a positive learning rate can be made to diverge by increasing the volatility of the true state process. Thus, we suspect $\lambda_{\max}(\mathbf{H}) \leq 2/\beta$ to be (near) necessary for the exponential stability of the ESD filter as in Definition 1. While for some ESD filters with $\beta = \infty$ it may be possible to demonstrate weaker notions of stability, this seems to necessitate some knowledge of the DGP, which we do not presume here. Rather, we are interested in showing a strong type of exponential filter stability that holds uniformly for *any* DGP. Indeed, the stability result in Theorem 1 is particularly robust in that it cannot be compromised even when the data $\{\mathbf{y}_t\}$ are generated with the express aim of making our filters diverge. The resulting conditions are intuitive, not overly stringent (i.e., hard to relax if the DGP is unknown), and readily verifiable.

4 Performance guarantees for score-driven filters

This section provides formal theoretical guarantees for the tracking accuracy of ESD and ISD filters, even when misspecified. To this end, we must reintroduce some consideration of the true process. To measure performance, we consider the weighted mean squared filtering error $\text{MSE}_{t|t}^{\mathbf{W}} := \mathbb{E}[\|\boldsymbol{\theta}_{t|t} - \boldsymbol{\theta}_t^*\|_{\mathbf{W}}^2]$ and the weighted mean squared prediction error $\text{MSE}_{t|t-1}^{\mathbf{W}} := \mathbb{E}[\|\boldsymbol{\theta}_{t|t-1} - \boldsymbol{\theta}_t^*\|_{\mathbf{W}}^2]$, where $\mathbf{W} \succ \mathbf{O}_k$ is a positive-definite weight matrix and $\boldsymbol{\theta}_t^*$ denotes the pseudo-true parameter defined below. The introduction of a *weighted* MSE allows for some flexibility even if we are ultimately interested in the usual case $\mathbf{W} = \mathbf{I}_k$. For example, the usual MSE can be bounded as follows: $\text{MSE}_{t|t}^{\mathbf{I}_k} \leq 1/(\lambda_{\min}(\mathbf{P})) \text{MSE}_{t|t}^{\mathbf{P}}$.

Definition 2 (Pseudo-true parameter). *Consider a true distribution $p^0(\mathbf{y}_t|\boldsymbol{\vartheta}_t)$ modeled by some postulated distribution $p(\mathbf{y}_t|\boldsymbol{\theta}_t)$. Then $\boldsymbol{\theta}_t^* := \operatorname{argmax}_{\boldsymbol{\theta} \in \Theta} \int p^0(\mathbf{y}|\boldsymbol{\vartheta}_t) \ell(\mathbf{y}|\boldsymbol{\theta}) d\mathbf{y}$ is the pseudo-true parameter, provided a unique solution exists. If $p(\mathbf{y}_t|\cdot) = p^0(\mathbf{y}_t|\cdot)$, then $\boldsymbol{\theta}_t^* = \boldsymbol{\vartheta}_t$.*

To track the pseudo-true parameter path $\{\boldsymbol{\theta}_t^*\}$, we require three moment conditions. First, the increments of the pseudo-true process must have a finite covariance matrix. Second, the score evaluated at the pseudo-truth must have a bounded unconditional second moment. Third, if the unconditional variance of the pseudo-true parameter $\boldsymbol{\theta}_t^*$ does not exist, our prediction step must be the identity mapping (i.e., we must set $\boldsymbol{\Phi} = \mathbf{I}_k$ in (3)). Although these assumptions are almost entirely nonrestrictive, they will, along with Assumption 1, be sufficient to derive MSE bounds for misspecified SD filters.

Assumption 2 (Moment conditions involving pseudo-truth). *Consider a true distribution $p^0(\mathbf{y}_t|\boldsymbol{\vartheta}_t)$ modeled by a postulated distribution $p(\mathbf{y}_t|\boldsymbol{\theta}_t)$. Assume for $t = 1, \dots, T$ that:*

a. *The pseudo-truth $\boldsymbol{\theta}_t^*$ exists and its increments have finite second (cross) moments.*

That is, $\text{cov}(\boldsymbol{\theta}_t^ - \boldsymbol{\theta}_{t-1}^*) \preceq \mathbf{Q}$, where $\mathbf{O}_k \preceq \mathbf{Q} \in \mathbb{R}^{k \times k}$ with $q^2 := \text{tr}(\mathbf{Q}) < \infty$.*

b. *The first moment of the postulated score, evaluated at the pseudo-truth, is zero; that*

is, $\mathbb{E}_{\mathbf{y}_t}[\nabla \ell(\mathbf{y}_t|\boldsymbol{\theta}_t^)] = \int p^0(\mathbf{y}|\boldsymbol{\vartheta}_t) \nabla \ell(\mathbf{y}|\boldsymbol{\theta}_t^*) d\mathbf{y} = \mathbf{0}_k$. Moreover, its second unconditional moment is bounded, which is ensured by $\mathbb{E}[\|\nabla \ell(\mathbf{y}_t|\boldsymbol{\theta}_t^*)\|^2] \leq \sigma^2 < \infty$.*

c. *At least one of the following two conditions holds: (i) the unconditional second moment of $\boldsymbol{\theta}_t^*$ is bounded, implying $s_\omega^2 := \sup_t \mathbb{E}[\|\boldsymbol{\theta}_t^* - \omega\|^2] < \infty$, $\forall \omega \in \mathbb{R}^k$, (ii) $\boldsymbol{\Phi} = \mathbf{I}_k$.*

Assumption 2(a) is weaker than many assumptions in the literature, which typically require (pseudo-)true parameter increments to be *uniformly* bounded (e.g., Wilson et al., 2019; Simonetto et al., 2020; Lanconelli and Lauria, 2024). Assumption 2(b) follows Toulis and Airola (2017, Ass. 2.1) in bounding the expected squared score at $\boldsymbol{\theta}_t^*$, which is less stringent than versions that bound the same quantity uniformly for all $\boldsymbol{\theta} \in \boldsymbol{\Theta}$ (e.g., Lehmann and Casella, 1998). Assumption 2(c) is intuitive, as tracking a unit-root (pseudo-true) process is feasible only if we set $\boldsymbol{\Phi} = \mathbf{I}_k$ in the prediction step (3).

Based on Assumption 2, Theorem 2 below gives specific values for each filter such that

the \mathbf{P} -weighted MSE at each time step t can be bounded as follows:

$$\text{updating-error bound : } \text{MSE}_{t|t}^{\mathbf{P}} \leq a \text{MSE}_{t|t-1}^{\mathbf{P}} + \underbrace{b}_{\text{noise}} \quad (10)$$

$$\text{prediction-error bound: } \text{MSE}_{t+1|t}^{\mathbf{P}} \leq c \text{MSE}_{t|t}^{\mathbf{P}} + \underbrace{d}_{\text{drift}} \quad (11)$$

for all $t \geq 1$. We refer to a and c as the contraction rates, while b and d are the additive constants. The values of a and b depend on which update step is used (ISD or ESD). The contraction rate a relates to α and β as per Assumption 1, while b relates to σ^2 as per Assumption 2(b). The value of c reflects the contraction rate in the prediction step via the autoregressive matrix Φ , while d relates to q^2 and s_{ω}^2 as per Assumptions 2(a) and (c).

Using a standard geometric-series result, the pair (10)–(11) yields the following *finite-sample error bound* for all $t \geq 1$ provided that $a c \neq 1$:

$$\text{MSE}_{t|t}^{\mathbf{P}} \leq \underbrace{a^t c^{t-1} \text{MSE}_{1|0}^{\mathbf{P}}}_{\text{initialization}} + \underbrace{\frac{1 - a^t c^t}{1 - a c} b}_{\text{noisy scores, } \sigma^2} + \underbrace{\frac{1 - a^{t-1} c^{t-1}}{1 - a c} a d}_{\text{drifting states, } q^2 \text{ and } s_{\omega}^2}, \quad (12)$$

where three contributions to the weighted MSE are indicated. Assuming $a c < 1$ and letting $t \rightarrow \infty$, we obtain the following *asymptotic error bounds*:

$$\limsup_{t \rightarrow \infty} \text{MSE}_{t|t}^{\mathbf{P}} \leq \frac{b + a d}{1 - a c}, \quad \limsup_{t \rightarrow \infty} \text{MSE}_{t+1|t}^{\mathbf{P}} \leq \frac{b c + d}{1 - a c}, \quad (13)$$

where the effect of the initialization has disappeared. Both bounds increase with the product $a c$, which can be interpreted as a joint contraction rate analogous to τ_{im} or τ_{ex} in Theorem 1. Indeed, if $\tau_{\text{im}}, \tau_{\text{ex}} < 1$, then we can find values of a and c such that $a c < 1$. If, moreover, the additive constants b and d are bounded, then (finite) MSE bounds exist.

Theorem 2 (MSE bounds for misspecified SD filters). *Let Assumptions 1–2 hold. Let the contraction conditions $\tau_{\text{im}} < 1$ and $\tau_{\text{ex}} < 1$ in Theorem 1 hold. Let $\mathcal{H}(\mathbf{y}_t, \boldsymbol{\theta})$ be Riemann*

integrable in $\boldsymbol{\theta}$ with probability one in \mathbf{y}_t . Finite MSE bounds then exist; specifically, the (non-)asymptotic bounds (12)–(13) hold with a, b, c , and d as stated in Table 1. In these bounds, the free parameters $\epsilon > 0$ and $\chi > 0$ can (and should) be chosen to ensure $a c < 1$.

Table 1: Values of a, b, c , and d in the (non-)asymptotic error bounds (12)–(13)

Step	Filter	Contraction rate	Additive constant
Update	ISD	$a = \left(1 - \frac{\alpha^+}{\lambda_{\max}(\mathbf{P}) + \alpha^+} + \frac{\alpha^-}{\lambda_{\min}(\mathbf{P}) - \alpha^-}\right)^2$	$b = a \times \frac{\sigma^2}{\lambda_{\min}(\mathbf{P})}$
	ESD	$a = \left(1 - \min \left\{ \frac{\alpha^+}{\lambda_{\max}(\mathbf{P})} - \frac{\alpha^-}{\lambda_{\min}(\mathbf{P})}, \frac{2\lambda_{\min}(\mathbf{P}) - \beta}{\lambda_{\min}(\mathbf{P})} \right\} \right)^2 + \frac{\chi^2 L^2}{\lambda_{\min}(\mathbf{P})^2}$	$b = \frac{(1+1/\chi^2)\sigma^2}{\lambda_{\min}(\mathbf{P})}$
Prediction		$c = (1 + \epsilon^2) \ \Phi\ _{\mathbf{P}}^2$	$d = \lambda_{\max}(\mathbf{P}) (1 + \frac{1}{\epsilon^2}) \times (\ \mathbf{I}_k - \Phi\ s_{\omega} + q)^2$

Note: $\boldsymbol{\omega}$, Φ , and \mathbf{P} are the parameters in the filter. For the definition of α and β , see Assumption 1(a), while $L := \max\{\alpha^-, \beta\}$. For q^2 , σ^2 , and s_{ω}^2 , see Assumptions 2(a), (b), and (c), respectively. Parameters $\epsilon > 0$ and $\chi > 0$ can be freely chosen as long as $a c < 1$.

The proof is presented in Appendix A.5. Under the conditions of Theorem 2, Table 1 expresses the coefficients a, b, c , and d appearing in the MSE bounds (12)–(13) in terms of the filter’s static parameters $\boldsymbol{\omega}$, Φ , and \mathbf{P} (as set by the researcher), α and β (as defined in Assumption 1), and q , σ^2 and σ_{ω}^2 (as defined in Assumption 2). For the update step of the ESD filter, a and b also contain the free parameter $\chi > 0$. For the prediction step, c and d similarly contain the free parameter $\epsilon > 0$. These free parameters arise from our application of Young’s inequality, which, for two vectors \mathbf{u} and \mathbf{v} , and a compatible matrix $\mathbf{W} \succ \mathbf{O}$, reads $\|\mathbf{u} + \mathbf{v}\|_{\mathbf{W}}^2 \leq (1 + \epsilon^2) \|\mathbf{u}\|_{\mathbf{W}}^2 + (1 + 1/\epsilon^2) \|\mathbf{v}\|_{\mathbf{W}}^2$ for all $\epsilon > 0$ (see Appendix A.5).

Theorem 2 therefore defines a *family* of admissible bounds, indexed by the two Young’s parameters $\chi > 0$ and $\epsilon > 0$, which influence both the numerator and denominator of the bounds. Naturally, we can select the free parameters to yield the best possible bound. Indeed, Appendix B.2 derives the smallest bound for the ISD filter in closed form.

As finite MSE bounds exist under the same conditions for which exponential stability in Theorem 1 holds, much of the discussion there remains relevant. For the ISD filter, log concavity of the postulated density (i.e., $\alpha \geq 0$) along with restrictions on Φ is sufficient

to yield $ac < 1$. For the ESD filter, in contrast, if we want to ensure $a < 1$ we additionally need $\beta < \infty$ and $\lambda_{\max}(\mathbf{H}) < 2/\beta$. As we will see in Section 5, these additional restrictions are no artifacts: it is easy to show that misspecified ESD filters can be divergent if $\beta = \infty$.

For our MSE bounds to be finite, we require $d < \infty$. We observe from Table 1 that d contains the term $\|\mathbf{I}_k - \Phi\| \times s_\omega^2$, where $s_\omega^2 := \sup_t \mathbb{E}[\|\boldsymbol{\theta}_t^* - \boldsymbol{\omega}\|^2]$. The boundedness of this term is ensured by Assumption 2(c), which imposes that (i) $s_\omega^2 < \infty$ and/or (ii) $\Phi = \mathbf{I}_k$. If $s_\omega^2 < \infty$, the resulting bound is minimized if s_ω^2 is minimized, which occurs if $\boldsymbol{\omega} = \mathbb{E}[\boldsymbol{\theta}_t^*]$; that is, ideally $\boldsymbol{\omega}$ should be the unconditional mean of $\boldsymbol{\theta}_t^*$. If $s_\omega^2 = \infty$, on the other hand, $d < \infty$ is ensured by $\Phi = \mathbf{I}_k$.

While choosing $\Phi = \mathbf{I}_k$ ensures $d < \infty$, the prediction step is no longer contractive as $c = 1 + \epsilon^2 > 1$, although ϵ may be arbitrarily small. To obtain a finite MSE bound, we then require $a < 1$ to ensure $ac < 1$. For the ISD filter, this can be achieved if $\alpha > 0$, which essentially means that each observation must carry a minimum (non-zero) amount of information. Thus, ISD filters can successfully track unit-root (pseudo-)true states (i.e., achieving an asymptotically bounded MSE) if the postulated density is strongly log concave. For ESD filters, as before, we additionally require $\beta < \infty$ and $\lambda_{\max}(\mathbf{H}) < 2/\beta$.

4.1 Special case: Linear state dynamics and known observation density

Naturally, our performance guarantees can be further improved if the DGP is known. To investigate this setting, we assume the DGP is a known state-space model with linear (but possibly non-Gaussian) state dynamics and a known observation density.

Assumption 3 (Known state-space model with linear state dynamics). *For all $t = 1, \dots, T$, let the true density $p^0(\cdot|\cdot)$ coincide with the postulated density $p(\cdot|\cdot)$, while the true state evolves as $\boldsymbol{\vartheta}_t = (\mathbf{I}_k - \Phi_0)\boldsymbol{\omega}_0 + \Phi_0\boldsymbol{\vartheta}_{t-1} + \boldsymbol{\xi}_t$, where $\boldsymbol{\xi}_t \sim \text{i.i.d. } (\mathbf{0}_k, \boldsymbol{\Sigma}_\xi)$ with finite covariance matrix $\mathbf{O}_k \preceq \boldsymbol{\Sigma}_\xi \in \mathbb{R}^{k \times k}$ and $\sigma_\xi^2 := \text{tr}(\boldsymbol{\Sigma}_\xi) < \infty$. The intercept parameter vector $\boldsymbol{\omega}_0 \in \mathbb{R}^d$ and autoregressive matrix $\Phi_0 \in \mathbb{R}^{k \times k}$ are known.*

When Assumption 3 holds, our filters employ the true observation density $p(\mathbf{y}_t|\cdot) = p^0(\mathbf{y}_t|\cdot)$, while also using the true state-transition parameters, $\boldsymbol{\omega} = \boldsymbol{\omega}_0$ and $\boldsymbol{\Phi} = \boldsymbol{\Phi}_0$. In this case, the pseudo-true and true parameters coincide; that is, $\boldsymbol{\theta}_t^* = \boldsymbol{\vartheta}_t$ for $t = 1, \dots, T$. However, as the DGP is a state-space model, our SD filters remain misspecified.

Proposition 1. *Let Assumptions 1, 2(a,b), and 3 hold. Let contraction conditions $\tau_{\text{im}}, \tau_{\text{ex}} < 1$ of Theorem 1 and the Riemann integrability condition of Theorem 2 hold. Then the MSE bounds (12)–(13) hold with a and b as in Table 1 and $c = \|\boldsymbol{\Phi}_0\|_{\mathbf{P}}^2$ and $d = \lambda_{\max}(\mathbf{P})\sigma_{\xi}^2$.*

The proof is contained in Appendix A.6. Under Assumption 3, the values of $c = \|\boldsymbol{\Phi}_0\|_{\mathbf{P}}^2$ and $d = \lambda_{\max}(\mathbf{P})\sigma_{\xi}^2$ are automatically bounded and no longer contain any free parameters. Although the MSE bound of the ESD filter still contains one free parameter (i.e., $\chi > 0$), the MSE bound of the ISD filter now exclusively depends on α , \mathbf{P} , $\boldsymbol{\Phi}_0$, σ^2 , and σ_{ξ}^2 . Some freedom remains in selecting the penalty matrix or, equivalently, the learning-rate matrix. In Appendix B.3, we take this matrix to be a scalar multiple of the identity, enabling us to analytically derive the scalar learning rate that minimizes the asymptotic (Euclidean) MSE bound. This closed-form solution can be used to “tune” the learning rate if σ^2 and σ_{ξ}^2 are known or can be approximated. Moreover, in a special case related to the Kalman filter, Appendix B.4 shows that this minimized MSE bound is tight (i.e., cannot be improved).

5 Simulation studies

We present three simulation studies comparing SD filters in terms of stability and performance. Specifically, we investigate a linear setting with high-dimensional states as in Cutler et al. (2023) (Section 5.1), nine non-linear DGPs with univariate states as in Koopman et al. (2016) (Section 5.2), and the popular dynamic Poisson count model (Section 5.3).

5.1 Least-squares recovery as in Cutler et al. (2023)

Observation equation. Following Madden et al. (2021, pp. 453–4) and Cutler et al. (2023, pp. 41–2), we investigate a high-dimensional linear model. Conditional on the true latent state $\boldsymbol{\vartheta}_t \in \mathbb{R}^k$, each observation $\mathbf{y}_t \in \mathbb{R}^n$ is independently drawn from a Gaussian distribution $N(\mathbf{A}\boldsymbol{\vartheta}_t, \boldsymbol{\Sigma})$. The (static) matrix $\mathbf{A} \in \mathbb{R}^{n \times k}$ is generated using Haar-distributed orthogonal matrices to ensure that it has rank $k \leq n$, with singular values equally spaced in the interval $[\sqrt{\alpha}, \sqrt{\beta}]$, where $0 < \alpha \leq \beta < \infty$. As we will see, this corresponds with the notation in Assumption 1. The covariance matrix $\boldsymbol{\Sigma}$ is set as $\sigma^2/(n\beta)\mathbf{I}_n$ with $0 < \sigma^2 < \infty$, ensuring that $\sigma^2 < \infty$ matches the notation in Assumption 2(b).

State transition. The latent state $\boldsymbol{\vartheta}_t \in \mathbb{R}^k$ evolves according to a random walk $\boldsymbol{\vartheta}_{t+1} = \boldsymbol{\vartheta}_t + \boldsymbol{\xi}_t$, where $\boldsymbol{\xi}_t$ is i.i.d. and non-Gaussian, drawn uniformly from the surface of a k -dimensional sphere with radius $\sigma_\xi > 0$, aligning with the notation in Assumption 3. The initial state $\boldsymbol{\vartheta}_0$ is drawn from the surface of a sphere with radius 10.

Postulated density. Following Cutler et al. (2023), we are interested in least-squares recovery, meaning that all directions are equally important. Therefore, we postulate a Gaussian density with the identity as the covariance matrix:

$$\ell(\mathbf{y}_t|\boldsymbol{\theta}) = -\frac{1}{2}\|\mathbf{A}\boldsymbol{\theta} - \mathbf{y}_t\|^2 - \frac{k}{2}\log(2\pi). \quad (14)$$

The Hessian with respect to $\boldsymbol{\theta}$ is constant at $\boldsymbol{\mathcal{H}} = -\mathbf{A}'\mathbf{A}$. Due to the construction of \mathbf{A} , the eigenvalues of $-\boldsymbol{\mathcal{H}}$ lie in $[\alpha, \beta]$ with $0 < \alpha \leq \beta < \infty$, consistent with the notation in Assumption 1(a). Although the observation log density (14) is technically misspecified, the pseudo-true parameter still equals the true parameter (i.e., $\boldsymbol{\vartheta}_t = \boldsymbol{\theta}_t^*, \forall t$). Moreover, taking the postulated covariance matrix to be a *scalar multiple* of the identity would lead to identical updates, differing only in the learning rate. Parameter σ^2 matches the notation in Assumption 2(b), as $\mathbb{E}\|\nabla(\mathbf{y}_t|\boldsymbol{\vartheta}_t)\|^2 = \mathbb{E}\|\mathbf{A}'(\mathbf{y}_t - \mathbf{A}\boldsymbol{\vartheta}_t)\|^2 = \text{tr}(\mathbf{A}'\boldsymbol{\Sigma}\mathbf{A}) \leq \beta \text{tr}(\boldsymbol{\Sigma}) = \sigma^2 < \infty$.

Filter specification. Our filters are initialized at the origin and use the identity mapping for their prediction steps; that is, $\boldsymbol{\theta}_{0|0}^j = \mathbf{0}_k$ and $\boldsymbol{\theta}_{t+1|t}^j = \boldsymbol{\theta}_{t|t}^j$ with $j \in \{\text{ex, im}\}$. Following Cutler et al. (2023), we consider learning-rate matrices that are scalar multiples of the identity. The ESD update with $\mathbf{H}_t^{\text{ex}} = \eta^{\text{ex}} \mathbf{I}_k$ and $\eta^{\text{ex}} > 0$ then equals

$$\text{ESD update: } \boldsymbol{\theta}_{t|t}^{\text{ex}} = \boldsymbol{\theta}_{t|t-1}^{\text{ex}} + \eta^{\text{ex}} \mathbf{A}'(\mathbf{y}_t - \mathbf{A}\boldsymbol{\theta}_{t|t-1}^{\text{ex}}),$$

where $\nabla(\mathbf{y}_t | \boldsymbol{\theta}_{t|t-1}^{\text{ex}}) = \mathbf{A}'(\mathbf{y}_t - \mathbf{A}\boldsymbol{\theta}_{t|t-1}^{\text{ex}})$ is the (explicit) score. For the ISD update, the first-order condition $\boldsymbol{\theta}_{t|t}^{\text{im}} = \boldsymbol{\theta}_{t|t-1}^{\text{im}} + \eta^{\text{im}} \mathbf{A}'(\mathbf{y}_t - \mathbf{A}\boldsymbol{\theta}_{t|t-1}^{\text{im}})$ can be solved for $\boldsymbol{\theta}_{t|t}^{\text{im}}$ to yield

$$\begin{aligned} \text{ISD update: } \boldsymbol{\theta}_{t|t}^{\text{im}} &= (\mathbf{I}_k + \eta^{\text{im}} \mathbf{A}' \mathbf{A})^{-1} \left(\boldsymbol{\theta}_{t|t-1}^{\text{im}} + \eta^{\text{im}} \mathbf{A}' \mathbf{y}_t \right), \\ &= \boldsymbol{\theta}_{t|t-1}^{\text{im}} + \eta^{\text{im}} (\mathbf{I}_k + \eta^{\text{im}} \mathbf{A}' \mathbf{A})^{-1} \mathbf{A}'(\mathbf{y}_t - \mathbf{A}\boldsymbol{\theta}_{t|t-1}^{\text{im}}), \end{aligned}$$

which is a shrunken version of the ESD update with shrinkage coefficient $(\mathbf{I}_k + \eta^{\text{im}} \mathbf{A}' \mathbf{A})^{-1}$. This ensures that the ISD update remains bounded as the learning rate η^{im} increases.

Error bounds. For both filters in this setup, Theorem 2 holds with $c^{\text{im}} = c^{\text{ex}} = 1$ and

$$\begin{aligned} a^{\text{ex}} &= (1 - \min\{\alpha\eta^{\text{ex}}, 2 - \beta\eta^{\text{ex}}\})^2 + (\chi\beta\eta^{\text{ex}})^2, & b^{\text{ex}} &= (1 + 1/\chi^2)\sigma^2\eta^{\text{ex}}, & d^{\text{ex}} &= \sigma_\xi^2/\eta^{\text{ex}}. \\ a^{\text{im}} &= (1 + \alpha\eta^{\text{im}})^{-2}, & b^{\text{im}} &= a^{\text{im}}\sigma^2\eta^{\text{im}}, & d^{\text{im}} &= \sigma_\xi^2/\eta^{\text{im}}. \end{aligned}$$

These values can be substituted into equations (12)–(13) to obtain finite-sample and asymptotic error bounds in the \mathbf{P}^j -norm, respectively. As we are interested in least squares, we multiply these bounds by $1/\lambda_{\min}(\mathbf{P}^j) = \eta^j$ to obtain (Euclidean) MSE bounds. We then minimize these MSE bounds by selecting the learning rates η^j for $j \in \{\text{im, ex}\}$. For the ISD filter, we use the analytic minimizer $\eta_\star^{\text{im}} = 1/\rho_\star^{\text{im}}$ given in Appendix B.3. For the ESD filter, we numerically minimize the MSE bound with respect to both the learning rate η^{ex} and the free parameter χ .

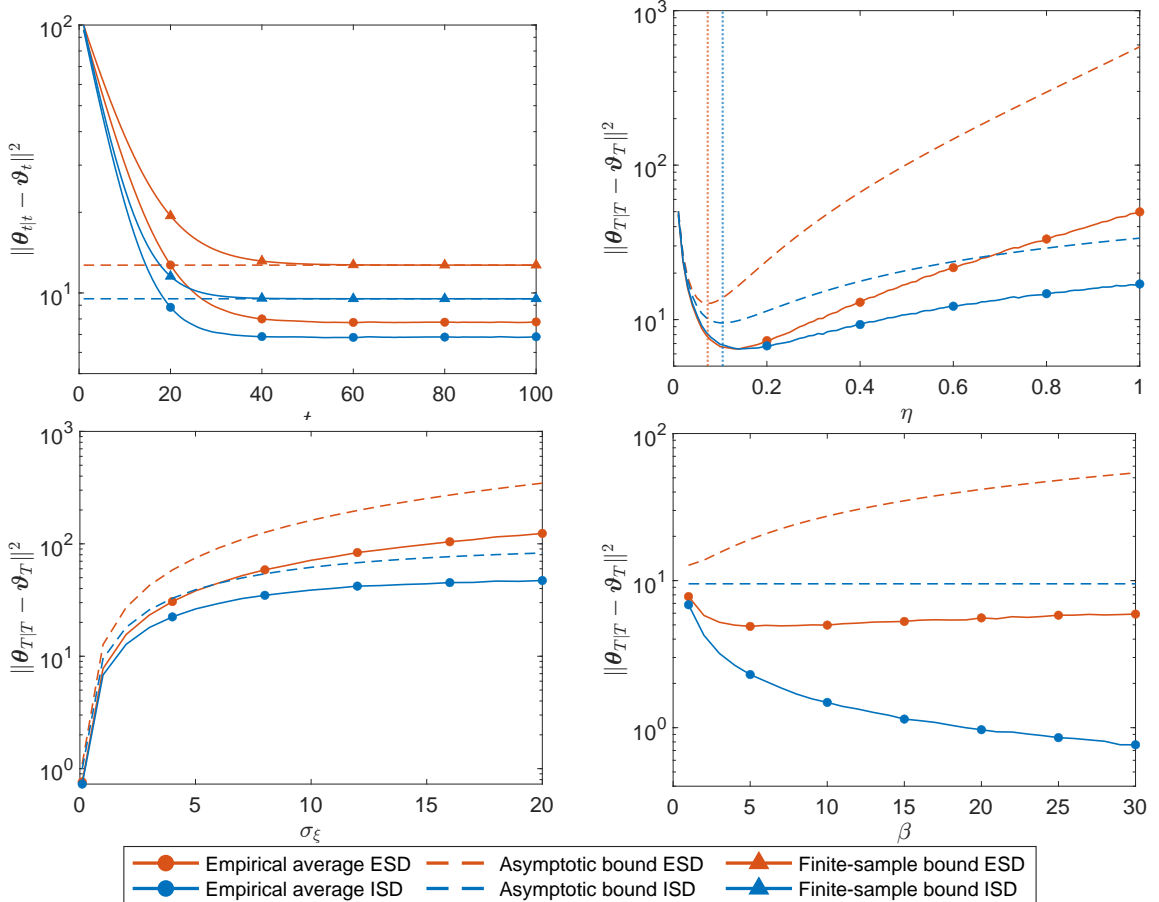


Figure 1: Semilog plots of empirical MSEs and MSE bounds (dotted) for least-squares recovery with respect to the time step t , learning rate η , state volatility σ_ξ , and Lipschitz gradient constant β , with average errors computed at horizon $T = 500$ for the latter three plots. Empirical averages are computed over 1,000 replications. Unless stated otherwise, parameters are $k = 50$, $n = 100$, $\alpha = \beta = 1$, $\sigma = 10$, and $\sigma_\xi = 1$, while learning rates η^j for $j \in \{\text{im}, \text{ex}\}$ are found by minimizing the asymptotic MSE bounds.

Simulation setup. As in Cutler et al. (2023), our default parameters are $k = 50$, $n = 100$, $\alpha = \beta = 1$, $\sigma = 10$, and $\sigma_\xi = 1$. We simulate 1,000 paths of length $T = 500$. For each replication, we compute the final squared error $\|\boldsymbol{\theta}_{T|T}^j - \boldsymbol{\vartheta}_T\|^2$ for $j \in \{\text{im}, \text{ex}\}$. We compute MSEs by averaging over all replications.

Findings for SD filters. Figure 1 shows the empirical MSEs of both SD filters for various values of t , η , σ_ξ , and β . The ISD filter achieves lower MSEs than the ESD filter across the entire range of settings considered. The top-left plot shows that the ISD filter has the lowest empirical MSE and MSE bound at all time steps. The initial MSE for both filters is 100, as they are initialized at the origin while the true process starts on a sphere of radius 10. The top-right plot shows the performance of both filters for different learning

rates, illustrating that the advantage of ISD filter grows as the learning rate increases. Vertical lines indicate the learning rates that minimize the MSE bounds, which in both cases lie slightly to the left of the learning rates that minimize the empirical MSEs.

The bottom-left plot shows that the advantage of ISD filters increases when the true state is more volatile (i.e., for larger values of σ_ξ). Similarly, the bottom-right plot shows that this advantage also grows for larger values of β . Intuitively, while the ISD filter can take advantage of the increased curvature in the postulated density (i.e., when observations are more informative), the ESD filter cannot, as its learning rate must be capped at $2/\beta$.

Three additional tracking algorithms. Next, we consider three recent tracking algorithms: (i) the online version of Nesterov’s cornerstone modern optimization method (ONM; Nesterov, 1983) as discussed in Nesterov (2018), (ii) the online gradient descent algorithm from Madden et al. (2021), and (iii) the stochastic gradient method from Cutler et al. (2023). For ONM, we follow the implementation provided in Madden et al. (2021, sec. 6.1), where the method performed well empirically, although no performance guarantees (in finite-dimensional spaces) are known. The algorithms by Madden et al. (2021) and Cutler et al. (2023) both use explicit gradient methods and, other than using different learning rates, are equivalent to our ESD filter. These authors also derive error bounds and select their learning rates to minimize these bounds; for details, see Cutler et al. (2023, Thm. 15), and Madden et al. (2021, Thm. 3.1). Interestingly, Cutler et al. (2023) cap the learning rate at $1/(2\beta)$, while our learning-rate cap for the ESD filter is four times higher at $2/\beta$, which still guarantees stability by way of Theorem 1. When $\alpha = \beta$, ONM is identical to online gradient descent as in by Madden et al. (2021). The learning rate in Madden et al. (2021) is $2/(\alpha + \beta)$, which differs from ours and Cutler et al.’s in that it is independent of the gradient noise σ^2 . The bounds in Madden et al. (2021) use a different norm and are thus not shown in our graphs.

Comparison of five tracking algorithms. To investigate the differences between

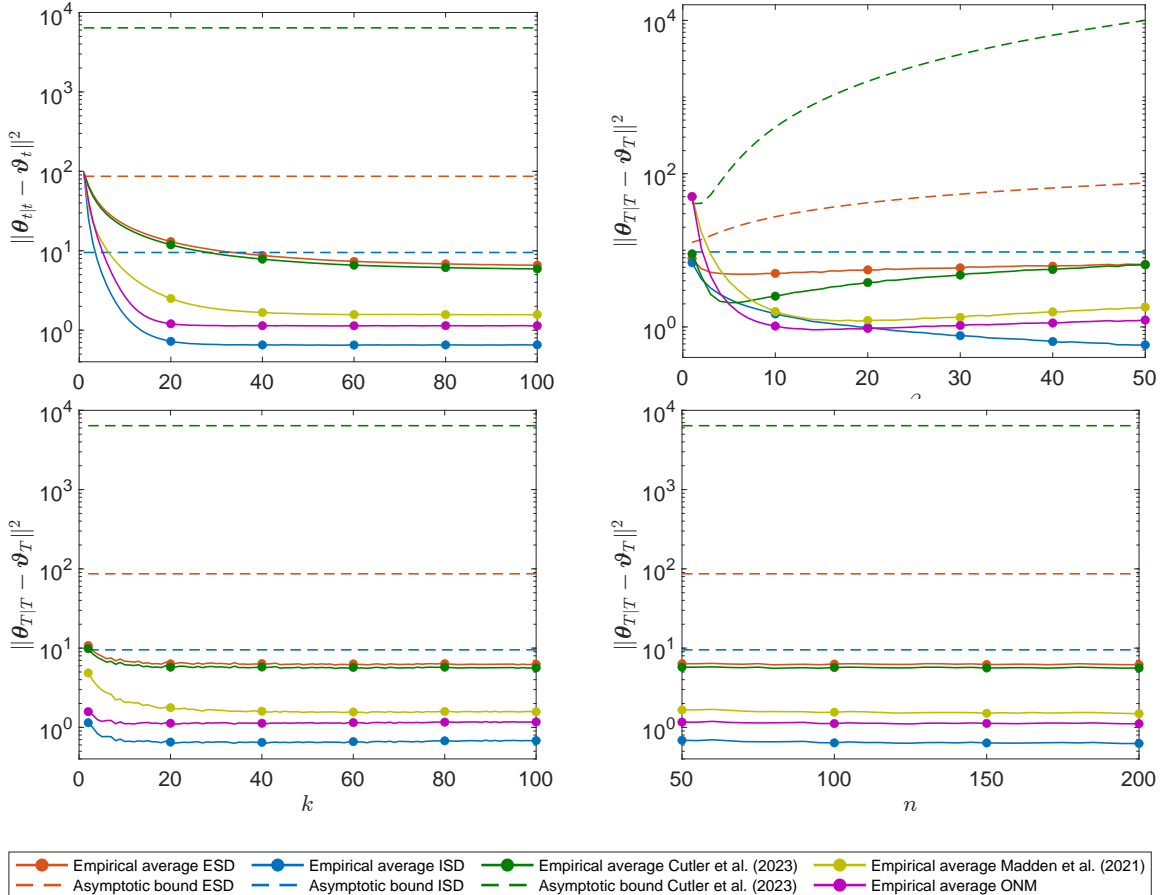


Figure 2: Semilog plots of guaranteed bounds and empirical tracking errors for least-squares recovery with respect to iteration t , Lipschitz gradient constant β , state dimension k , and observation dimension n , with average errors computed at horizon $T = 500$ for the latter three plots. Empirical averages are computed over 1,000 trials. Default parameter values: $\alpha = 1, \beta = 40, \sigma = 10, \sigma_\xi = 1, \eta = \eta_*, k = 50, n = 100$.

all five tracking algorithms, we consider a setting with a large disparity between α and β , taking $\alpha = 1$ and $\beta = 40$. For completeness, results for our default parameters (for which $\alpha = \beta = 1$ as in Cutler et al., 2023), are given in Appendix C.2. Figure 2 shows the MSEs of all five algorithms and, when available, the asymptotic MSE bounds.

We find that the ISD filter (i) outperforms all other methods across all time steps t , (ii) is the only algorithm that yields consistently lower MSEs when the Lipschitz constant β is increased, (iii) has the lowest MSE for all investigated state dimensions k and observation dimensions n , and (iv) provides the strongest (non-)asymptotic performance guarantees (i.e., the lowest MSE bounds). Of the alternatives, ONM performs best overall, echoing the findings in Madden et al. (2021), although there are no known guarantees for this algorithm.

5.2 Performance guarantees for nine DGPs in Koopman et al. (2016)

DGPs. We take nine distributions from Koopman et al. (2016), listed in Table 2 with exact specifications in Appendix C.3, and combine them with linear state dynamics $\vartheta_t = \phi_0 \vartheta_{t-1} + \xi_t$ initialized at $\vartheta_0 = 0$, where the state innovations $\xi_t \sim \text{i.i.d.}(0, \sigma_\xi^2)$ are Student's t distributed with six degrees of freedom. As our theoretical guarantees only require two moments, we allow fat-tailed state increments. For completeness, we also consider the Gaussian case (in Appendix C.3). In both cases, the state ϑ_t takes values in \mathbb{R} , such that all distributions contain link functions (e.g., mapping ϑ_t to $\mathbb{R}_{>0}$ for volatility).

The static parameters are $\phi_0 = 0.97$ and $\sigma_\xi \in \{0.15, 0.3, 0.6\}$ for low-, medium-, and high-volatility settings. Koopman et al. (2016) investigated only the low-volatility case ($\sigma_\xi = 0.15$) with Gaussian state innovations, finding that (explicit) SD filters perform relatively accurately. We take no stance on which volatility setting is more realistic; we are merely interested in investigating the implications for SD filter accuracy. Are there, for example, values of σ_ξ for which SD filters lose track of the underlying state and/or diverge?

Filters. We follow Koopman et al. (2016) in assuming that the observation densities in Table 2 are correctly specified, meaning that our postulated density $p(\cdot|\vartheta_t)$ matches (the functional form of) the true density $p^0(\cdot|\vartheta_t)$. This also implies that the ISD and ESD filters are implemented using the same (correctly specified) link functions. Because the DGP is a state-space model, however, both SD filters remain misspecified. Some densities include additional shape parameters, which are treated as unknown and estimated via maximum likelihood (6). While ESD updates (2) are given in closed form, ISD updates (4) can be computed using standard numerical methods (for details, see Appendix C.4).

MSE bounds. For each density, Table 2 reports the corresponding values of α and β from Assumption 1(a), where $\alpha \geq 0$ indicates log concavity and $\beta < \infty$ signifies a bounded Hessian. For the two non-concave cases, we impose the condition $\mathbf{P} = \rho > \alpha^-$ to ensure that Assumption 1(b) holds; in our simulations, this restriction was never binding.

Assumption 1(c) is automatically satisfied for all DGPs, as the state space is unbounded (i.e., $\Theta = \mathbb{R}$). Given the linear state equation, Assumption 2 also holds. Using the specified values of α and β , Table 2 indicates with check marks whether MSE bounds for the ISD and ESD filters exist (i.e., are finite). This is the case for nine and two DGPs, respectively.

Simulation setting. For each DGP, we simulate 1,000 time series of length 10,000. The “in-sample” period of the first 1,000 observations is used for the estimation of static parameters (i.e., ω, ϕ, ρ and shape parameters), while the remaining “out-of-sample” period is used to compute MSEs of predictions $\{\theta_{t|t-1}^j\}$ for $j \in \{\text{im, ex}\}$ relative to true states $\{\vartheta_t\}$.

Table 2: Out-of-sample MSE of $\{\theta_{t|t-1}^j\}$ for $j \in \{\text{im, ex}\}$ relative to true states $\{\vartheta_t\}$.

DGP		Assum. 1		MSE bound?		Low vol. ($\sigma_\xi = 0.15$)		Med. vol. ($\sigma_\xi = 0.30$)		High vol. ($\sigma_\xi = 0.60$)	
Type	Distribution	α	β	ISD	ESD	ISD	ESD	ISD	ESD	ISD	ESD
Count	Poisson	0	∞	✓	✗	.146	.149	.408	∞	1.74	∞
Count	Neg. Binomial	0	∞	✓	✗	.159	.160	.430	∞	1.68	∞
Intensity	Exponential	0	∞	✓	✗	.146	.150	.370	.899	1.06	$\sim 10^3$
Duration	Gamma	0	∞	✓	✗	.157	.162	.481	.577	1.32	$\sim 10^6$
Duration	Weibull	0	∞	✓	✗	.125	.128	.307	.345	0.80	$\sim 10^3$
Volatility	Gaussian	0	∞	✓	✗	.193	.199	.506	.647	1.51	$\sim 10^7$
Volatility	Student's t	0	$\frac{\nu+1}{8}$	✓	✓	.226	.226	.608	.615	1.56	1.61
Dependence	Gaussian	$-\frac{1}{4}$	∞	✓	✗	.237	.239 [†]	.593	∞	1.58	∞
Dependence	Student's t	$-\frac{1}{4}$	$\frac{\nu+1}{4}$	✓	✓	.251	.251	.619	.624	1.52	1.55

Note: MSE = mean squared error. ISD = implicit score driven. ESD = explicit score driven. [†] For the Gaussian dependence model in the low-volatility setting, the ESD filter diverged in the out-of-sample period for a single replication; for simplicity, we ignore this path and report a finite MSE.

Findings. Table 2 shows that the ISD filter outperforms the ESD filter across all DGPs and volatility settings. In the low-volatility setting (as in Koopman et al., 2016), the differences in performance are marginal. Although the ESD filter diverged during the out-of-sample period for one replication of the Gaussian dependence model, for simplicity we ignore this path and report a finite MSE. This divergence may explain why Koopman et al. (2016) further reduced the state volatility for both dependence DGPs to $\sigma_\xi = 0.10$.

In the medium-volatility setting, the performance gap becomes more pronounced. For three DGPs, the ESD filter diverges during the out-of-sample period, with a substantial proportion of paths affected (e.g., $\sim 10\%$ of paths for the Gaussian dependence model).

We report the corresponding MSEs as infinite. For two DGPs with $\beta < \infty$, the difference between the ISD and ESD filters remains marginal.

In the high-volatility setting, the potential instability of the ESD filter becomes evident across all models except those with $\beta < \infty$. Even when it does not strictly diverge (i.e., to infinity), the resulting MSEs can still be extremely large (e.g., $\sim 10^7$). In contrast, the MSE of the ISD filter never exceeds 1.74 (for the Poisson distribution).

In sum, ESD filters remain competitive across all volatility scenarios only when an MSE bound is available. Otherwise, they are prone to eventual divergence, whether in the low-, medium-, or high-volatility setting. For the Gaussian dependence model, even the low-volatility setting is problematic, although the probability of divergence appears to be quite low. The value of σ_ξ for which we start to see a substantial proportion of paths diverging is model dependent. This possibility of divergence of misspecified (explicit) SD filters was not identified in Koopman et al. (2016), likely because their analysis focused on empirical performance (i.e., without theoretical guarantees) in a low-volatility context.

Although our focus has been on ESD filters with constant learning rates, these stability issues do not disappear—and may even worsen—when using time-varying learning rates. In the next subsection, we demonstrate that such instability persists for the Poisson count model across all standard learning-rate approaches.

5.3 Poisson count model with various link and scaling functions

DGP. We consider count observations $y_t \in \mathbb{N}$ generated by a dynamic Poisson distribution $p^0(y_t|\mu_t) = \mu_t^{y_t} \exp(-\mu_t)/y_t!$ with mean $\mu_t = \exp(\vartheta_t)$, where $\mu_t > 0$ is strictly positive due to the exponential link. The latent process $\{\vartheta_t\}$ follows linear dynamics $\vartheta_t = 0.98\vartheta_{t-1} + \xi_t$ with Gaussian increments $\xi_t \sim \text{i.i.d. } N(0, \sigma_\xi^2)$. This model, along with slight variations, has been extensively studied in the literature, with notable applications including the modeling of U.K. van-driver deaths (Harvey and Fernandes, 1989; Durbin and Koopman, 1997, 2000).

ESD filter. Explicit SD filters for the Poisson count model have been considered in Davis et al. (2003, sec. 2.3), Gorgi (2018, sec. 5.2) and Gorgi et al. (2024, sec. 4.3). In line with this literature, we assume that the Poisson distribution and the exponential link $\mu_t = \exp(\vartheta_t)$ are known to the researcher, such that they can be used to calculate the score $y_t - \exp(\theta)$ and Fisher's information quantity $\exp(\theta)$. We follow the literature in considering several *scaling* options by multiplying the score by the inverse Fisher information to the power $\zeta \in \{0, 1/2, 1\}$. However, since the resulting scaled score $\exp(-\zeta\theta) [y_t - \exp(\theta)]$ fails to be Lipschitz continuous in $\theta \in \mathbb{R}$ for any scaling $\zeta \in \{0, 1/2, 1\}$, neither stability nor performance guarantees can be established for the ESD filter.

ISD filter. For the ISD filter, we consider only a static learning rate. While the Poisson distribution is again assumed to be known, we explore scenarios where the relationship between ϑ_t and μ_t is unknown. Specifically, we consider two cases in which the researcher postulates either (i) an exponential link $\mu_{t|t}^{\text{im}} = \exp(\theta_{t|t}^{\text{im}})$, which is correct, or (ii) a quadratic link $\mu_{t|t}^{\text{im}} = (\theta_{t|t}^{\text{im}})^2$, which is misspecified.

The parameter space Θ is \mathbb{R} under the exponential link and $\mathbb{R}_{\geq 0}$ under the quadratic link (this ensures monotonicity). For the quadratic link, simple parameter constraints (i.e., positivity of ω and ϕ) ensure that the prediction step (3) maps $\mathbb{R}_{\geq 0}$ to itself. This capacity to handle bounded parameter spaces is a distinctive feature of the ISD filter.

Under the two link functions, the logarithmic Poisson distribution is either (i) concave in $\theta \in \mathbb{R}$ (i.e., $\alpha = 0$), or (ii) strongly concave in $\theta \in \mathbb{R}_{\geq 0}$ (with $\alpha = 2$) as can easily be seen. In both cases, Assumptions 1(a,b) are satisfied. For the exponential link, the ISD update can be computed using Newton's optimization method (see Appendix C.4). For the quadratic link, a closed-form solution is available (see Appendix C.5). Notably, if the prediction lies in the interior of $\Theta = \mathbb{R}_{\geq 0}$, then so does the update. Even when both the prediction and the update lie on the boundary (which may occur when $y_t = 0$), the first-order condition (1) is still satisfied. Thus, while Assumption 1(c) is not strictly met, it can

be effectively circumvented. Finally, Assumption 2 holds in both cases (see Appendix C.5).

In sum, performance guarantees are available for both versions of the ISD filter. When the correct (exponential) link function is used, these bounds apply to the tracking error relative to the true states $\{\vartheta_t\}$. In contrast, when the incorrect (quadratic) link is employed, the bounds pertain to the tracking error relative to the pseudo-true states $\{\theta_t^*\} = \{\exp(\vartheta_t/2)\}$. In the latter case, the bound includes a free parameter, for which we substitute an analytic expression that minimizes the bound (see Appendix B.2). The resulting minimized MSE bound further depends on $q^2 = \sup_t \mathbb{E}[\|\theta_t^* - \theta_{t-1}^*\|^2] < \infty$ and $s_\omega^2 = \sup_t \mathbb{E}[\|\theta_t^* - \omega\|^2] < \infty$. For the purpose of computing the bound, both quantities are assumed to be known; this is standard practice in the stochastic-optimization literature (e.g., Nesterov, 2018, p. 8).

Simulation setup. We vary the state variation σ_ξ over the range $(0, 0.5]$. For each value of σ_ξ , we simulate 500 time series of length 10,000. The “in-sample” period, consisting of the first 1,000 observations, is used to estimate the static parameters, while the remaining “out-of-sample” period is used to assess the filtering performance.

Parameter estimation. Filters with exponential link functions are implemented with Assumption 3, meaning the true parameters $\omega_0 = 0$ and $\phi_0 = 0.98$ are used in the prediction step (3) (i.e., we set $\omega^j = \omega_0$ and $\phi^j = \phi_0$ for $j \in \{\text{im, ex}\}$) and the learning rates η^j for $j \in \{\text{im, ex}\}$ are estimated using (6). For the ISD filter with the quadratic link, all static parameters $(\omega^{\text{im}}, \phi^{\text{im}}, \eta^{\text{im}})$ are estimated using (6).

Findings. The left-hand panel of Figure 3 shows the out-of-sample Kullback-Leibler (KL) divergence between the filtered distribution $p(\cdot|\mu_{t|t})$ and the true distribution $p^0(\cdot|\mu_t)$, given by $\text{KL}\{p(\cdot|\mu_{t|t}), p^0(\cdot|\mu_t)\} = \mu_t \log(\mu_t/\mu_{t|t}) + \mu_{t|t} - \mu_t$. Because each filter assumes a Poisson distribution, the KL divergence depends solely on the discrepancy between the filtered mean $\mu_{t|t}^j$ for $j \in \{\text{im, ex}\}$ and the true mean μ_t . At low levels of state volatility, all filters achieve comparable KL divergence values. However, as state variability increases, all three ESD filters become unstable. Both ISD filters remain stable across all state variations,

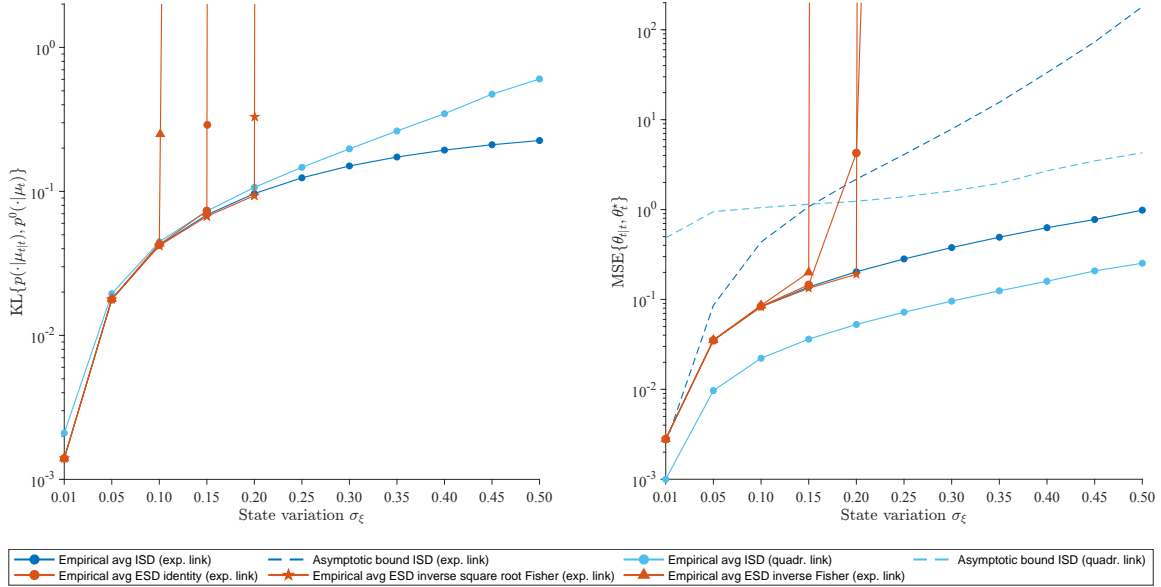


Figure 3: Plots of the out-of-sample empirical errors and guaranteed bounds for tracking (the logarithm of the rate of) a dynamic Poisson distribution (i.e., the true state $\{\vartheta_t\}$) with respect to its variation σ_ξ . The left-hand plot shows the Kullback-Leibler (KL) divergence between the postulated and true densities $p(\cdot|\mu_{t|t})$ and $p^0(\cdot|\mu_t)$, where $\mu_{t|t}$ and μ_t denote the filtered and true rates, respectively. The right-hand plot shows the MSE between the filtered state $\theta_{t|t}$ and the pseudo-true state θ_t^* ($= \vartheta_t$ if Assumption 3 holds). Empirical averages are computed over 500 trials.

even as their estimated learning rates are considerably higher (see Appendix C.5).

The right-hand panel of Figure 3 shows the out-of-sample MSEs of the filtered states $\{\theta_{t|t}^j\}$, evaluated against the true states $\{\vartheta_t\}$ when using the exponential link, or against the pseudo-true states $\{\theta_t^* = \exp(\vartheta_t/2)\}$ when using the quadratic link. Meaningful comparisons can only be made between filters that use the same link function. As the state variability increases, all three ESD filters become unstable. In contrast—and consistent with our theoretical results—both ISD filters remain stable across all state variations.

6 Conclusion

This paper has established theoretical guarantees for the stability and filtering performance of multivariate explicit and implicit score-driven (ESD and ISD) filters under potential model misspecification. First, we derived novel sufficient conditions for the exponential stability of the multivariate filtered parameter path. These conditions are verifiable in practice and yield stability uniformly for any data sequence. Proving stability for ESD filters

necessitated a Lipschitz-continuous score and a sufficiently small learning rate. Second, we combined these sufficient conditions for filter stability with mild conditions on the DGP to obtain (non-)asymptotic mean squared error (MSE) bounds that quantify the distance between the filtered parameter path and the pseudo-true path.

In three Monte Carlo studies, we validated the theoretical findings and demonstrated the advantages of ISD over ESD filters. In a high-dimensional linear model, our newly derived filtering bounds improved upon existing results by up to three orders of magnitude. Across a wide range of nonlinear settings, we demonstrated that misspecified ESD filters may diverge when no finite MSE bounds exist and the underlying state is sufficiently volatile—a finding that aligns with our theoretical framework, but is, to our knowledge, not (yet) widely recognized in the score-driven filtering literature. Conversely, we have shown in theory and practice that ISD filters remain stable, even when misspecified, while accurately tracking the (pseudo-)true parameter. Our newly derived MSE bounds can be minimized, often analytically, to facilitate the tuning of static (hyper-)parameters, such as the learning rate.

Acknowledgments

We thank Mariia Artemova, Janneke van Brummelen, Timo Dimitriadis, Andrew Harvey, Bernd Heidergott, Frank Kleibergen, Stan Koobs, Yicong Lin, André Lucas, Sam van Meer, Ramon de Punder, Alberto Quaini, Bernhard van der Sluis, Pierluigi Vallarino, and Phyllis Wan for their comments and suggestions. We also thank the participants of the EIPC 2024, Tinbergen Institute PhD seminar 2024, Oxford Dynamic Econometrics Conference 2024, New York Camp Econometrics 2024, NESG 2024, ISEO Summer School 2024, IAAE 2024, EEA-ESEM 2024, Brown Bag seminar VU Amsterdam 2025, and SoFiE 2025.

Disclosure statement

We have no conflicts of interest to disclose.

References

Artemova, M. (2023). An order-invariant score-driven dynamic factor model. *Preprint*. <https://papers.tinbergen.nl/23067.pdf>.

Artemova, M., F. Blasques, J. van Brummelen, and S. J. Koopman (2022). Score-driven models: Methodology and theory. In *Oxford Research Encyclopedia of Economics and Finance*. OUP.

Beutner, E. A., Y. Lin, and A. Lucas (2023). Consistency, distributional convergence, and optimality of score-driven filters. *Preprint*. <https://papers.tinbergen.nl/23051.pdf>.

Blasques, F., C. Francq, and S. Laurent (2023). Quasi score-driven models. *Journal of Econometrics* 234(1), 251–275.

Blasques, F., P. Gorgi, S. J. Koopman, and O. Wintenberger (2018). Feasible invertibility conditions and maximum likelihood estimation for observation-driven models. *Electronic Journal of Statistics* 12(1), 1019–1052.

Blasques, F., J. van Brummelen, S. J. Koopman, and A. Lucas (2022). Maximum likelihood estimation for score-driven models. *Journal of Econometrics* 227(2), 325–346.

Bougerol, P. (1993). Kalman filtering with random coefficients and contractions. *SIAM Journal on Control and Optimization* 31(4), 942–959.

Boyd, S. P. and L. Vandenberghe (2004). *Convex Optimization*. CUP.

Brandt, A. (1986). The stochastic equation $Y_{n+1} = A_n Y_n + B_n$ with stationary coefficients. *Advances in Applied Probability* 18(1), 211–220.

Brownlees, C. and J. Llorens-Terrazas (2024). Empirical risk minimization for time series: Nonparametric performance bounds for prediction. *Journal of Econometrics* 244(1), 105849.

Chen, X., J. D. Lee, X. T. Tong, and Y. Zhang (2020). Statistical inference for model parameters in stochastic gradient descent. *Annals of Statistics* 48(1), 251–273.

Creal, D., S. J. Koopman, and A. Lucas (2013). Generalized autoregressive score models with applications. *Journal of Applied Econometrics* 28(5), 777–795.

Cutler, J., D. Drusvyatskiy, and Z. Harchaoui (2023). Stochastic optimization under distributional drift. *Journal of Machine Learning Research* 24(147), 1–56.

Davis, R. A., W. T. Dunsmuir, and S. B. Streett (2003). Observation-driven models for Poisson counts. *Biometrika* 90(4), 777–790.

Durbin, J. and S. J. Koopman (1997). Monte Carlo maximum likelihood estimation for non-Gaussian state space models. *Biometrika* 84(3), 669–684.

Durbin, J. and S. J. Koopman (2000). Time series analysis of non-Gaussian observations based on state space models from both classical and Bayesian perspectives. *Journal of the Royal Statistical Society Series B: Statistical Methodology* 62(1), 3–56.

Durbin, J. and S. J. Koopman (2012). *Time Series Analysis by State Space Methods*. OUP.

Gorgi, P. (2018). Integer-valued autoregressive models with survival probability driven by a stochastic recurrence equation. *Journal of Time Series Analysis* 39(2), 150–171.

Gorgi, P., C. Lauria, and A. Luati (2024). On the optimality of score-driven models. *Biometrika* 111(3), 865–880.

Guo, L. and L. Ljung (1995). Exponential stability of general tracking algorithms. *IEEE Transactions on Automatic Control* 40(8), 1376–1387.

Harvey, A. C. (2013). *Dynamic Models for Volatility and Heavy Tails: With Applications to Financial and Economic Time Series*. CUP.

Harvey, A. C. (2022). Score-driven time series models. *Annual Review of Statistics and Its Application* 9(1), 321–342.

Harvey, A. C. and C. Fernandes (1989). Time series models for count or qualitative observations. *Journal of Business & Economic Statistics* 7(4), 407–417.

Harvey, A. C. and R.-J. Lange (2018). Modeling the interactions between volatility and returns using EGARCH-M. *Journal of Time Series Analysis* 39(6), 909–919.

Jungers, R. (2009). *The Joint Spectral Radius: Theory and Applications*. Springer.

Kalman, R. E. (1960). A new approach to linear filtering and prediction problems. *Journal of Basic Engineering* 82(1), 35–45.

Koopman, S. J., A. Lucas, and M. Scharth (2016). Predicting time-varying parameters with parameter-driven and observation-driven models. *Review of Economics and Statistics* 98(1), 97–110.

Krengel, U. (1985). *Ergodic Theorems*. Walter de Gruyter.

Lanconelli, A. and C. S. Lauria (2024). Maximum likelihood with a time varying parameter. *Statistical Papers* 65(4), 2555–2566.

Lange, R.-J. (2024). Bellman filtering and smoothing for state-space models. *Journal of Econometrics* 238(2), 105632.

Lange, R.-J., B. van Os, and D. J. van Dijk (2024). Implicit score-driven filters for time-varying parameter models. *Preprint*. <https://ssrn.com/abstract=4227958>.

Lehmann, E. L. and G. Casella (1998). *Theory of Point Estimation*. Springer.

Liang, T. and W. J. Su (2019). Statistical inference for the population landscape via moment-adjusted stochastic gradients. *Journal of the Royal Statistical Society Series B: Statistical Methodology* 81(2), 431–456.

Madden, L., S. Becker, and E. Dall’Anese (2021). Bounds for the tracking error of first-order online optimization methods. *Journal of Optimization Theory and Applications* 189, 437–457.

Nesterov, Y. (1983). A method for unconstrained convex minimization problem with the rate of convergence $O(1/k^2)$. *Doklady AN SSSR* 269, 543–547.

Nesterov, Y. (2018). *Lectures on Convex Optimization*. Springer.

Pötscher, B. M. and I. Prucha (1997). *Dynamic Nonlinear Econometric Models: Asymptotic Theory*. Springer.

Simonetto, A., E. Dall’Anese, S. Paternain, G. Leus, and G. B. Giannakis (2020). Time-varying convex optimization: Time-structured algorithms and applications. *Proceedings of the IEEE* 108(11), 2032–2048.

Straumann, D. and T. Mikosch (2006). Quasi-maximum-likelihood estimation in conditionally heteroscedastic time series: A stochastic recurrence equations approach. *Annals of Statistics* 34(5), 2449–2495.

Toulis, P. and E. M. Airoldi (2017). Asymptotic and finite-sample properties of estimators based on stochastic gradients. *Annals of Statistics* 45(4), 1694–1727.

Wilson, C., V. V. Veeravalli, and A. Nedić (2019). Adaptive sequential stochastic optimization. *IEEE Transactions on Automatic Control* 64(2), 496–509.

Wu, L. and W. J. Su (2023). The implicit regularization of dynamical stability in stochastic gradient descent. In *International Conference on Machine Learning*, pp. 37656–37684. PMLR.

Online supplement to:
“Stability and performance guarantees for
misspecified multivariate score-driven filters”

Simon Donker van Heel, Rutger-Jan Lange, Bram van Os, and Dick van Dijk

August 19, 2025

A Proofs of main results

A.1 Preliminaries

Throughout our proofs, we make extensive use of the squared weighted norm $\|\mathbf{x}\|_{\mathbf{W}}^2 := \mathbf{x}'\mathbf{W}\mathbf{x}$ for any $\mathbf{x} \in \mathbb{R}^k$ and any positive-definite matrix $\mathbf{W} \in \mathbb{R}^{k \times k}$. With slight abuse of notation, we also use the shorthand $\|\mathbf{x}\|_{\mathbf{W}}^2$ for a matrix \mathbf{W} that is not positive definite; in this case, the expression remains well defined but strictly speaking does not constitute a norm. We also use the \mathbf{W} -weighted (induced) matrix norm, defined as

$$\|\mathbf{A}\|_{\mathbf{W}}^2 := \sup_{\mathbf{y} \in \mathbb{R}^k \setminus \{\mathbf{0}_k\}} \frac{\|\mathbf{A}\mathbf{y}\|_{\mathbf{W}}^2}{\|\mathbf{y}\|_{\mathbf{W}}^2} \geq \frac{\|\mathbf{A}\mathbf{x}\|_{\mathbf{W}}^2}{\|\mathbf{x}\|_{\mathbf{W}}^2}, \quad \forall \mathbf{x} \in \mathbb{R}^k \setminus \{\mathbf{0}_k\}.$$

The inequality demonstrates that the usual submultiplicative property holds, i.e.,

$$\|\mathbf{A}\mathbf{x}\|_{\mathbf{W}}^2 \leq \|\mathbf{A}\|_{\mathbf{W}}^2 \|\mathbf{x}\|_{\mathbf{W}}^2, \quad \forall \mathbf{x} \in \mathbb{R}^k, \tag{A.1}$$

for any matrix $\mathbf{A} \in \mathbb{R}^{k \times k}$ and any positive-definite matrix $\mathbf{W} \in \mathbb{R}^{k \times k}$.

The notation $\mathbf{A}^{1/2}$ for positive-semidefinite $\mathbf{A} \in \mathbb{R}^{k \times k}$ refers to the symmetric matrix square root that can be obtained via eigendecomposition. Specifically, let $\mathbf{V} \in \mathbb{R}^{k \times k}$ denote the matrix of eigenvectors of \mathbf{A} and let $\mathbf{D} \in \mathbb{R}^{k \times k}$ denote the diagonal matrix of eigenvalues in corresponding order such that $\mathbf{A} = \mathbf{V}\mathbf{D}\mathbf{V}'$; then, $\mathbf{A}^{1/2} := \mathbf{V}\tilde{\mathbf{D}}\mathbf{V}'$, where $\tilde{\mathbf{D}} \in \mathbb{R}^{k \times k}$ is a diagonal matrix containing the principal square root eigenvalues such that $\tilde{\mathbf{D}}\tilde{\mathbf{D}} = \mathbf{D}$. From this definition and the orthogonality of \mathbf{V} it is immediately apparent that $\mathbf{A}^{1/2}$ is symmetric and that $\mathbf{A}^{1/2}\mathbf{A}^{1/2} = \mathbf{V}\tilde{\mathbf{D}}\mathbf{V}'\mathbf{V}\tilde{\mathbf{D}}\mathbf{V}' = \mathbf{V}\tilde{\mathbf{D}}\mathbf{I}_k\tilde{\mathbf{D}}\mathbf{V}' = \mathbf{V}\mathbf{D}\mathbf{V}' = \mathbf{A}$. It can also be established that $\mathbf{A}^{1/2}$ is the unique symmetric matrix such that $\mathbf{A}^{1/2}\mathbf{A}^{1/2} = \mathbf{A}$, see Horn and Johnson (2012, Thm. 7.2.6a).

A.2 Lemma 1

The next eigenvalue property is used in the proof of Lemma 2, which in turn is used in the proofs of Theorems 1 and 2.

Lemma 1. *Let $\mathbf{A}, \mathbf{B} \in \mathbb{R}^{k \times k}$ be symmetric, while \mathbf{B} is positive definite. Then*

$$\min \left\{ \frac{\lambda_{\min}(\mathbf{A})}{\lambda_{\min}(\mathbf{B})}, \frac{\lambda_{\min}(\mathbf{A})}{\lambda_{\max}(\mathbf{B})} \right\} \mathbf{I}_k \preceq \mathbf{B}^{-\frac{1}{2}} \mathbf{A} \mathbf{B}^{-\frac{1}{2}} \preceq \max \left\{ \frac{\lambda_{\max}(\mathbf{A})}{\lambda_{\min}(\mathbf{B})}, \frac{\lambda_{\max}(\mathbf{A})}{\lambda_{\max}(\mathbf{B})} \right\} \mathbf{I}_k. \quad (\text{A.2})$$

Proof. First, we prove the inequality relating to the minimum eigenvalue, i.e.

$$\min \left\{ \frac{\lambda_{\min}(\mathbf{A})}{\lambda_{\min}(\mathbf{B})}, \frac{\lambda_{\min}(\mathbf{A})}{\lambda_{\max}(\mathbf{B})} \right\} \leq \lambda_{\min} \left(\mathbf{B}^{-\frac{1}{2}} \mathbf{A} \mathbf{B}^{-\frac{1}{2}} \right).$$

To see this, we write the smallest eigenvalue as

$$\lambda_{\min} \left(\mathbf{B}^{-\frac{1}{2}} \mathbf{A} \mathbf{B}^{-\frac{1}{2}} \right) = \min_{\mathbf{x} \neq \mathbf{0}_k} \frac{\mathbf{x}' \mathbf{B}^{-\frac{1}{2}} \mathbf{A} \mathbf{B}^{-\frac{1}{2}} \mathbf{x}}{\mathbf{x}' \mathbf{x}} = \min_{\mathbf{y} \neq \mathbf{0}_k} \frac{\mathbf{y}' \mathbf{A} \mathbf{y}}{\mathbf{y}' \mathbf{B} \mathbf{y}},$$

where we used $\mathbf{y} = \mathbf{B}^{-1/2} \mathbf{x}$. Depending on the sign of $\lambda_{\min}(\mathbf{A})$, there are two cases:

$$\begin{aligned} \lambda_{\min}(\mathbf{A}) \geq 0 &\Rightarrow \min_{\mathbf{y} \neq \mathbf{0}_k} \frac{\mathbf{y}' \mathbf{A} \mathbf{y}}{\mathbf{y}' \mathbf{B} \mathbf{y}} \geq \frac{\lambda_{\min}(\mathbf{A})}{\lambda_{\max}(\mathbf{B})}, \\ \lambda_{\min}(\mathbf{A}) < 0 &\Rightarrow \min_{\mathbf{y} \neq \mathbf{0}_k} \frac{\mathbf{y}' \mathbf{A} \mathbf{y}}{\mathbf{y}' \mathbf{B} \mathbf{y}} = \min_{\mathbf{y}: \mathbf{y}' \mathbf{A} \mathbf{y} < 0} \frac{\mathbf{y}' \mathbf{A} \mathbf{y}}{\mathbf{y}' \mathbf{B} \mathbf{y}} \geq \min_{\mathbf{y} \neq \mathbf{0}_k} \frac{\mathbf{y}' \mathbf{A} \mathbf{y}}{\lambda_{\min}(\mathbf{B}) \mathbf{y}' \mathbf{y}} = \frac{\lambda_{\min}(\mathbf{A})}{\lambda_{\min}(\mathbf{B})}. \end{aligned}$$

In both cases, the numerator is the smallest eigenvalue of \mathbf{A} . When the numerator is positive (negative), the denominator is the largest (smallest) eigenvalue of \mathbf{B} . Hence the minimum of both possible fractions is the relevant one.

Second, we prove the inequality relating to the maximum eigenvalue, i.e.

$$\lambda_{\max} \left(\mathbf{B}^{-\frac{1}{2}} \mathbf{A} \mathbf{B}^{-\frac{1}{2}} \right) \leq \max \left\{ \frac{\lambda_{\max}(\mathbf{A})}{\lambda_{\min}(\mathbf{B})}, \frac{\lambda_{\max}(\mathbf{A})}{\lambda_{\max}(\mathbf{B})} \right\}.$$

To see this, we write the largest eigenvalue as

$$\lambda_{\max} \left(\mathbf{B}^{-\frac{1}{2}} \mathbf{A} \mathbf{B}^{-\frac{1}{2}} \right) = \max_{\mathbf{x} \neq \mathbf{0}_k} \frac{\mathbf{x}' \mathbf{B}^{-\frac{1}{2}} \mathbf{A} \mathbf{B}^{-\frac{1}{2}} \mathbf{x}}{\mathbf{x}' \mathbf{x}} = \max_{\mathbf{y} \neq \mathbf{0}_k} \frac{\mathbf{y}' \mathbf{A} \mathbf{y}}{\mathbf{y}' \mathbf{B} \mathbf{y}},$$

where we used $\mathbf{y} = \mathbf{B}^{-1/2} \mathbf{x}$. Depending on the sign of $\lambda_{\max}(\mathbf{A})$, there are two cases:

$$\begin{aligned} \lambda_{\max}(\mathbf{A}) \geq 0 &\Rightarrow \max_{\mathbf{y} \neq \mathbf{0}_k} \frac{\mathbf{y}' \mathbf{A} \mathbf{y}}{\mathbf{y}' \mathbf{B} \mathbf{y}} \leq \frac{\lambda_{\max}(\mathbf{A})}{\lambda_{\min}(\mathbf{B})}, \\ \lambda_{\max}(\mathbf{A}) < 0 &\Rightarrow \max_{\mathbf{y} \neq \mathbf{0}_k} \frac{\mathbf{y}' \mathbf{A} \mathbf{y}}{\mathbf{y}' \mathbf{B} \mathbf{y}} = \max_{\mathbf{y}: \mathbf{y}' \mathbf{A} \mathbf{y} < 0} \frac{\mathbf{y}' \mathbf{A} \mathbf{y}}{\mathbf{y}' \mathbf{B} \mathbf{y}} \leq \max_{\mathbf{y} \neq \mathbf{0}_k} \frac{\mathbf{y}' \mathbf{A} \mathbf{y}}{\lambda_{\max}(\mathbf{B}) \mathbf{y}' \mathbf{y}} = \frac{\lambda_{\max}(\mathbf{A})}{\lambda_{\max}(\mathbf{B})}. \end{aligned}$$

In both cases, the numerator is the largest eigenvalue of \mathbf{A} . When the numerator is positive (negative), the denominator is the smallest (largest) eigenvalue of \mathbf{B} . Hence the maximum of both possible fractions is the relevant one. \square

A.3 Lemma 2

Lemma 2 relies on Lemma 1 in the previous section. Lemma 2 will be used in the proofs of Theorems 1 and 2.

Lemma 2 (Update stability). *Let Assumption 1 hold. Fix $t \geq 1$. Consider two predictions $\boldsymbol{\theta}_{t|t-1}^j \in \Theta$ with $j \in \{\text{im}, \text{ex}\}$ and associated ISD and ESD updates (1) and (2), yielding $\boldsymbol{\theta}_{t|t}^{\text{im}}$ and $\boldsymbol{\theta}_{t|t}^{\text{ex}}$, respectively. Then, uniformly in $\boldsymbol{\theta}_{t|t-1}^j, \boldsymbol{\theta}_{t|t-1}^j \in \Theta$ and for all \mathbf{y}_t ,*

$$\left\| \frac{d\boldsymbol{\theta}_{t|t}^{\text{im}}}{d\boldsymbol{\theta}_{t|t-1}^{\text{im}}} \right\|_{\mathbf{P}} \leq 1 - \frac{\alpha^+}{\lambda_{\max}(\mathbf{P}) + \alpha^+} + \frac{\alpha^-}{\lambda_{\min}(\mathbf{P}) - \alpha^-}, \quad (\text{A.3})$$

$$\left\| \frac{d\boldsymbol{\theta}_{t|t}^{\text{ex}}}{d\boldsymbol{\theta}_{t|t-1}^{\text{ex}}} \right\|_{\mathbf{P}} \leq 1 - \min \left\{ \frac{\alpha^+}{\lambda_{\max}(\mathbf{P})} - \frac{\alpha^-}{\lambda_{\min}(\mathbf{P})}, 2 - \frac{\beta}{\lambda_{\min}(\mathbf{P})} \right\}. \quad (\text{A.4})$$

Discussion of Lemma 2. The lemma considers the sensitivity of the updated parameter with respect to the predicted parameter, as measured by the Jacobian matrix, in the \mathbf{P} -weighted matrix norm. We call the updating step stable (in the \mathbf{P} -norm) if the weighted

norm does not exceed unity. By equation (A.3), for the implicit update to be stable for all observations \mathbf{y}_t and all predictions, it is both necessary and sufficient to have $\alpha \geq 0$, in which case the right-hand side does not exceed unity. In particular, the update is always stable if $\alpha > 0$, while it may be expansive if $\alpha < 0$. The largest possible expansion is bounded due to Assumption 1(b) (i.e., $\lambda_{\min}(\mathbf{P}) > \alpha^-$).

As inequality (A.4) shows, ESD update stability additionally requires $\beta < \infty$; otherwise the right-hand side would be unbounded. While $\alpha \geq 0$ remains necessary, it is no longer sufficient: if β is large, such that the second argument of $\min\{\cdot, \cdot\}$ dominates, we also need $2 - \beta/\lambda_{\min}(\mathbf{P})$ to be positive. Using $1/\lambda_{\min}(\mathbf{P}) = \lambda_{\max}(\mathbf{H})$, this additional requirement can be concisely written as $\lambda_{\max}(\mathbf{H}) \leq 2/\beta$.

Proof. Update stability for ISD filters. For the clarity of exposition, we omit the superscript on $\boldsymbol{\theta}_{t|t-1}$. Differentiating the ISD update step (1), the Jacobian of the implicit update with respect to the prediction $\boldsymbol{\theta}_{t|t-1}$ is

$$\frac{d\boldsymbol{\theta}_{t|t}^{\text{im}}}{d\boldsymbol{\theta}'_{t|t-1}} = \mathbf{I}_k + \mathbf{P}^{-1} \mathcal{H}_t^{\text{im}} \frac{d\boldsymbol{\theta}_{t|t}^{\text{im}}}{d\boldsymbol{\theta}'_{t|t-1}}, \quad (\text{A.5})$$

where $\mathcal{H}_t^{\text{im}} := \nabla^2 \ell(\mathbf{y}_t \mid \boldsymbol{\theta}_{t|t}^{\text{im}})$ is the Hessian matrix evaluated at the ISD update. Premultiply by the penalty matrix \mathbf{P} to get

$$\mathbf{P} \frac{d\boldsymbol{\theta}_{t|t}^{\text{im}}}{d\boldsymbol{\theta}'_{t|t-1}} = \mathbf{P} + \mathcal{H}_t^{\text{im}} \frac{d\boldsymbol{\theta}_{t|t}^{\text{im}}}{d\boldsymbol{\theta}'_{t|t-1}}, \quad (\text{A.6})$$

and solve for the Jacobian to obtain

$$\frac{d\boldsymbol{\theta}_{t|t}^{\text{im}}}{d\boldsymbol{\theta}'_{t|t-1}} = (\mathbf{P} - \mathcal{H}_t^{\text{im}})^{-1} \mathbf{P} = (\mathbf{I}_k - \mathbf{P}^{-1} \mathcal{H}_t^{\text{im}})^{-1}. \quad (\text{A.7})$$

Here, we note that the inverse of $\mathbf{P} - \mathcal{H}_t^{\text{im}}$ exists as $\mathbf{P} - \mathcal{H}_t^{\text{im}} \succ \mathbf{O}$ by Assumption 1, i.e. the penalty exceeds any possible non-concavity of the log density such that the regularized

objective in optimization (4) is strictly concave. The second equality follows from $(\mathbf{P} - \mathcal{H}_t^{\text{im}})^{-1} \mathbf{P} = [\mathbf{P}^{-1}(\mathbf{P} - \mathcal{H}_t^{\text{im}})]^{-1} = (\mathbf{I}_k - \mathbf{P}^{-1}\mathcal{H}_t^{\text{im}})^{-1}$. Next, we investigate

$$\begin{aligned}
\left\| \frac{d\boldsymbol{\theta}_{t|t}^{\text{im}}}{d\boldsymbol{\theta}_{t|t-1}'} \right\|_{\mathbf{P}} &= \|(\mathbf{I}_k - \mathbf{P}^{-1}\mathcal{H}_t^{\text{im}})^{-1}\|_{\mathbf{P}} \quad \text{by (A.7)} \\
&= \left\| \mathbf{P}^{1/2} (\mathbf{I}_k - \mathbf{P}^{-1}\mathcal{H}_t^{\text{im}})^{-1} \mathbf{P}^{-1/2} \right\| \quad \text{as } \|\mathbf{A}\|_{\mathbf{B}} = \|\mathbf{B}^{1/2}\mathbf{A}\mathbf{B}^{-1/2}\| \\
&= \left\| (\mathbf{I}_k + \mathbf{P}^{-1/2}(-\mathcal{H}_t^{\text{im}})\mathbf{P}^{-1/2})^{-1} \right\| \quad \text{as } \mathbf{B}^{1/2}\mathbf{A}^{-1}\mathbf{B}^{-1/2} = (\mathbf{B}^{1/2}\mathbf{A}\mathbf{B}^{-1/2})^{-1} \\
&= \lambda_{\max} \left([\mathbf{I}_k + \mathbf{P}^{-1/2}(-\mathcal{H}_t^{\text{im}})\mathbf{P}^{-1/2}]^{-1} \right) \quad \text{as } \|\mathbf{B}\| = \lambda_{\max}(\mathbf{B}) \text{ if } \mathbf{B} \text{ is p.d.} \\
&= 1/\lambda_{\min}(\mathbf{I}_k + \mathbf{P}^{-1/2}(-\mathcal{H}_t^{\text{im}})\mathbf{P}^{-1/2}) \\
&= [1 + \lambda_{\min}(\mathbf{P}^{-1/2}(-\mathcal{H}_t^{\text{im}})\mathbf{P}^{-1/2})]^{-1}. \tag{A.8}
\end{aligned}$$

The fourth line uses that $\mathbf{I}_k - \mathbf{P}^{-1/2}\mathcal{H}_t^{\text{im}}\mathbf{P}^{-1/2}$ is (symmetric and) positive definite, which follows from the symmetry of \mathbf{P} along with $\mathbf{P} - \mathcal{H}_t^{\text{im}} \succ \mathbf{O}_k$ as implied by Assumption 1. The last two lines use $\lambda_{\max}(\mathbf{A}^{-1}) = 1/\lambda_{\min}(\mathbf{A})$ and $\lambda_{\min}(\mathbf{I}_k + \mathbf{A}) = 1 + \lambda_{\min}(\mathbf{A})$ for arbitrary matrix $\mathbf{A} \in \mathbb{R}^{k \times k}$. To upper bound the last quantity, we must lower bound $\lambda_{\min}(\mathbf{P}^{-1/2}(-\mathcal{H}_t^{\text{im}})\mathbf{P}^{-1/2}) > -1$. (Note that $1/(1+x)$ is decreasing in x for $x > -1$.) To this end we use Lemma 1 in Appendix A.2 to yield

$$\begin{aligned}
\left\| \frac{d\boldsymbol{\theta}_{t|t}^{\text{im}}}{d\boldsymbol{\theta}_{t|t-1}'} \right\|_{\mathbf{P}} &\leq \left[1 + \min \left\{ \frac{\lambda_{\min}(-\mathcal{H}_t^{\text{im}})}{\lambda_{\min}(\mathbf{P})}, \frac{\lambda_{\min}(-\mathcal{H}_t^{\text{im}})}{\lambda_{\max}(\mathbf{P})} \right\} \right]^{-1} \quad \text{by (A.8) and Lemma 1} \\
&\leq \left[1 + \min \left\{ \frac{\alpha}{\lambda_{\min}(\mathbf{P})}, \frac{\alpha}{\lambda_{\max}(\mathbf{P})} \right\} \right]^{-1} \quad \text{as } \alpha \leq \lambda_{\min}(-\mathcal{H}_t^{\text{im}}) \text{ by Assumption 1} \\
&= \left[1 + \frac{\alpha^+}{\lambda_{\max}(\mathbf{P})} - \frac{\alpha^-}{\lambda_{\min}(\mathbf{P})} \right]^{-1} \quad \text{as } \alpha = \alpha^+ - \alpha^- \text{ and } \lambda_{\min}(\mathbf{P}) > 0 \\
&= 1 - \frac{\alpha^+}{\lambda_{\max}(\mathbf{P}) + \alpha^+} + \frac{\alpha^-}{\lambda_{\min}(\mathbf{P}) - \alpha^-}, \quad \text{by algebra} \tag{A.9}
\end{aligned}$$

where $\alpha^+ := \max\{0, \alpha\}$ and $\alpha^- := \max\{0, -\alpha\}$. In sum, in the concave case (i.e., $\alpha \geq 0$), we obtain the standard contraction coefficient $1 - \alpha^+ / (\lambda_{\max}(\mathbf{P}) + \alpha^+) = \lambda_{\max}(\mathbf{P}) / (\lambda_{\max}(\mathbf{P}) + \alpha^+) \leq 1$ (see also Lange et al., 2024, p. 9). In the non-concave case (i.e., $\alpha < 0$), we obtain

the maximal expansion coefficient $1 + \alpha^- / (\lambda_{\min}(\mathbf{P}) - \alpha^-) = \lambda_{\min}(\mathbf{P}) / (\lambda_{\min}(\mathbf{P}) - \alpha^-)$. The strict concavity of the regularized objective (Assumption 1) implies $\lambda_{\max}(\mathbf{P}) \geq \lambda_{\min}(\mathbf{P}) > \alpha^-$, such that the denominator is strictly positive in either case.

Update stability for ESD filters. For the clarity of exposition, we omit the superscript on $\boldsymbol{\theta}_{t|t-1}$. Differentiating the ESD update step (2), the Jacobian of the update with respect to the prediction is

$$\frac{d\boldsymbol{\theta}_{t|t}^{\text{ex}}}{d\boldsymbol{\theta}'_{t|t-1}} = \mathbf{I}_k + \mathbf{P}^{-1} \mathcal{H}_t^{\text{ex}}, \quad (\text{A.10})$$

where $\mathcal{H}_t^{\text{ex}} := \nabla^2(\mathbf{y}_t | \boldsymbol{\theta}_{t|t-1}^{\text{ex}})$ is the Hessian matrix evaluated at the ESD prediction. Then

$$\begin{aligned} \left\| \frac{d\boldsymbol{\theta}_{t|t}^{\text{ex}}}{d\boldsymbol{\theta}'_{t|t-1}} \right\|_{\mathbf{P}} &= \left\| \mathbf{I}_k + \mathbf{P}^{-1} \mathcal{H}_t^{\text{ex}} \right\|_{\mathbf{P}} = \left\| \mathbf{P}^{1/2} (\mathbf{I}_k + \mathbf{P}^{-1} \mathcal{H}_t^{\text{ex}}) \mathbf{P}^{-1/2} \right\| \\ &= \left\| \mathbf{I}_k + \mathbf{P}^{-1/2} \mathcal{H}_t^{\text{ex}} \mathbf{P}^{-1/2} \right\| \\ &= \max \left\{ \lambda_{\max}(\mathbf{I}_k + \mathbf{P}^{-1/2} \mathcal{H}_t^{\text{ex}} \mathbf{P}^{-1/2}), -\lambda_{\min}(\mathbf{I}_k + \mathbf{P}^{-1/2} \mathcal{H}_t^{\text{ex}} \mathbf{P}^{-1/2}) \right\}, \quad (\text{A.11}) \end{aligned}$$

where the first line uses the definition of the induced matrix norm $\|\mathbf{A}\|_{\mathbf{W}} = \|\mathbf{W}^{1/2} \mathbf{A} \mathbf{W}^{-1/2}\|$ for any symmetric positive-definite matrix \mathbf{W} and square matrix \mathbf{A} of equal dimension, and the second line uses $\|\mathbf{A}\| = \sqrt{\lambda_{\max}(\mathbf{A}^2)} = \max\{\lambda_{\max}(\mathbf{A}), -\lambda_{\min}(\mathbf{A})\}$ for any symmetric matrix \mathbf{A} with real eigenvalues. Because we work exclusively with real-valued matrices, we have that symmetry is sufficient to guarantee that all eigenvalues are real.

First, focusing on the maximal eigenvalue of $\mathbf{I}_k + \mathbf{P}^{-1/2} \mathcal{H}_t^{\text{ex}} \mathbf{P}^{-1/2}$, we can bound it by using Lemma 1 in Appendix A.2 as follows:

$$\begin{aligned} \lambda_{\max}(\mathbf{I}_k + \mathbf{P}^{-1/2} \mathcal{H}_t^{\text{ex}} \mathbf{P}^{-1/2}) &= 1 + \lambda_{\max}(\mathbf{P}^{-1/2} \mathcal{H}_t^{\text{ex}} \mathbf{P}^{-1/2}) \\ &= 1 - \lambda_{\min}(\mathbf{P}^{-1/2} (-\mathcal{H}_t^{\text{ex}}) \mathbf{P}^{-1/2}) \\ &\leq 1 - \min \left\{ \frac{\lambda_{\min}(-\mathcal{H}_t^{\text{ex}})}{\lambda_{\min}(\mathbf{P})}, \frac{\lambda_{\min}(-\mathcal{H}_t^{\text{ex}})}{\lambda_{\max}(\mathbf{P})} \right\} \quad \text{by Lemma 1} \\ &\leq 1 - \min \left\{ \frac{\alpha}{\lambda_{\min}(\mathbf{P})}, \frac{\alpha}{\lambda_{\max}(\mathbf{P})} \right\} \quad \text{as } \alpha \leq -\mathcal{H}_t^{\text{ex}} \text{ by Assumption 1} \end{aligned}$$

$$= 1 - \frac{\alpha^+}{\lambda_{\max}(\mathbf{P})} + \frac{\alpha^-}{\lambda_{\min}(\mathbf{P})}. \quad (\text{A.12})$$

The first and second lines use $\lambda_{\max}(\mathbf{I}_k + \mathbf{A}) = 1 + \lambda_{\max}(\mathbf{A})$ and $\lambda_{\max}(\mathbf{A}) = -\lambda_{\min}(-\mathbf{A})$, respectively, for an arbitrary matrix $\mathbf{A} \in \mathbb{R}^{k \times k}$. The inequality in the third line holds because $1 - x$ is decreasing in x and we can lower bound $x = \lambda_{\min}(\mathbf{P}^{-1/2}(-\mathbf{H}_t^{\text{ex}})\mathbf{P}^{-1/2})$ by Lemma 1 in Appendix A.2 with $\mathbf{A} = -\mathbf{H}_t^{\text{ex}}$ and $\mathbf{B} = \mathbf{P}$. The inequality in the fourth line holds by Assumption 1. The final equality follows by $\alpha = \alpha^+ - \alpha^-$ (where $\alpha^+ := \max\{0, \alpha\}$ and $\alpha^- := \max\{0, -\alpha\}$) and $\lambda_{\min}(\mathbf{P}) > 0$.

Second, focusing on (the negative of) the smallest eigenvalue of $\mathbf{I}_k + \mathbf{P}^{-1/2}\mathbf{H}_t^{\text{ex}}\mathbf{P}^{-1/2}$, we again use Lemma 1 as follows:

$$\begin{aligned} -\lambda_{\min}(\mathbf{I}_k + \mathbf{P}^{-1/2}\mathbf{H}_t^{\text{ex}}\mathbf{P}^{-1/2}) &= \lambda_{\max}(-\mathbf{I}_k + \mathbf{P}^{-1/2}(-\mathbf{H}_t^{\text{ex}})\mathbf{P}^{-1/2}) \\ &= -1 + \lambda_{\max}(\mathbf{P}^{-1/2}(-\mathbf{H}_t^{\text{ex}})\mathbf{P}^{-1/2}) \\ &\leq -1 + \max \left\{ \frac{\lambda_{\max}(-\mathbf{H}_t^{\text{ex}})}{\lambda_{\min}(\mathbf{P})}, \frac{\lambda_{\max}(-\mathbf{H}_t^{\text{ex}})}{\lambda_{\max}(\mathbf{P})} \right\} \quad \text{by Lemma 1} \\ &\leq -1 + \frac{\beta}{\lambda_{\min}(\mathbf{P})} \quad \text{by Assumption 1} \\ &= 1 - \left(2 - \frac{\beta}{\lambda_{\min}(\mathbf{P})} \right). \end{aligned} \quad (\text{A.13})$$

The first and second lines use $-\lambda_{\min}(\mathbf{A}) = \lambda_{\max}(-\mathbf{A})$ and $\lambda_{\max}(-\mathbf{I}_k + \mathbf{A}) = -1 + \lambda_{\max}(\mathbf{A})$, respectively, for arbitrary matrix $\mathbf{A} \in \mathbb{R}^{k \times k}$. The inequality in the third line uses Lemma 1 in Appendix A.2 with $\mathbf{A} = -\mathbf{H}_t^{\text{ex}}$ and $\mathbf{B} = \mathbf{P}$. The inequality in the fourth line holds by Assumption 1 that says $\lambda_{\max}(-\mathbf{H}_t^{\text{ex}}) \leq \beta$. The final line, which holds trivially, is used below.

Third, combining (A.11) with bounds (A.12) and (A.13), we obtain

$$\left\| \frac{d\boldsymbol{\theta}_{t|t}^{\text{ex}}}{d\boldsymbol{\theta}'_{t|t-1}} \right\|_{\mathbf{P}} = \max \left\{ \lambda_{\max}(\mathbf{I}_k + \mathbf{P}^{-1/2}\mathbf{H}_t^{\text{ex}}\mathbf{P}^{-1/2}), -\lambda_{\min}(\mathbf{I}_k + \mathbf{P}^{-1/2}\mathbf{H}_t^{\text{ex}}\mathbf{P}^{-1/2}) \right\} \text{ by (A.11)}$$

$$\leq 1 - \min \left\{ \frac{\alpha^+}{\lambda_{\max}(\mathbf{P})} - \frac{\alpha^-}{\lambda_{\min}(\mathbf{P})}, 2 - \frac{\beta}{\lambda_{\min}(\mathbf{P})} \right\} \text{ by (A.12) and (A.13)} \quad (\text{A.14})$$

This concludes the proof. \square

A.4 Proof of Theorem 1

The proof of Theorem 1 makes use of Lemma 2 in the previous section.

Proof. Let $f_t^j : \Theta \rightarrow \Theta$ denote the update function at time t for $j \in \{\text{im}, \text{ex}\}$. For example, for the ISD update we have $\boldsymbol{\theta}_{t|t}^{\text{im}} = f_t^{\text{im}}(\boldsymbol{\theta}_{t|t-1}) = f^{\text{im}}(\boldsymbol{\theta}_{t|t-1} | \mathbf{y}_t, \mathbf{P}) = \operatorname{argmax}_{\boldsymbol{\theta} \in \Theta} \{\ell(\mathbf{y}_t | \boldsymbol{\theta}) - \frac{1}{2} \|\boldsymbol{\theta} - \boldsymbol{\theta}_{t|t-1}^{\text{im}}\|_{\mathbf{P}}^2\}$. Because the proof structure is not contingent on whether the update is explicit or implicit, we suppress the filter-type superscript in the proof below and use f_t and $\boldsymbol{\theta}_{t|t}$.

Next, let $g_t^{\mathbf{a}} : [0, 1] \rightarrow \mathbb{R}$ for some $\mathbf{a} \in \mathbb{R}^d$, where $g_t^{\mathbf{a}}(u) := \langle \mathbf{a}, f_t(u\boldsymbol{\theta}_{t|t-1} + (1-u)\tilde{\boldsymbol{\theta}}_{t|t-1}) \rangle$, $u \in [0, 1]$ and $\boldsymbol{\theta}_{t|t-1}, \tilde{\boldsymbol{\theta}}_{t|t-1} \in \Theta$ are two predictions. Note that by convexity of the parameter space Θ , we have $u\boldsymbol{\theta}_{t|t-1} + (1-u)\tilde{\boldsymbol{\theta}}_{t|t-1} \in \Theta, \forall u \in [0, 1]$, such that $g_t^{\mathbf{a}}$ is well defined.

For both the ISD and ESD update mappings, we have that the Jacobian of the update mapping f_t is well-defined if the Hessian of the log-likelihood exists, see again Lemma 2. In addition, if $f_t(\boldsymbol{\theta})$ is differentiable in $\boldsymbol{\theta}$ everywhere, then $g_t^{\mathbf{a}}(u)$ is differentiable in u everywhere. In sum, Assumption 1 implies $g_t^{\mathbf{a}}(u)$ is differentiable and hence continuous everywhere. Therefore, by the mean-value theorem, we have $\forall \mathbf{a} \in \mathbb{R}^d$ that $\exists u^* \in [0, 1]$ such that

$$\begin{aligned} \langle \mathbf{a}, \boldsymbol{\theta}_{t|t} - \tilde{\boldsymbol{\theta}}_{t|t-1} \rangle &= \langle \mathbf{a}, f_t(\boldsymbol{\theta}_{t|t-1}) - f_t(\tilde{\boldsymbol{\theta}}_{t|t-1}) \rangle \\ &= g_t^{\mathbf{a}}(1) - g_t^{\mathbf{a}}(0) \\ &= \frac{dg_t^{\mathbf{a}}(u)}{du} \Big|_{u=u^*} (1 - 0) \\ &= \langle \mathbf{a}, \mathcal{J}_{f_t}(\boldsymbol{\theta}_t^*) (\boldsymbol{\theta}_{t|t-1} - \tilde{\boldsymbol{\theta}}_{t|t-1}) \rangle, \end{aligned} \quad (\text{A.15})$$

where $\mathcal{J}_{f_t}(\boldsymbol{\theta}_t^*) := \frac{df_t}{d\boldsymbol{\theta}'} \Big|_{\boldsymbol{\theta}=\boldsymbol{\theta}_t^*}$ is the $k \times k$ Jacobian of the update function f_t evaluated at the midpoint $\boldsymbol{\theta}_t^* := u^* \boldsymbol{\theta}_{t|t-1} + (1 - u^*) \tilde{\boldsymbol{\theta}}_{t|t-1}$.

Next, we use our result with $\mathbf{a} = \mathbf{P}(\boldsymbol{\theta}_{t|t} - \tilde{\boldsymbol{\theta}}_{t|t})/\|\boldsymbol{\theta}_{t|t} - \tilde{\boldsymbol{\theta}}_{t|t}\|_{\mathbf{P}} \in \mathbb{R}^k$. This yields

$$\begin{aligned}
\|\boldsymbol{\theta}_{t|t} - \tilde{\boldsymbol{\theta}}_{t|t}\|_{\mathbf{P}} &= \langle \mathbf{P}(\boldsymbol{\theta}_{t|t} - \tilde{\boldsymbol{\theta}}_{t|t})/\|\boldsymbol{\theta}_{t|t} - \tilde{\boldsymbol{\theta}}_{t|t}\|_{\mathbf{P}}, \boldsymbol{\theta}_{t|t} - \tilde{\boldsymbol{\theta}}_{t|t} \rangle \\
&= \langle \mathbf{P}(\boldsymbol{\theta}_{t|t} - \tilde{\boldsymbol{\theta}}_{t|t})/\|\boldsymbol{\theta}_{t|t} - \tilde{\boldsymbol{\theta}}_{t|t}\|_{\mathbf{P}}, \mathcal{J}_{f_t}(\boldsymbol{\theta}_t^*)(\boldsymbol{\theta}_{t|t-1} - \tilde{\boldsymbol{\theta}}_{t|t-1}) \rangle \\
&= \|\boldsymbol{\theta}_{t|t} - \tilde{\boldsymbol{\theta}}_{t|t}\|_{\mathbf{P}}^{-1} \langle \mathbf{P}^{1/2}(\boldsymbol{\theta}_{t|t} - \tilde{\boldsymbol{\theta}}_{t|t}), \mathbf{P}^{1/2} \mathcal{J}_{f_t}(\boldsymbol{\theta}_t^*)(\boldsymbol{\theta}_{t|t-1} - \tilde{\boldsymbol{\theta}}_{t|t-1}) \rangle \\
&\leq \|\boldsymbol{\theta}_{t|t} - \tilde{\boldsymbol{\theta}}_{t|t}\|_{\mathbf{P}}^{-1} \|\boldsymbol{\theta}_{t|t} - \tilde{\boldsymbol{\theta}}_{t|t}\|_{\mathbf{P}} \|\mathcal{J}_{f_t}(\boldsymbol{\theta}_t^*)(\boldsymbol{\theta}_{t|t-1} - \tilde{\boldsymbol{\theta}}_{t|t-1})\|_{\mathbf{P}} \\
&\leq \|\mathcal{J}_{f_t}(\boldsymbol{\theta}_t^*)\|_{\mathbf{P}} \|\boldsymbol{\theta}_{t|t-1} - \tilde{\boldsymbol{\theta}}_{t|t-1}\|_{\mathbf{P}}, \tag{A.16}
\end{aligned}$$

where the second line uses the mean-value theorem (A.15) above, the fourth uses the Cauchy-Schwarz inequality and $\|\mathbf{P}^{1/2}\mathbf{x}\| = \|\mathbf{x}\|_{\mathbf{P}}, \forall \mathbf{x} \in \mathbb{R}^d$ and the final line uses the submultiplicative property (A.1) of the \mathbf{P} -weighted matrix norm.

Using the prediction step (3), we obtain

$$\begin{aligned}
\|\boldsymbol{\theta}_{t|t} - \tilde{\boldsymbol{\theta}}_{t|t}\|_{\mathbf{P}} &\leq \|\mathcal{J}_{f_t}(\boldsymbol{\theta}_t^*)\|_{\mathbf{P}} \|\boldsymbol{\theta}_{t|t-1} - \tilde{\boldsymbol{\theta}}_{t|t-1}\|_{\mathbf{P}} \\
&= \|\mathcal{J}_{f_t}(\boldsymbol{\theta}_t^*)\|_{\mathbf{P}} \|\boldsymbol{\Phi}(\boldsymbol{\theta}_{t-1|t-1} - \tilde{\boldsymbol{\theta}}_{t-1|t-1})\|_{\mathbf{P}} \\
&\leq \|\mathcal{J}_{f_t}(\boldsymbol{\theta}_t^*)\|_{\mathbf{P}} \|\boldsymbol{\Phi}\|_{\mathbf{P}} \|\boldsymbol{\theta}_{t-1|t-1} - \tilde{\boldsymbol{\theta}}_{t-1|t-1}\|_{\mathbf{P}}, \tag{A.17}
\end{aligned}$$

using again the submultiplicative property (A.1) of the \mathbf{P} -weighted norm. The result indicates that the update-to-update mapping at time t is contractive in the norm $\|\cdot\|_{\mathbf{P}}$ if $\|\mathcal{J}_{f_t}(\boldsymbol{\theta}_t^*)\|_{\mathbf{P}} \|\boldsymbol{\Phi}\|_{\mathbf{P}} < 1$.

In Lemma 2, we derived bounds for the ISD updates (A.9) and ESD updates (A.14).

Note that, with slight abuse of notation, we have $\mathcal{J}_{f_t^j}(\boldsymbol{\theta}_t^*) := \frac{df_t^j}{d\boldsymbol{\theta}'} \Big|_{\boldsymbol{\theta}=\boldsymbol{\theta}_t^*} = \frac{d\boldsymbol{\theta}_{t|t}^j}{d\boldsymbol{\theta}_{t|t-1}} \Big|_{\boldsymbol{\theta}_{t|t-1}=\boldsymbol{\theta}_t^*}$

for $j \in \{\text{im}, \text{ex}\}$. Substituting in these bounds into equation (A.17), we have

$$\|\boldsymbol{\theta}_{t|t}^j - \tilde{\boldsymbol{\theta}}_{t|t}^j\|_{\mathbf{P}} \leq \tau_j^{1/2} \|\boldsymbol{\theta}_{t-1|t-1}^j - \tilde{\boldsymbol{\theta}}_{t-1|t-1}^j\|_{\mathbf{P}}, \quad \text{where} \quad (\text{A.18})$$

$$\tau_{\text{im}}^{1/2} := \|\boldsymbol{\Phi}\|_{\mathbf{P}} \left(1 - \frac{\alpha^+}{\lambda_{\max}(\mathbf{P}) + \alpha^+} + \frac{\alpha^-}{\lambda_{\min}(\mathbf{P}) - \alpha^-} \right), \quad (\text{A.19})$$

$$\tau_{\text{ex}}^{1/2} := \|\boldsymbol{\Phi}\|_{\mathbf{P}} \left(1 - \min \left\{ \frac{\alpha^+}{\lambda_{\max}(\mathbf{P})} - \frac{\alpha^-}{\lambda_{\min}(\mathbf{P})}, 2 - \frac{\beta}{\lambda_{\min}(\mathbf{P})} \right\} \right), \quad (\text{A.20})$$

such that the ISD and ESD update-to-update mappings at time t are contractive if $\tau_{\text{im}}^{1/2} < 1$ and $\tau_{\text{ex}}^{1/2} < 1$, respectively. Because $\tau_{\text{im}}^{1/2}, \tau_{\text{ex}}^{1/2} \geq 0$ (see again the proofs of Lemma 2), we may equivalently state these conditions as $\tau^{\text{im}} < 1$ and $\tau^{\text{ex}} < 1$, which are exactly the sufficient conditions that are stated in Theorem 1

Since $\tau_{\text{im}}^{1/2}, \tau_{\text{ex}}^{1/2}, \|\cdot\| \geq 0$, squaring both sides of (A.18) and repeatedly applying it yields

$$\|\boldsymbol{\theta}_{t|t}^j - \tilde{\boldsymbol{\theta}}_{t|t}^j\|_{\mathbf{P}}^2 \leq (\tau_j)^t \|\boldsymbol{\theta}_{0|0} - \tilde{\boldsymbol{\theta}}_{0|0}\|_{\mathbf{P}}^2, \quad (\text{A.21})$$

where $\boldsymbol{\theta}_{0|0}^j, \tilde{\boldsymbol{\theta}}_{0|0}^j \in \boldsymbol{\Theta}$ are two starting points. Hence for each filter, Definition 1 is satisfied with $\mathbf{W} = \mathbf{P}$. Thus, under the (sufficient) condition $\tau^j < 1$, it follows that

$$\lim_{t \rightarrow \infty} \|\boldsymbol{\theta}_{t|t}^j - \tilde{\boldsymbol{\theta}}_{t|t}^j\|_{\mathbf{P}}^2 = 0. \quad (\text{A.22})$$

for any starting points $\boldsymbol{\theta}_{0|0}^j$ and $\tilde{\boldsymbol{\theta}}_{0|0}^j$ and any data sequence $\{\mathbf{y}_t\}$, and this convergence to zero is exponentially fast. Finally, we note that for any two positive-definite matrices $\mathbf{W}, \tilde{\mathbf{W}} \in \mathbb{R}^{k \times k}$, and for any $\mathbf{x} \in \mathbb{R}^k : \|\mathbf{x}\|_{\mathbf{W}}^2 = \mathbf{x}'\mathbf{W}\mathbf{x} = \mathbf{0}_k \Leftrightarrow \mathbf{x} = \mathbf{0}_k \Leftrightarrow \|\mathbf{x}\|_{\tilde{\mathbf{W}}}^2 = \mathbf{0}_k$ (norm equivalence), which also implies exponential convergence of the filtered paths in the Euclidean norm $\|\cdot\|$. \square

A.5 Proof of Theorem 2

The proof of Theorem 2 makes use of Lemma 2 in Appendix A.3.

Proof. Here, we derive the values of a, b, c, d given in Table 1 in terms of other quantities defined in Assumptions 1–2. Specifically, we derive a and b for the ISD and ESD updates, and c and d for the prediction step.

Preliminaries. Throughout this proof, we make use of two different expectation operators. First, we use the unconditional expectation $\mathbb{E}[\cdot]$, which acts on $\{\mathbf{y}_t\}$ using the true densities $\{p^0(\cdot | \boldsymbol{\vartheta}_t)\}$ and then on the true state path $\{\boldsymbol{\vartheta}_t\}$ using its joint density. Second, we use the conditional expectation operator that acts only on \mathbf{y}_t given a particular state $\boldsymbol{\vartheta}_t$. That is, $\mathbb{E}_{\mathbf{y}_t}[\cdot] := \int \cdot p^0(\mathbf{y} | \boldsymbol{\vartheta}_t) d\mathbf{y}$. By the tower property, it follows that $\mathbb{E}_{\mathbf{y}_t}[\mathbb{E}[\cdot]] = \mathbb{E}[\cdot]$.

Young's inequality. For both the ESD update and the prediction step, we make use of Young's inequality. Specifically, we use that for any $\mathbf{u}, \mathbf{v} \in \mathbb{R}^k$ and any positive definite $\mathbf{W} \in \mathbb{R}^{k \times k}$:

$$\begin{aligned}
\|\mathbf{u} + \mathbf{v}\|_{\mathbf{W}}^2 &= \|\mathbf{W}^{1/2}\mathbf{u} + \mathbf{W}^{1/2}\mathbf{v}\|^2 \\
&= \|\mathbf{W}^{1/2}\mathbf{u}\|^2 + \|\mathbf{W}^{1/2}\mathbf{v}\|^2 + 2\langle \mathbf{W}^{1/2}\mathbf{u}, \mathbf{W}^{1/2}\mathbf{v} \rangle \\
&\leq \|\mathbf{u}\|_{\mathbf{W}}^2 + \|\mathbf{v}\|_{\mathbf{W}}^2 + 2|\langle \mathbf{W}^{1/2}\mathbf{u}, \mathbf{W}^{1/2}\mathbf{v} \rangle| \\
&\leq \|\mathbf{u}\|_{\mathbf{W}}^2 + \|\mathbf{v}\|_{\mathbf{W}}^2 + 2\|\mathbf{W}^{1/2}\mathbf{u}\|\|\mathbf{W}^{1/2}\mathbf{v}\| \\
&\leq \|\mathbf{u}\|_{\mathbf{W}}^2 + \|\mathbf{v}\|_{\mathbf{W}}^2 + \epsilon^2\|\mathbf{W}^{1/2}\mathbf{u}\|^2 + (1/\epsilon^2)\|\mathbf{W}^{1/2}\mathbf{v}\|^2 \\
&= (1 + \epsilon^2)\|\mathbf{u}\|_{\mathbf{W}}^2 + (1 + 1/\epsilon^2)\|\mathbf{v}\|_{\mathbf{W}}^2,
\end{aligned} \tag{A.23}$$

for any $\epsilon > 0$, where in the fourth line we used the Cauchy-Schwarz inequality and in the fifth line Young's inequality for products (i.e., $2xy \leq \epsilon^2x^2 + 1/\epsilon^2y^2$ for all $x, y \geq 0, \epsilon > 0$).

Cauchy-Schwarz inequality. For the prediction step, we also use the Cauchy-Schwarz

inequality. For any $\mathbf{u}, \mathbf{v} \in \mathbb{R}^k$, we have

$$\begin{aligned}
\mathbb{E}[\|\mathbf{u} + \mathbf{v}\|^2] &= \mathbb{E}[\|\mathbf{u}\|^2 + \|\mathbf{v}\|^2 + 2\langle \mathbf{u}, \mathbf{v} \rangle] \\
&\leq \mathbb{E}[\|\mathbf{u}\|^2] + \mathbb{E}[\|\mathbf{v}\|^2] + 2\mathbb{E}[|\langle \mathbf{u}, \mathbf{v} \rangle|] \\
&\leq \mathbb{E}[\|\mathbf{u}\|^2] + \mathbb{E}[\|\mathbf{v}\|^2] + 2\mathbb{E}[\|\mathbf{u}\|\|\mathbf{v}\|] \\
&\leq \mathbb{E}[\|\mathbf{u}\|^2] + \mathbb{E}[\|\mathbf{v}\|^2] + 2\sqrt{\mathbb{E}[\|\mathbf{u}\|^2]\mathbb{E}[\|\mathbf{v}\|^2]} \\
&= \left(\sqrt{\mathbb{E}[\|\mathbf{u}\|^2]} + \sqrt{\mathbb{E}[\|\mathbf{v}\|^2]} \right)^2,
\end{aligned} \tag{A.24}$$

where the third line uses the Cauchy-Schwarz inequality and the penultimate line uses the Cauchy-Schwarz inequality for random variables: $|\mathbb{E}[XY]| \leq \sqrt{\mathbb{E}[X^2]\mathbb{E}[Y^2]}$ for scalar-valued random variables X, Y , which we use with $X = \|\mathbf{u}\|$ and $Y = \|\mathbf{v}\|$.

Analysis of ISD update step. The first-order condition of the ISD update for a static penalty matrix \mathbf{P} reads:

$$\boldsymbol{\theta}_{t|t} = \boldsymbol{\theta}_{t|t-1} + \mathbf{P}^{-1} \nabla \ell(\mathbf{y}_t \mid \boldsymbol{\theta}_{t|t}). \tag{A.25}$$

We move $\mathbf{P}^{-1} \nabla \ell(\mathbf{y}_t \mid \boldsymbol{\theta}_{t|t})$ to the left-hand side, pre-multiply both sides by the symmetric square root of the penalty matrix, denoted $\mathbf{P}^{\frac{1}{2}}$, and subtract $\mathbf{P}^{\frac{1}{2}} \boldsymbol{\theta}_t^* - \mathbf{P}^{-\frac{1}{2}} \nabla \ell(\mathbf{y}_t \mid \boldsymbol{\theta}_t^*)$ from both sides to obtain

$$\mathbf{P}^{\frac{1}{2}}(\boldsymbol{\theta}_{t|t} - \boldsymbol{\theta}_t^*) - \mathbf{P}^{-\frac{1}{2}}(\nabla \ell(\mathbf{y}_t \mid \boldsymbol{\theta}_{t|t}) - \nabla \ell(\mathbf{y}_t \mid \boldsymbol{\theta}_t^*)) = \mathbf{P}^{\frac{1}{2}}(\boldsymbol{\theta}_{t|t-1} - \boldsymbol{\theta}_t^*) + \mathbf{P}^{-\frac{1}{2}} \nabla \ell(\mathbf{y}_t \mid \boldsymbol{\theta}_t^*). \tag{A.26}$$

Using Riemann integrability of the Hessian of the log-likelihood function, we may write

$$\nabla \ell(\mathbf{y}_t \mid \boldsymbol{\theta}_{t|t}) - \nabla \ell(\mathbf{y}_t \mid \boldsymbol{\theta}_t^*) = \mathcal{H}_{t|t}^*(\boldsymbol{\theta}_{t|t} - \boldsymbol{\theta}_t^*), \tag{A.27}$$

where $\mathcal{H}_{t|t}^* := \int_0^1 \frac{\partial^2 \ell(\mathbf{y}_t \mid \boldsymbol{\theta})}{\partial \boldsymbol{\theta} \partial \boldsymbol{\theta}'} \Big|_{\boldsymbol{\theta} = u \boldsymbol{\theta}_{t|t} + (1-u) \boldsymbol{\theta}_t^*} du$ is the average Hessian between $\boldsymbol{\theta}_{t|t}$ and $\boldsymbol{\theta}_t^*$.

Substituting this result into equation (A.26) produces

$$(\mathbf{I}_k - \mathbf{P}^{-1/2} \mathcal{H}_{t|t}^* \mathbf{P}^{-1/2}) \mathbf{P}^{\frac{1}{2}} (\boldsymbol{\theta}_{t|t} - \boldsymbol{\theta}_t^*) = \mathbf{P}^{\frac{1}{2}} (\boldsymbol{\theta}_{t|t-1} - \boldsymbol{\theta}_t^*) + \mathbf{P}^{-\frac{1}{2}} \nabla \ell(\mathbf{y}_t \mid \boldsymbol{\theta}_t^*), \quad (\text{A.28})$$

where by Assumption 1, $\mathbf{P} \succ \mathcal{H}_{t|t}^* \Rightarrow \mathbf{I}_k \succ \mathbf{P}^{-1/2} \mathcal{H}_{t|t}^* \mathbf{P}^{-1/2} \Rightarrow \mathbf{I}_k - \mathbf{P}^{-1/2} \mathcal{H}_{t|t}^* \mathbf{P}^{-1/2} \succ \mathbf{O}_k$,

such that taking the inner product on both sides gives

$$\begin{aligned} & \|\mathbf{P}^{1/2} (\boldsymbol{\theta}_{t|t} - \boldsymbol{\theta}_t^*)\|_{(\mathbf{I}_k - \mathbf{P}^{-1/2} \mathcal{H}_{t|t}^* \mathbf{P}^{-1/2})^2}^2 \\ &= \|\boldsymbol{\theta}_{t|t-1} - \boldsymbol{\theta}_t^*\|_{\mathbf{P}}^2 + \|\nabla \ell(\mathbf{y}_t \mid \boldsymbol{\theta}_t^*)\|_{\mathbf{P}^{-1}}^2 + 2\langle \boldsymbol{\theta}_{t|t-1} - \boldsymbol{\theta}_t^*, \nabla \ell(\mathbf{y}_t \mid \boldsymbol{\theta}_t^*) \rangle. \end{aligned} \quad (\text{A.29})$$

Next, we take the unconditional expectation on both sides and use that $\mathbb{E}[\|\nabla \ell(\mathbf{y}_t \mid \boldsymbol{\theta}_t^*)\|_{\mathbf{P}^{-1}}^2] \leq \lambda_{\max}(\mathbf{P}^{-1}) \mathbb{E}[\|\nabla \ell(\mathbf{y}_t \mid \boldsymbol{\theta}_t^*)\|_{\mathbf{P}^{-1}}^2] \leq \sigma^2 / \lambda_{\min}(\mathbf{P})$ by Assumption 2(b) and that $\mathbb{E}[\langle \boldsymbol{\theta}_{t|t-1} - \boldsymbol{\theta}_t^*, \nabla \ell(\mathbf{y}_t \mid \boldsymbol{\theta}_t^*) \rangle] = \mathbb{E}[\mathbb{E}_{\mathbf{y}_t}[\langle \boldsymbol{\theta}_{t|t-1} - \boldsymbol{\theta}_t^*, \nabla \ell(\mathbf{y}_t \mid \boldsymbol{\theta}_t^*) \rangle]] = \mathbb{E}[\langle \boldsymbol{\theta}_{t|t-1} - \boldsymbol{\theta}_t^*, \mathbb{E}_{\mathbf{y}_t}[\nabla \ell(\mathbf{y}_t \mid \boldsymbol{\theta}_t^*)] \rangle] = 0$ by the tower property and the fact that $\mathbb{E}_{\mathbf{y}_t}[\nabla \ell(\mathbf{y}_t \mid \boldsymbol{\theta}_t^*)] = 0$ because the pseudo-true parameter uniquely maximizes the expected log likelihood (see Definition 2). This produces

$$\mathbb{E}[\|\mathbf{P}^{1/2} (\boldsymbol{\theta}_{t|t} - \boldsymbol{\theta}_t^*)\|_{(\mathbf{I}_k - \mathbf{P}^{-1/2} \mathcal{H}_{t|t}^* \mathbf{P}^{-1/2})^2}^2] \leq \mathbb{E}[\|\boldsymbol{\theta}_{t|t-1} - \boldsymbol{\theta}_t^*\|_{\mathbf{P}}^2] + \sigma^2 / \lambda_{\min}(\mathbf{P}). \quad (\text{A.30})$$

For the left-hand side, we may use the following lower bound

$$\lambda_{\min}((\mathbf{I}_k - \mathbf{P}^{-1/2} \mathcal{H}_{t|t}^* \mathbf{P}^{-1/2})^2) \|\boldsymbol{\theta}_{t|t} - \boldsymbol{\theta}_t^*\|_{\mathbf{P}}^2 \leq \|\mathbf{P}^{1/2} (\boldsymbol{\theta}_{t|t} - \boldsymbol{\theta}_t^*)\|_{(\mathbf{I}_k - \mathbf{P}^{-1/2} \mathcal{H}_{t|t}^* \mathbf{P}^{-1/2})^2}^2, \quad (\text{A.31})$$

as $\mathbf{I}_k - \mathbf{P}^{-1/2} \mathcal{H}_{t|t}^* \mathbf{P}^{-1/2} \succ \mathbf{O}_k$, it follows that $\lambda_{\min}((\mathbf{I}_k - \mathbf{P}^{-1/2} \mathcal{H}_{t|t}^* \mathbf{P}^{-1/2})^2) = \lambda_{\min}(\mathbf{I}_k - \mathbf{P}^{-1/2} \mathcal{H}_{t|t}^* \mathbf{P}^{-1/2})^2 > 0$. Using the lower bound in (A.30) and dividing both sides by $\lambda_{\min}(\mathbf{I}_k - \mathbf{P}^{-1/2} \mathcal{H}_{t|t}^* \mathbf{P}^{-1/2})^2$ gives

$$\mathbb{E}[\|\boldsymbol{\theta}_{t|t} - \boldsymbol{\theta}_t^*\|_{\mathbf{P}}^2] \leq \lambda_{\min}(\mathbf{I}_k - \mathbf{P}^{-1/2} \mathcal{H}_{t|t}^* \mathbf{P}^{-1/2})^{-2} (\mathbb{E}[\|\boldsymbol{\theta}_{t|t-1} - \boldsymbol{\theta}_t^*\|_{\mathbf{P}}^2] + \sigma^2 / \lambda_{\min}(\mathbf{P})). \quad (\text{A.32})$$

Using the same methodology as in the proof of Lemma 2, equation (A.9), we may obtain:

$$\lambda_{\min}(\mathbf{I}_k - \mathbf{P}^{-1/2} \mathcal{H}_{t|t}^* \mathbf{P}^{-1/2})^{-1} \leq 1 - \frac{\alpha^+}{\lambda_{\max}(\mathbf{P}) + \alpha^+} + \frac{\alpha^-}{\lambda_{\min}(\mathbf{P}) - \alpha^-}. \quad (\text{A.33})$$

As both sides are nonnegative, we may square both sides. Using the definition of the \mathbf{P} -weighted MSE produces the final result:

$$\text{MSE}_{t|t}^{\mathbf{P}} \leq a \text{MSE}_{t|t-1}^{\mathbf{P}} + b, \quad (\text{A.34})$$

where $a = \left(1 - \frac{\alpha^+}{\lambda_{\max}(\mathbf{P}) + \alpha^+} + \frac{\alpha^-}{\lambda_{\min}(\mathbf{P}) - \alpha^-}\right)^2$ and $b = a\sigma^2/\lambda_{\min}(\mathbf{P})$, which confirms the expressions for the ISD filter in Table 1

Analysis of ESD update step. The ESD update reads:

$$\boldsymbol{\theta}_{t|t} = \boldsymbol{\theta}_{t|t-1} + \mathbf{P}^{-1} \nabla \ell(\mathbf{y}_t \mid \boldsymbol{\theta}_{t|t-1}), \quad (\text{A.35})$$

where pre-multiplying both sides with $\mathbf{P}^{1/2}$ and subtracting $\mathbf{P}^{1/2} \boldsymbol{\theta}_t^*$ on both sides yields

$$\mathbf{P}^{1/2}(\boldsymbol{\theta}_{t|t} - \boldsymbol{\theta}_t^*) = \mathbf{P}^{1/2}(\boldsymbol{\theta}_{t|t-1} - \boldsymbol{\theta}_t^*) + \mathbf{P}^{-1/2} \nabla \ell(\mathbf{y}_t \mid \boldsymbol{\theta}_{t|t-1}). \quad (\text{A.36})$$

Computing the squared norm on both sides and taking an unconditional expectation yields

$$\begin{aligned} & \mathbb{E}[\|\boldsymbol{\theta}_{t|t} - \boldsymbol{\theta}_t^*\|_{\mathbf{P}}^2] \\ &= \mathbb{E}[\|\boldsymbol{\theta}_{t|t} - \boldsymbol{\theta}_t^*\|_{\mathbf{P}}^2] + 2\mathbb{E}[\langle \nabla \ell(\mathbf{y}_t \mid \boldsymbol{\theta}_{t|t-1}), \boldsymbol{\theta}_{t|t-1} - \boldsymbol{\theta}_t^* \rangle] + \mathbb{E}[\|\nabla \ell(\mathbf{y}_t \mid \boldsymbol{\theta}_{t|t-1})\|_{\mathbf{P}^{-1}}^2]. \end{aligned} \quad (\text{A.37})$$

For the second term on the right-hand side of (A.37), we may write

$$2\mathbb{E}[\langle \nabla \ell(\mathbf{y}_t \mid \boldsymbol{\theta}_{t|t-1}), \boldsymbol{\theta}_{t|t-1} - \boldsymbol{\theta}_t^* \rangle] = 2\mathbb{E}_{\mathbf{y}_t}[\mathbb{E}[\langle \nabla \ell(\mathbf{y}_t \mid \boldsymbol{\theta}_{t|t-1}), \boldsymbol{\theta}_{t|t-1} - \boldsymbol{\theta}_t^* \rangle]]$$

$$\begin{aligned}
&= 2\mathbb{E}[\langle \mathbb{E}[\nabla \ell(\mathbf{y}_t \mid \boldsymbol{\theta}_{t|t-1}) - \nabla \ell(\mathbf{y}_t \mid \boldsymbol{\theta}_t^*)], \boldsymbol{\theta}_{t|t-1} - \boldsymbol{\theta}_t^* \rangle] \\
&= 2\mathbb{E}[\mathbb{E}[\langle \nabla \ell(\mathbf{y}_t \mid \boldsymbol{\theta}_{t|t-1}) - \nabla \ell(\mathbf{y}_t \mid \boldsymbol{\theta}_t^*), \boldsymbol{\theta}_{t|t-1} - \boldsymbol{\theta}_t^* \rangle]] \\
&= 2\mathbb{E}[\langle \mathcal{H}_{t|t-1}^*(\boldsymbol{\theta}_{t|t-1} - \boldsymbol{\theta}_t^*), \boldsymbol{\theta}_{t|t-1} - \boldsymbol{\theta}_t^* \rangle] \\
&= \mathbb{E}[\|\boldsymbol{\theta}_{t|t-1} - \boldsymbol{\theta}_t^*\|_{2\mathcal{H}_{t|t-1}^*}^2], \tag{A.38}
\end{aligned}$$

where the first and fourth line use the tower property, the second that $\mathbb{E}_{\mathbf{y}_t}[\nabla \ell(\mathbf{y}_t \mid \boldsymbol{\theta}_t^*)] = 0$ by Assumption 2(b) and the fourth that

$$\nabla \ell(\mathbf{y}_t \mid \boldsymbol{\theta}_{t|t-1}) - \nabla \ell(\mathbf{y}_t \mid \boldsymbol{\theta}_t^*) = \mathcal{H}_{t|t-1}^*(\boldsymbol{\theta}_{t|t-1} - \boldsymbol{\theta}_t^*), \tag{A.39}$$

where $\mathcal{H}_{t|t-1}^* := \int_0^1 \frac{\partial^2 \ell(\mathbf{y}_t \mid \boldsymbol{\theta})}{\partial \boldsymbol{\theta} \partial \boldsymbol{\theta}'} \Big|_{\boldsymbol{\theta} = u \boldsymbol{\theta}_{t|t-1} + (1-u) \boldsymbol{\theta}_t^*} du$ is the average Hessian between $\boldsymbol{\theta}_{t|t-1}$ and $\boldsymbol{\theta}_t^*$. Equation (A.38) technically contains an abuse of notation as the Hessian matrix typically is not positive definite; below, however, this term will be combined with others, resulting in a proper norm.

For the final term on the right-hand side of (A.37), we have that

$$\begin{aligned}
&\mathbb{E}[\|\nabla \ell(\mathbf{y}_t \mid \boldsymbol{\theta}_{t|t-1})\|_{\mathbf{P}^{-1}}^2] = \mathbb{E}[\|\nabla \ell(\mathbf{y}_t \mid \boldsymbol{\theta}_{t|t-1}) - \nabla \ell(\mathbf{y}_t \mid \boldsymbol{\theta}_t^*) + \nabla \ell(\mathbf{y}_t \mid \boldsymbol{\theta}_t^*)\|_{\mathbf{P}^{-1}}^2] \\
&\leq \mathbb{E}[(1 + \chi^2)\|\nabla \ell(\mathbf{y}_t \mid \boldsymbol{\theta}_{t|t-1}) - \nabla \ell(\mathbf{y}_t \mid \boldsymbol{\theta}_t^*)\|_{\mathbf{P}^{-1}}^2 + (1 + 1/\chi^2)\|\nabla \ell(\mathbf{y}_t \mid \boldsymbol{\theta}_t^*)\|_{\mathbf{P}^{-1}}^2] \\
&= (1 + \chi^2)\mathbb{E}[\|\mathcal{H}_{t|t-1}^*(\boldsymbol{\theta}_{t|t-1} - \boldsymbol{\theta}_t^*)\|_{\mathbf{P}^{-1}}^2] + (1 + 1/\chi^2)\mathbb{E}[\|\nabla \ell(\mathbf{y}_t \mid \boldsymbol{\theta}_t^*)\|_{\mathbf{P}^{-1}}^2] \\
&\leq (1 + \chi^2)\mathbb{E}[\|\boldsymbol{\theta}_{t|t-1} - \boldsymbol{\theta}_t^*\|_{\mathcal{H}_{t|t-1}^* \mathbf{P}^{-1} \mathcal{H}_{t|t-1}^*}^2] + (1 + 1/\chi^2)\sigma^2/\lambda_{\min}(\mathbf{P}), \tag{A.40}
\end{aligned}$$

where the second line uses Young's inequality as specified in (A.23) with $\epsilon = \chi$, $\mathbf{u} = \nabla \ell(\mathbf{y}_t \mid \boldsymbol{\theta}_{t|t-1}) - \nabla \ell(\mathbf{y}_t \mid \boldsymbol{\theta}_t^*)$, $\mathbf{v} = \nabla \ell(\mathbf{y}_t \mid \boldsymbol{\theta}_t^*)$ and $\mathbf{W} = \mathbf{P}^{-1}$, the third uses the definition of $\mathcal{H}_{t|t-1}^*$ and the fourth that $\mathbb{E}[\|\nabla \ell(\mathbf{y}_t \mid \boldsymbol{\theta}_t^*)\|_{\mathbf{P}^{-1}}^2] \leq \sigma^2/\lambda_{\min}(\mathbf{P})$ by Assumption 2(b).

Substituting (A.38) and (A.40) into equation (A.37), we obtain

$$\begin{aligned}
& \mathbb{E}[\|\boldsymbol{\theta}_{t|t} - \boldsymbol{\theta}_t^*\|_{\mathbf{P}}^2] \\
& \leq \mathbb{E}[\|\boldsymbol{\theta}_{t|t} - \boldsymbol{\theta}_t^*\|_{\mathbf{P}}^2] + \mathbb{E}[\|\boldsymbol{\theta}_{t|t} - \boldsymbol{\theta}_t^*\|_{2\mathbf{H}_{t|t-1}^*}^2] + (1 + \chi^2)\mathbb{E}\left[\|\boldsymbol{\theta}_{t|t-1} - \boldsymbol{\theta}_t^*\|_{\mathbf{H}_{t|t-1}^* \mathbf{P}^{-1} \mathbf{H}_{t|t-1}^*}^2\right] \\
& \quad + \frac{(1 + 1/\chi^2)\sigma^2}{\lambda_{\min}(\mathbf{P})} \\
& = \mathbb{E}[\|\boldsymbol{\theta}_{t|t} - \boldsymbol{\theta}_t^*\|_{\mathbf{P} + 2\mathbf{H}_{t|t-1}^* + (1 + \chi^2)\mathbf{H}_{t|t-1}^* \mathbf{P}^{-1} \mathbf{H}_{t|t-1}^*}^2] + \frac{(1 + 1/\chi^2)\sigma^2}{\lambda_{\min}(\mathbf{P})} \\
& = \mathbb{E}[\|\mathbf{P}^{1/2}(\boldsymbol{\theta}_{t|t} - \boldsymbol{\theta}_t^*)\|_{(\mathbf{I}_k + \mathbf{P}^{-1/2}\mathbf{H}_{t|t-1}^* \mathbf{P}^{-1/2})^2}^2 + \frac{(1 + 1/\chi^2)\sigma^2}{\lambda_{\min}(\mathbf{P})} \\
& \quad + \chi^2\mathbb{E}[\|\mathbf{P}^{1/2}(\boldsymbol{\theta}_{t|t} - \boldsymbol{\theta}_t^*)\|_{\mathbf{P}^{-1/2}\mathbf{H}_{t|t-1}^* \mathbf{P}^{-1} \mathbf{H}_{t|t-1}^* \mathbf{P}^{-1/2}}^2. \tag{A.41}
\end{aligned}$$

Using the eigenvalue bounds for $\mathbf{I}_k + \mathbf{P}^{-1/2}\mathbf{H}_t^{\text{ex}}\mathbf{P}^{-1/2}$ in inequality (A.14) from Lemma 2, we may square both sides as they are both nonnegative, to obtain

$$\lambda_{\max}(\mathbf{I}_k + \mathbf{P}^{-1/2}\mathbf{H}_{t|t-1}^* \mathbf{P}^{-1/2})^2 \leq \left(1 - \min\left\{\frac{\alpha^+}{\lambda_{\max}(\mathbf{P})} - \frac{\alpha^-}{\lambda_{\min}(\mathbf{P})}, 2 - \frac{\beta}{\lambda_{\min}(\mathbf{P})}\right\}\right)^2. \tag{A.42}$$

Using again inequality (A.14) in Lemma 2, we also have

$$\begin{aligned}
\lambda_{\max}(\mathbf{P}^{-1/2}\mathbf{H}_{t|t-1}^* \mathbf{P}^{-1} \mathbf{H}_{t|t-1}^* \mathbf{P}^{-1/2}) & = \lambda_{\max}((\mathbf{P}^{-1/2}\mathbf{H}_{t|t-1}^* \mathbf{P}^{-1/2})^2) \\
& = \max\{\lambda_{\max}(\mathbf{P}^{-1/2}\mathbf{H}_{t|t-1}^* \mathbf{P}^{-1/2}), -\lambda_{\min}(\mathbf{P}^{-1/2}\mathbf{H}_{t|t-1}^* \mathbf{P}^{-1/2})\}^2 \\
& = \max\{\lambda_{\max}(\mathbf{I}_k + \mathbf{P}^{-1/2}\mathbf{H}_{t|t-1}^* \mathbf{P}^{-1/2}) - 1, 1 - \lambda_{\min}(\mathbf{I}_k + \mathbf{P}^{-1/2}\mathbf{H}_{t|t-1}^* \mathbf{P}^{-1/2})\}^2 \\
& \leq \max\left\{\max\left\{\frac{\lambda_{\max}(\mathbf{P}) - \alpha}{\lambda_{\max}(\mathbf{P})}, \frac{\lambda_{\min}(\mathbf{P}) - \alpha}{\lambda_{\min}(\mathbf{P})}\right\} - 1, 1 + \frac{\beta - \lambda_{\min}(\mathbf{P})}{\lambda_{\min}(\mathbf{P})}\right\}^2 \\
& \leq \max\left\{\frac{-\alpha}{\lambda_{\max}(\mathbf{P})}, \frac{-\alpha}{\lambda_{\min}(\mathbf{P})}, \frac{\beta}{\lambda_{\min}(\mathbf{P})}\right\}^2 \\
& \leq \max\left\{\frac{\alpha^-}{\lambda_{\min}(\mathbf{P})}, \frac{\beta}{\lambda_{\min}(\mathbf{P})}\right\}^2 = \frac{L^2}{\lambda_{\min}(\mathbf{P})^2}, \tag{A.43}
\end{aligned}$$

using $\beta > 0$, $\alpha^-/\lambda_{\min}(\mathbf{P}) \geq \alpha^-/\lambda_{\max}(\mathbf{P})$, and $L := \max\{\alpha^-, \beta\}$. In the penultimate line, $-\alpha/\lambda_{\max}(\mathbf{P})$ cannot be the largest of the three numbers, so that it can be dropped.

Combining these results, we obtain the final result:

$$\text{MSE}_{t|t}^{\mathbf{P}} \leq a \text{MSE}_{t|t-1}^{\mathbf{P}} + b, \quad (\text{A.44})$$

where $a = \left(1 - \min\left\{\frac{\alpha^+}{\lambda_{\max}(\mathbf{P})} - \frac{\alpha^-}{\lambda_{\min}(\mathbf{P})}, 2 - \frac{\beta}{\lambda_{\min}(\mathbf{P})}\right\}\right)^2 + \frac{\chi^2 L^2}{\lambda_{\min}(\mathbf{P})^2}$ and $b = \frac{(1+1/\chi^2)\sigma^2}{\lambda_{\min}(\mathbf{P})}$, which confirms the expressions for the ESD filter in Table 1.

Analysis of the prediction step. We start by subtracting the pseudo-true state $\boldsymbol{\theta}_t^*$ from the prediction step in equation (3), multiplying by $\mathbf{P}^{1/2}$ and taking the squared norm:

$$\begin{aligned} \|\boldsymbol{\theta}_{t+1|t} - \boldsymbol{\theta}_{t+1}^*\|_{\mathbf{P}}^2 &= \|(\mathbf{I}_k - \boldsymbol{\Phi})\boldsymbol{\omega} + \boldsymbol{\Phi}\boldsymbol{\theta}_{t|t} - \boldsymbol{\theta}_{t+1}^*\|_{\mathbf{P}}^2 \\ &= \|\boldsymbol{\Phi}(\boldsymbol{\theta}_{t|t} - \boldsymbol{\theta}_t^*) + (\boldsymbol{\Phi} - \mathbf{I}_k)(\boldsymbol{\theta}_t^* - \boldsymbol{\omega}) + (\boldsymbol{\theta}_t^* - \boldsymbol{\theta}_{t+1}^*)\|_{\mathbf{P}}^2 \\ &\leq (1 + \epsilon^2) \|\boldsymbol{\Phi}(\boldsymbol{\theta}_{t|t} - \boldsymbol{\theta}_t^*)\|_{\mathbf{P}}^2 \\ &\quad + \left(1 + \frac{1}{\epsilon^2}\right) \|(\boldsymbol{\Phi} - \mathbf{I}_k)(\boldsymbol{\theta}_t^* - \boldsymbol{\omega}) + (\boldsymbol{\theta}_t^* - \boldsymbol{\theta}_{t+1}^*)\|_{\mathbf{P}}^2, \end{aligned} \quad (\text{A.45})$$

where in the second line we added and subtracted $(\boldsymbol{\Phi} - \mathbf{I}_k)\boldsymbol{\theta}_t^*$ and the third line uses Young's inequality as specified in (A.23) with $\mathbf{u} = \boldsymbol{\Phi}(\boldsymbol{\theta}_{t|t} - \boldsymbol{\theta}_t^*)$, $\mathbf{v} = (\boldsymbol{\Phi} - \mathbf{I}_k)(\boldsymbol{\theta}_t^* - \boldsymbol{\omega}) + (\boldsymbol{\theta}_t^* - \boldsymbol{\theta}_{t+1}^*)$ and $\mathbf{W} = \mathbf{P}$. Using the submultiplicative property (A.1) of the \mathbf{P} -weighted matrix norm and taking the unconditional expectation of (A.45) yields

$$\text{MSE}_{t+1|t}^{\mathbf{P}} \leq (1 + \epsilon^2) \|\boldsymbol{\Phi}\|_{\mathbf{P}}^2 \text{MSE}_{t|t}^{\mathbf{P}} + \left(1 + \frac{1}{\epsilon^2}\right) \mathbb{E}[\|(\boldsymbol{\Phi} - \mathbf{I}_k)(\boldsymbol{\theta}_t^* - \boldsymbol{\omega}) + (\boldsymbol{\theta}_t^* - \boldsymbol{\theta}_{t+1}^*)\|_{\mathbf{P}}^2], \quad (\text{A.46})$$

where $\|\boldsymbol{\Phi}\|_{\mathbf{P}}^2$ is the squared matrix norm of $\boldsymbol{\Phi}$ induced by the vector norm $\|\tilde{\mathbf{u}}\|_{\mathbf{P}}^2$ for $\tilde{\mathbf{u}} \in \mathbb{R}^k$.

Using preliminary result (A.24) with $\mathbf{u} = (\boldsymbol{\Phi} - \mathbf{I}_k)(\boldsymbol{\theta}_t^* - \boldsymbol{\omega})$ and $\mathbf{v} = \boldsymbol{\theta}_t^* - \boldsymbol{\theta}_{t+1}^*$, we obtain

$$\begin{aligned} &\mathbb{E}[\|(\boldsymbol{\Phi} - \mathbf{I}_k)(\boldsymbol{\theta}_t^* - \boldsymbol{\omega}) + (\boldsymbol{\theta}_t^* - \boldsymbol{\theta}_{t+1}^*)\|_{\mathbf{P}}^2] \\ &\leq \lambda_{\max}(\mathbf{P}) \left(\sqrt{\mathbb{E}[\|(\boldsymbol{\Phi} - \mathbf{I}_k)(\boldsymbol{\theta}_t^* - \boldsymbol{\omega})\|^2]} + \sqrt{\mathbb{E}[\|\boldsymbol{\theta}_t^* - \boldsymbol{\theta}_{t+1}^*\|^2]} \right)^2 \end{aligned}$$

$$\begin{aligned}
&\leq \lambda_{\max}(\mathbf{P}) \left(\sqrt{\mathbb{E}[\|\Phi - \mathbf{I}_k\|^2 \|\boldsymbol{\theta}_t^* - \boldsymbol{\omega}\|^2]} + \sqrt{\mathbb{E}[\|\boldsymbol{\theta}_{t+1}^* - \boldsymbol{\theta}_t^*\|^2]} \right)^2 \\
&= \lambda_{\max}(\mathbf{P}) \left(\|\mathbf{I}_k - \Phi\| \sqrt{\mathbb{E}[\|\boldsymbol{\theta}_t^* - \boldsymbol{\omega}\|^2]} + \sqrt{\mathbb{E}[\|\boldsymbol{\theta}_{t+1}^* - \boldsymbol{\theta}_t^*\|^2]} \right)^2 \\
&\leq \lambda_{\max}(\mathbf{P}) (\|\mathbf{I}_k - \Phi\| s_\omega + q)^2,
\end{aligned} \tag{A.47}$$

where the third lines uses that the definition of induced matrix norm and the final line that

$$s_\omega^2 := \mathbb{E}[\|\boldsymbol{\theta}_t^* - \boldsymbol{\omega}\|^2] \text{ and } \mathbb{E}[\|\boldsymbol{\theta}_{t+1}^* - \boldsymbol{\theta}_t^*\|^2] = \mathbb{E}[\text{tr}((\boldsymbol{\theta}_{t+1}^* - \boldsymbol{\theta}_t^*)(\boldsymbol{\theta}_{t+1}^* - \boldsymbol{\theta}_t^*)')] = \text{tr}(\mathbb{E}[(\boldsymbol{\theta}_{t+1}^* - \boldsymbol{\theta}_t^*)(\boldsymbol{\theta}_{t+1}^* - \boldsymbol{\theta}_t^*)']) \leq \text{tr}(\mathbf{Q}) =: q^2 < \infty.$$

Combining inequalities (A.47) and (A.46) yields the final result

$$\text{MSE}_{t+1|t}^{\mathbf{P}} \leq c \text{MSE}_{t|t}^{\mathbf{P}} + d, \tag{A.48}$$

where $c = (1 + \epsilon^2) \|\Phi\|_{\mathbf{P}}^2$ and $d = (1 + \frac{1}{\epsilon^2}) \lambda_{\max}(\mathbf{P}) (\|\mathbf{I}_k - \Phi\| s_\omega + q)^2$, which confirms the expressions for the prediction step in Table 1. \square

A.6 Proof of Proposition 1

Proof. If, in addition to Assumptions 1 and 2(a,b), Assumption 3 holds, then

$$\begin{aligned}
\text{MSE}_{t+1|t}^{\mathbf{P}} &= \mathbb{E}[\|\boldsymbol{\theta}_{t+1|t} - \boldsymbol{\vartheta}_{t+1}\|_{\mathbf{P}}^2] \\
&= \mathbb{E}[\|(\mathbf{I}_k - \Phi)\boldsymbol{\omega} + \Phi\boldsymbol{\theta}_{t|t} - (\mathbf{I}_k - \Phi_0)\boldsymbol{\omega}_0 - \Phi_0\boldsymbol{\vartheta}_t - \boldsymbol{\xi}_{t+1}\|_{\mathbf{P}}^2] \\
&= \mathbb{E}[\|\Phi_0(\boldsymbol{\theta}_{t|t} - \boldsymbol{\vartheta}_t) - \boldsymbol{\xi}_{t+1}\|_{\mathbf{P}}^2] \\
&= \mathbb{E}[\|\Phi_0(\boldsymbol{\theta}_{t|t} - \boldsymbol{\vartheta}_t)\|_{\mathbf{P}}^2] + \mathbb{E}[\|\boldsymbol{\xi}_{t+1}\|_{\mathbf{P}}^2] - 2\mathbb{E}[\langle \mathbf{P}\Phi_0(\boldsymbol{\theta}_{t|t} - \boldsymbol{\vartheta}_t), \boldsymbol{\xi}_{t+1} \rangle] \\
&= \mathbb{E}[\|\Phi_0(\boldsymbol{\theta}_{t|t} - \boldsymbol{\vartheta}_t)\|_{\mathbf{P}}^2] + \mathbb{E}[\|\boldsymbol{\xi}_{t+1}\|_{\mathbf{P}}^2] \\
&\leq \|\Phi_0\|_{\mathbf{P}}^2 \mathbb{E}[\|\boldsymbol{\theta}_{t|t} - \boldsymbol{\vartheta}_t\|_{\mathbf{P}}^2] + \lambda_{\max}(\mathbf{P}) \mathbb{E}[\|\boldsymbol{\xi}_{t+1}\|^2] \\
&\leq \|\Phi_0\|_{\mathbf{P}}^2 \text{MSE}_{t|t}^{\mathbf{P}} + \lambda_{\max}(\mathbf{P}) \sigma_\xi^2,
\end{aligned} \tag{A.49}$$

where the third line uses that $\boldsymbol{\omega} = \boldsymbol{\omega}_0$ and $\boldsymbol{\Phi} = \boldsymbol{\Phi}_0$, the fifth that $\boldsymbol{\xi}_{t+1}$ is independent of $\boldsymbol{\Phi}_0(\boldsymbol{\theta}_{t|t} - \boldsymbol{\vartheta}_t)$ and with $\mathbb{E}[\boldsymbol{\xi}_{t+1}] = \mathbf{0}_k$, while the sixth line uses the submultiplicative property (A.1) of the \mathbf{P} -weighted matrix norm. The last line uses that $\mathbb{E}[\|\boldsymbol{\xi}_{t+1}\|^2] = \mathbb{E}[\text{tr}(\boldsymbol{\xi}_{t+1}\boldsymbol{\xi}'_{t+1})] = \text{tr}(\mathbb{E}[\boldsymbol{\xi}_{t+1}\boldsymbol{\xi}'_{t+1}]) = \text{tr}(\boldsymbol{\Sigma}_\xi) = \sigma_\xi^2 < \infty$. We conclude that $c = \|\boldsymbol{\Phi}_0\|_{\mathbf{P}}^2$ and $d = \lambda_{\max}(\mathbf{P})\sigma_\xi^2$. \square

B Further theoretical results

B.1 Kalman filter as ISD and ESD update

Although the ISD and ESD filters generally produce different outcomes, they yield identical results (albeit with different learning rates) in the case of a Gaussian observation density where the mean is a linear transformation of the parameter being tracked.

Example 1 (Kalman's (1960) level update as both ISD and ESD). *Consider the observation $\mathbf{y}_t = \mathbf{d} + \mathbf{Z}\boldsymbol{\vartheta}_t + \boldsymbol{\varepsilon}_t$, where $\mathbf{y}_t, \mathbf{d} \in \mathbb{R}^n$, $\mathbf{Z} \in \mathbb{R}^{n \times k}$, $\boldsymbol{\vartheta}_t \in \mathbb{R}^k$, and $\boldsymbol{\varepsilon}_t \sim \text{i.i.d. } \mathcal{N}(\mathbf{0}_n, \boldsymbol{\Sigma}_\varepsilon)$ with $\boldsymbol{\Sigma}_\varepsilon \succ \mathbf{O}_n$. Consider Kalman's predicted and updated covariance matrices $\mathbf{P}_{t|t-1}^{\text{KF}}, \mathbf{P}_{t|t}^{\text{KF}} \succ \mathbf{O}_k$, which are both \mathcal{F}_{t-1} measurable. Assume the postulated density $p(\cdot|\cdot)$ matches the true density $p^0(\cdot|\cdot)$. Then, Kalman's level update can be interpreted as (i) an ISD update as in equation (1), with the learning-rate matrix $\mathbf{H}_t^{\text{im}} = \mathbf{P}_{t|t-1}^{\text{KF}}$; and (ii) an ESD update as in equation (2), with $\mathbf{H}_t^{\text{ex}} = \mathbf{P}_{t|t}^{\text{KF}}$. Note that the implicit learning rate exceeds the explicit one, in that $\mathbf{H}_t^{\text{im}} \succeq \mathbf{H}_t^{\text{ex}}$, since $\mathbf{P}_{t|t-1}^{\text{KF}} \succeq \mathbf{P}_{t|t}^{\text{KF}}$. This dual interpretation suggests that generalizations of the Kalman filter may be constructed from either its ISD or ESD representation, as in Lange (2024a) and Ollivier (2018), respectively.*

Proof. **Linear Gaussian observation equation.** Observations $\mathbf{y}_t \in \mathbb{R}^n$ are generated by

$$\mathbf{y}_t = \mathbf{d} + \mathbf{Z}\boldsymbol{\vartheta}_t + \boldsymbol{\varepsilon}_t, \quad \boldsymbol{\varepsilon}_t \sim \text{i.i.d. } \mathcal{N}(\mathbf{0}_n, \boldsymbol{\Sigma}_\varepsilon), \quad (\text{B.1})$$

where $\mathbf{d}, \boldsymbol{\varepsilon}_t \in \mathbb{R}^n$, $\mathbf{Z} \in \mathbb{R}^{n \times k}$, $\boldsymbol{\vartheta}_t \in \mathbb{R}^k$ and $\boldsymbol{\Sigma}_\varepsilon \succ \mathbf{O}_n$. If the postulated density $p(\cdot|\boldsymbol{\theta})$ matches the true density $p^0(\cdot|\boldsymbol{\vartheta})$, then the log-likelihood function and score are

$$\begin{aligned} \text{log density:} \quad \ell(\mathbf{y}|\boldsymbol{\theta}) &\propto -\frac{1}{2}(\mathbf{y} - \mathbf{d} - \mathbf{Z}\boldsymbol{\theta})'\boldsymbol{\Sigma}_\varepsilon^{-1}(\mathbf{y} - \mathbf{d} - \mathbf{Z}\boldsymbol{\theta}), \\ \text{score:} \quad \nabla \ell(\mathbf{y}|\boldsymbol{\theta}) &= \mathbf{Z}'\boldsymbol{\Sigma}_\varepsilon^{-1}(\mathbf{y} - \mathbf{d} - \mathbf{Z}\boldsymbol{\theta}). \end{aligned} \quad (\text{B.2})$$

Let the predicted parameter $\boldsymbol{\theta}_{t|t-1} \in \mathbb{R}^k$ be given and fixed, which is used to compute both the ISD update (1) and the ESD update (2); hence, we omit the superscript on $\boldsymbol{\theta}_{t|t-1}$.

Kalman's covariance update. Let Kalman's predicted and updated covariance matrices $\mathbf{P}_{t|t-1}^{\text{KF}} \succ \mathbf{O}_k$ and $\mathbf{P}_{t|t}^{\text{KF}} \succ \mathbf{O}_k$ be given and fixed. They are related via

$$\begin{aligned} \mathbf{P}_{t|t}^{\text{KF}} &= \mathbf{P}_{t|t-1}^{\text{KF}} - \mathbf{P}_{t|t-1}^{\text{KF}} \mathbf{Z}' (\mathbf{Z} \mathbf{P}_{t|t-1}^{\text{KF}} \mathbf{Z}' + \boldsymbol{\Sigma}_\varepsilon)^{-1} \mathbf{Z} \mathbf{P}_{t|t-1}^{\text{KF}}, \\ &= [(\mathbf{P}_{t|t-1}^{\text{KF}})^{-1} + \mathbf{Z}' \boldsymbol{\Sigma}_\varepsilon^{-1} \mathbf{Z}]^{-1}. \end{aligned} \quad (\text{B.3})$$

The first line gives the standard covariance-matrix updating step; see Harvey (1989, p. 106) or Durbin and Koopman (2012, p. 86). The second line is used below and can be found in several places (e.g. Fahrmeir, 1992, p. 504, Lambert et al., 2022, eq. 36); it follows from the Woodbury matrix-inversion lemma (see equation (B.8) below).

Kalman update as ISD update. We take the ISD update (1) with $\mathbf{H}_t^{\text{im}} = \mathbf{P}_{t|t-1}^{\text{KF}}$ and substitute the score (B.2) to yield

$$\begin{aligned} \boldsymbol{\theta}_{t|t}^{\text{im}} &= \boldsymbol{\theta}_{t|t-1} + \mathbf{P}_{t|t-1}^{\text{KF}} \nabla \ell(\mathbf{y}_t|\boldsymbol{\theta}_{t|t}^{\text{im}}), \\ &= \boldsymbol{\theta}_{t|t-1} + \mathbf{P}_{t|t-1}^{\text{KF}} \mathbf{Z}' \boldsymbol{\Sigma}_\varepsilon^{-1} (\mathbf{y}_t - \mathbf{d} - \mathbf{Z}\boldsymbol{\theta}_{t|t}^{\text{im}}). \end{aligned} \quad (\text{B.4})$$

Pre-multiplying by $(\mathbf{P}_{t|t-1}^{\text{KF}})^{-1}$ and isolating $\boldsymbol{\theta}_{t|t}^{\text{im}}$ on the left-hand side, we obtain

$$\boldsymbol{\theta}_{t|t}^{\text{im}} = (\mathbf{Z}' \boldsymbol{\Sigma}_\varepsilon^{-1} \mathbf{Z} + (\mathbf{P}_{t|t-1}^{\text{KF}})^{-1})^{-1} [(\mathbf{P}_{t|t-1}^{\text{KF}})^{-1} \boldsymbol{\theta}_{t|t-1} + \mathbf{Z}' \boldsymbol{\Sigma}_\varepsilon^{-1} (\mathbf{y}_t - \mathbf{d})],$$

$$\begin{aligned}
&= (\mathbf{Z}' \boldsymbol{\Sigma}_\varepsilon^{-1} \mathbf{Z} + (\mathbf{P}_{t|t-1}^{\text{KF}})^{-1})^{-1} [\{(\mathbf{P}_{t|t-1}^{\text{KF}})^{-1} + \cancel{\mathbf{Z}' \boldsymbol{\Sigma}_\varepsilon^{-1} \mathbf{Z}} - \cancel{\mathbf{Z}' \boldsymbol{\Sigma}_\varepsilon^{-1} \mathbf{Z}}\} \boldsymbol{\theta}_{t|t-1} + \mathbf{Z}' \boldsymbol{\Sigma}_\varepsilon^{-1} (\mathbf{y}_t - \mathbf{d})], \\
&= \boldsymbol{\theta}_{t|t-1} + (\mathbf{Z}' \boldsymbol{\Sigma}_\varepsilon^{-1} \mathbf{Z} + (\mathbf{P}_{t|t-1}^{\text{KF}})^{-1})^{-1} \mathbf{Z}' \boldsymbol{\Sigma}_\varepsilon^{-1} (\mathbf{y}_t - \mathbf{d} - \mathbf{Z} \boldsymbol{\theta}_{t|t-1}), \\
&= \boldsymbol{\theta}_{t|t-1} + \mathbf{P}_{t|t-1}^{\text{KF}} \mathbf{Z}' (\mathbf{Z} \mathbf{P}_{t|t-1}^{\text{KF}} \mathbf{Z}' + \boldsymbol{\Sigma}_\varepsilon)^{-1} (\mathbf{y}_t - \mathbf{d} - \mathbf{Z} \boldsymbol{\theta}_{t|t-1}),
\end{aligned} \tag{B.5}$$

where the last line, which follows from a standard matrix-inversion lemma (see equation (B.7) below), is the standard Kalman-filter level update; see e.g. Harvey (1989, p. 106) or Durbin and Koopman (2012, p. 86).

Kalman update as ESD update. We take the ESD update (2) with $\mathbf{H}_t^{\text{ex}} = \mathbf{P}_{t|t}^{\text{KF}}$ and substitute the score (B.2) to yield

$$\begin{aligned}
\boldsymbol{\theta}_{t|t}^{\text{ex}} &= \boldsymbol{\theta}_{t|t-1} + \mathbf{P}_{t|t}^{\text{KF}} \nabla \ell(\mathbf{y}_t | \boldsymbol{\theta}_{t|t-1}), \\
&= \boldsymbol{\theta}_{t|t-1} + \mathbf{P}_{t|t}^{\text{KF}} \mathbf{Z}' \boldsymbol{\Sigma}_\varepsilon^{-1} (\mathbf{y}_t - \mathbf{d} - \mathbf{Z} \boldsymbol{\theta}_{t|t-1}), \\
&\stackrel{(B.3)}{=} \boldsymbol{\theta}_{t|t-1} + ((\mathbf{P}_{t|t-1}^{\text{KF}})^{-1} + \mathbf{Z}' \boldsymbol{\Sigma}_\varepsilon^{-1} \mathbf{Z})^{-1} \mathbf{Z}' \boldsymbol{\Sigma}_\varepsilon^{-1} (\mathbf{y}_t - \mathbf{d} - \mathbf{Z} \boldsymbol{\theta}_{t|t-1}), \\
&= \boldsymbol{\theta}_{t|t-1} + \mathbf{P}_{t|t-1}^{\text{KF}} \mathbf{Z}' (\mathbf{Z} \mathbf{P}_{t|t-1}^{\text{KF}} \mathbf{Z}' + \boldsymbol{\Sigma}_\varepsilon)^{-1} (\mathbf{y}_t - \mathbf{d} - \mathbf{Z} \boldsymbol{\theta}_{t|t-1}),
\end{aligned} \tag{B.6}$$

where the last line, which follows from the same matrix-inversion lemma (see equation (B.7) below), is again the standard form of Kalman's level update (see references given above).

Matrix-inversion lemmas. The above derivation relied on two matrix-inversion lemmas for positive-definite matrices \mathbf{A} , $\mathbf{B} \succ \mathbf{O}_k$ and an arbitrary (size-compatible) matrix \mathbf{C} :

$$(\mathbf{A} + \mathbf{C}' \mathbf{B}^{-1} \mathbf{C})^{-1} \mathbf{C}' \mathbf{B}^{-1} = \mathbf{A}^{-1} \mathbf{C}' (\mathbf{B} + \mathbf{C} \mathbf{A}^{-1} \mathbf{C}')^{-1}. \tag{B.7}$$

$$(\mathbf{A} + \mathbf{C}' \mathbf{B}^{-1} \mathbf{C})^{-1} = \mathbf{A}^{-1} - \mathbf{A}^{-1} \mathbf{C}' (\mathbf{B} + \mathbf{C} \mathbf{A}^{-1} \mathbf{C}')^{-1} \mathbf{C} \mathbf{A}^{-1}. \tag{B.8}$$

While the second identity is a special case of the Woodbury matrix identity (e.g. Sherman and Morrison, 1950 and Henderson and Searle, 1981), a simple proof for the first identity is hard to find. A short proof of both identities can be found in Lange (2024b). \square

B.2 Minimizing MSE bound of ISD filter w.r.t. Young's parameter

For the ISD filter when Assumption 2 holds but Assumption 3 does not, the MSE bound contains a single free parameter, $\epsilon > 0$, which can be analytically optimized.

Corollary 1 (Optimal Young's parameter for the ISD filter). *Let Assumptions 1–2 hold and assume that sufficient condition (8) for stability in Theorem 1 is met, implying $\tau_{\text{im}} = ac/(1 + \epsilon^2) < 1$ for some $\epsilon > 0$. For $0 < \tau_{\text{im}} < 1$, the value of the Young's parameter $\epsilon^2 > 0$ that minimizes the asymptotic MSE bound (13) is then given by*

$$\epsilon_*^2 = \frac{1 - \tau_{\text{im}}}{\tau_{\text{im}} + \sqrt{\tau_{\text{im}} + \tau_{\text{im}}(1 - \tau_{\text{im}}) \frac{\sigma^2}{\lambda_{\max}(\mathbf{P})\lambda_{\min}(\mathbf{P})(\|\mathbf{I}_k - \mathbf{\Phi}\| s_\omega + q)^2}}} < \infty. \quad (\text{B.9})$$

Proof. Computing the bound. Consider the ISD filter in case Assumption 2 holds, but Assumption 3 does not. In addition, let $\tau_{\text{im}} = ac/(1 + \epsilon^2) < 1$ (see equation (8)) and define $\tilde{d} := d/(1 + \frac{1}{\epsilon^2})$, where d is as in Table 1. Note that \tilde{d} , unlike d , is independent of ϵ^2 . As we must ensure $ac < 1$ to guarantee finite asymptotic MSE bounds, it is convenient to take $\epsilon^2 := (\kappa(1 - \tau_{\text{im}}))/\tau_{\text{im}}$, such that $ac = \tau_{\text{im}}(1 + \epsilon^2) = \tau_{\text{im}} + \kappa(1 - \tau_{\text{im}}) < 1$, $\forall \kappa \in (0, 1)$. Intuitively, κ controls the extent to which ϵ^2 closes the “gap” between τ_{im} and unity; i.e., the denominator in the asymptotic MSE bound reads $1 - ac = 1 - \tau_{\text{im}} - \kappa(1 - \tau_{\text{im}}) = 1 - \tau_{\text{im}} - \kappa + \kappa\tau_{\text{im}} = (1 - \tau_{\text{im}})(1 - \kappa) \in (0, 1)$.

The asymptotic MSE bound $\forall \kappa \in (0, 1)$ is given by

$$\begin{aligned} \limsup_{t \rightarrow \infty} \text{MSE}_{t|t}^{\mathbf{P}} &\leq \frac{b + ad}{1 - ac} \\ &= \frac{b + a\tilde{d}(1 + \frac{1}{\epsilon^2})}{1 - \tau_{\text{im}}(1 + \epsilon^2)} \\ &= \frac{b + a\tilde{d}(1 + \frac{\tau_{\text{im}}}{\kappa(1 - \tau_{\text{im}})})}{(1 - \tau_{\text{im}})(1 - \kappa)} \\ &= \frac{b + a\tilde{d}}{1 - \tau_{\text{im}}} \frac{1}{1 - \kappa} + \frac{\tau_{\text{im}}a\tilde{d}}{(1 - \tau_{\text{im}})^2} \frac{1}{\kappa(1 - \kappa)} \\ &= A \frac{1}{1 - \kappa} + B \frac{1}{\kappa(1 - \kappa)}, \end{aligned} \quad (\text{B.10})$$

where the second line uses the definition of \tilde{d} and τ_{im} and the third line uses our specification of ϵ^2 in terms of κ . From the final line, it follows that $A, B \geq 0$ are given by

$$A := \frac{b + a\tilde{d}}{1 - \tau_{\text{im}}}, \quad B := \frac{\tau_{\text{im}}a\tilde{d}}{(1 - \tau_{\text{im}})^2}. \quad (\text{B.11})$$

For future reference, we note that

$$\frac{A}{B} = \frac{\frac{b + a\tilde{d}}{1 - \tau_{\text{im}}}}{\frac{\tau_{\text{im}}a\tilde{d}}{(1 - \tau_{\text{im}})^2}} = \frac{1 - \tau_{\text{im}}}{\tau_{\text{im}}} \frac{b + a\tilde{d}}{a\tilde{d}}. \quad (\text{B.12})$$

Minimizing the bound. In case $\tau_{\text{im}} = 0$, we have that $\epsilon = \infty$ minimizes the MSE bound, as can be seen in the second line of (B.10). We therefore proceed with the case $\tau_{\text{im}} > 0$, which implies $B > 0$ as $\tau_{\text{im}} = ac/(1 + \epsilon^2) \neq 0 \Rightarrow a \neq 0$ and $q > 0 \Rightarrow \tilde{d} > 0$; see (B.11). Equation (B.10) illustrates that as $A, B > 0$, we have that $\kappa \in (0, 1)$ should not approach either boundary too closely.

Minimizing the bound (B.10) with respect to κ yields the following first-order condition:

$$0 = \frac{A}{(1 - \kappa)^2} + \frac{B(2\kappa - 1)}{\kappa^2(1 - \kappa)^2}, \quad (\text{B.13})$$

where we may multiply by $\kappa^2(1 - \kappa)^2 \in (0, 1)$ to obtain

$$0 = A\kappa^2 + 2B\kappa - B, \quad (\text{B.14})$$

which is a quadratic equation in κ , the solution of which reads

$$\kappa_{\pm} = \frac{-2B \pm \sqrt{4B^2 + 4AB}}{2A}. \quad (\text{B.15})$$

Because A and B are positive, we have $\kappa_+ > 0$ and $\kappa_- < 0$. Only the positive solution is

of interest. Specifically, we have

$$\begin{aligned}
\kappa_\star = \kappa_+ &= \frac{-2B + \sqrt{4B^2 + 4AB}}{2A} \\
&= \frac{-2B + \sqrt{4B^2 + 4AB}}{2A} \times \underbrace{\frac{2B + \sqrt{4B^2 + 4AB}}{2B + \sqrt{4B^2 + 4AB}}}_{=1} \\
&= \frac{4AB}{4AB + 2A\sqrt{4B^2 + 4AB}} \\
&= \frac{4AB}{4AB + \sqrt{(4AB)^2 + 16A^3B}} \\
&= \frac{1}{1 + \sqrt{1 + A/B}},
\end{aligned} \tag{B.16}$$

which shows that $\kappa_\star \in (0, 1/2)$.

Using the expression for A/B in (B.12) and $\epsilon^2 = \frac{1-\tau_{\text{im}}}{\tau_{\text{im}}} \kappa$, we obtain

$$\begin{aligned}
\epsilon_\star^2 &= \frac{1-\tau_{\text{im}}}{\tau_{\text{im}}} \kappa_\star = \frac{1-\tau_{\text{im}}}{\tau_{\text{im}}} \frac{1}{1 + \sqrt{1 + A/B}} \\
&= \frac{1-\tau_{\text{im}}}{\tau_{\text{im}} + \sqrt{\tau_{\text{im}}^2 + \tau_{\text{im}}(1-\tau_{\text{im}})\frac{b+a\tilde{d}}{ad}}} \\
&= \frac{1-\tau_{\text{im}}}{\tau_{\text{im}} + \sqrt{\tau_{\text{im}}^2 + \tau_{\text{im}}(1-\tau_{\text{im}})(\frac{b}{ad} + 1)}} \\
&= \frac{1-\tau_{\text{im}}}{\tau_{\text{im}} + \sqrt{\tau_{\text{im}}^2 + \tau_{\text{im}}(1-\tau_{\text{im}})\frac{b}{ad} + \tau_{\text{im}}(1-\tau_{\text{im}})}} \\
&= \frac{1-\tau_{\text{im}}}{\tau_{\text{im}} + \sqrt{\tau_{\text{im}} + \tau_{\text{im}}(1-\tau_{\text{im}})\frac{b}{ad}}}, \\
&= \frac{1-\tau_{\text{im}}}{\tau_{\text{im}} + \sqrt{\tau_{\text{im}} + \tau_{\text{im}}(1-\tau_{\text{im}})\frac{\sigma^2}{\lambda_{\max}(\mathbf{P})\lambda_{\min}(\mathbf{P})(\|\mathbf{I}_k - \mathbf{\Phi}\| s_\omega + q)^2}}},
\end{aligned} \tag{B.17}$$

where the final line uses the values of b and d for the ISD filter from Table 1. Note that coerciveness (the bounds tend to infinity as κ approaches either zero or one) and continuity imply that this unique stationary point is, in fact, a global minimum. \square

B.3 Minimizing MSE bound of ISD filter w.r.t. learning rate

Under Assumptions 2–3, the (Euclidean) MSE bound for the ISD filter derived from Theorem 2 contains no free parameters, although some freedom remains in selecting the penalty matrix. If we take the penalty matrix to be a scalar multiple of the identity, the value of this multiple that minimizes the asymptotic MSE bound can be derived analytically.

Corollary 2 (Optimal penalty parameter for the ISD filter). *Let Assumptions 1, 2(a,b) and 3 hold. Furthermore, assume that (i) the postulated log-likelihood contribution is strongly concave (i.e., $\alpha > 0$), (ii) the penalty matrix is a scalar multiple of the identity matrix (i.e., $\mathbf{P} = \rho \mathbf{I}_k$ for some $\rho > 0$), and (iii) $\sigma, \sigma_\xi > 0$ such $b, d > 0$. Then the value of $\rho > 0$ that minimizes the asymptotic (Euclidean) MSE bound for the ISD filter is*

$$\rho_* = \frac{\sigma^2 (1 - \|\Phi_0\|^2) - \alpha^2 \sigma_\xi^2 + \sqrt{(\alpha^2 \sigma_\xi^2 - \sigma^2 (1 - \|\Phi_0\|^2))^2 + 4\alpha^2 \sigma^2 \sigma_\xi^2}}{2\alpha \sigma_\xi^2} < \infty. \quad (\text{B.18})$$

Proof. Using the result of Theorem 2 and that $\mathbf{P} = \rho \mathbf{I}_k$, we have that $a = \left(\frac{\rho}{\rho+\alpha}\right)^2 \in (0, 1)$ and $b = a\rho^{-1}\sigma^2$ for the ISD filter with strong concavity ($\alpha > 0$). In addition, when the DGP is a known state-space model (Assumption 3 holds) and again using $\mathbf{P} = \rho \mathbf{I}_k$, we have that $c = \|\Phi_0\|_{\mathbf{P}}^2 = \|\mathbf{P}^{1/2} \Phi_0 \mathbf{P}^{-1/2}\|^2 = \|\rho^{1/2} \mathbf{I}_k \Phi_0 \rho^{-1/2} \mathbf{I}_k\|^2 = \|\Phi_0\|^2$ and $d = \rho \sigma_\xi^2$. Substituting these into the asymptotic filter \mathbf{P} -weighted MSE bound in (13) and converting to the (Euclidean) MSE bound, we obtain

$$\begin{aligned} \limsup_{t \rightarrow \infty} \text{MSE}_{t|t} &= \frac{1}{\rho} \limsup_{t \rightarrow \infty} \text{MSE}_{t|t}^{\mathbf{P}} \leq \frac{1}{\rho} \frac{b + ad}{1 - ac} = \frac{a\sigma^2/\rho^2 + a\sigma_\xi^2}{1 - a\|\Phi_0\|^2} \\ &= \frac{\sigma^2/\rho^2 + \sigma_\xi^2}{a^{-1} - \|\Phi_0\|^2} = \frac{\sigma^2/\rho^2 + \sigma_\xi^2}{\left(\frac{\rho+\alpha}{\rho}\right)^2 - \|\Phi_0\|^2} = \frac{\sigma^2 + \rho^2 \sigma_\xi^2}{(\rho + \alpha)^2 - \rho^2 \|\Phi_0\|^2}, \end{aligned} \quad (\text{B.19})$$

where the second line first multiplies with $a^{-1}/a^{-1} = 1$ and subsequently with $\rho^2/\rho^2 = 1$.

To optimize the bound with respect to ρ , we consider the first-order condition:

$$\begin{aligned}
0 &= \frac{d}{d\rho} \frac{\sigma^2 + \rho^2 \sigma_\xi^2}{(\rho + \alpha)^2 - \rho^2 \|\Phi_0\|^2} \\
&= \frac{2\rho \sigma_\xi^2 ((\rho + \alpha)^2 - \rho^2 \|\Phi_0\|^2) - (\sigma^2 + \rho^2 \sigma_\xi^2)(2(\rho + \alpha) - 2\rho \|\Phi_0\|^2)}{((\rho + \alpha)^2 - \rho^2 \|\Phi_0\|^2)^2} \\
&= \frac{2\rho \sigma_\xi^2 ((\rho + \alpha)^2 - \rho^2 \|\Phi_0\|^2) - (\sigma^2 + \rho^2 \sigma_\xi^2)(2(\rho + \alpha) - 2\rho \|\Phi_0\|^2)}{\rho^4(a^{-1} + c)^2}, \tag{B.20}
\end{aligned}$$

where the second line multiplies with $\frac{1}{\rho^4(a^{-1} + c)^2} = 1$ followed by using the definition of a and c .

The contraction condition $ac < 1$ is assumed to hold, which implies that the denominator in (B.20) is positive; that is, $ac < 1 \Rightarrow 1 - ac > 0 \Rightarrow a^{-1} - c > 0 \Rightarrow \rho^4(a^{-1} + c)^2 > 0$. This means that to solve the first-order condition, we need to set the numerator equal to 0, i.e.,

$$\begin{aligned}
0 &= 2\rho \sigma_\xi^2 ((\rho + \alpha)^2 - \rho^2 \|\Phi_0\|^2) - (\sigma^2 + \rho^2 \sigma_\xi^2)(2(\rho + \alpha) - 2\rho \|\Phi_0\|^2) \\
&= 2\rho \sigma_\xi^2 (\rho + \alpha)^2 - 2\rho^3 \sigma_\xi^2 \|\Phi_0\|^2 - \sigma^2 (2(\rho + \alpha) - 2\rho \|\Phi_0\|^2) - 2\rho^2 \sigma_\xi^2 (\rho + \alpha) + 2\rho^3 \sigma_\xi^2 \|\Phi_0\|^2 \\
&= 2\rho \sigma_\xi^2 (\rho + \alpha)^2 - 2\sigma^2 (\rho + \alpha) + 2\rho \sigma^2 \|\Phi_0\|^2 - 2\rho^2 \sigma_\xi^2 (\rho + \alpha) \\
&= 2\rho^3 \sigma_\xi^2 + 2\rho \sigma_\xi^2 \alpha^2 + 4\rho^2 \sigma_\xi^2 \alpha - 2\rho \sigma^2 - 2\sigma^2 \alpha + 2\rho \sigma^2 \|\Phi_0\|^2 - 2\rho^3 \sigma_\xi^2 - 2\rho^2 \sigma_\xi^2 \alpha \\
&= 2\rho \sigma_\xi^2 \alpha^2 + 4\rho^2 \sigma_\xi^2 \alpha - 2\rho \sigma^2 - 2\sigma^2 \alpha + 2\rho \sigma^2 \|\Phi_0\|^2 - 2\rho^2 \sigma_\xi^2 \alpha \\
&= \rho^2 (2\sigma_\xi^2 \alpha) + \rho (2\sigma_\xi^2 \alpha^2 - 2\sigma^2 (1 - \|\Phi_0\|^2)) - 2\sigma^2 \alpha \\
&= A\rho^2 + B\rho + C, \tag{B.21}
\end{aligned}$$

which yields a quadratic equation in ρ with coefficients $A = 2\sigma_\xi^2 \alpha$, $B = 2\sigma_\xi^2 \alpha^2 - 2\sigma^2 (1 - \|\Phi_0\|^2)$ and $C = -2\sigma^2 \alpha$ and solution

$$\rho_\pm = \frac{-B \pm \sqrt{B^2 - 4AC}}{2A}. \tag{B.22}$$

Because $AC = -4\sigma_\xi^2 \sigma^2 \alpha^2 < 0$ and $A = 2\sigma_\xi^2 \alpha > 0$, we have that $\rho_- < 0$ and $\rho_+ > 0$, the latter is therefore the solution to the minimization problem at hand. Specifically, the final

result reads

$$\begin{aligned}\rho_\star &= \rho_+ = \frac{-2\sigma_\xi^2\alpha^2 + 2\sigma^2(1 - \|\Phi_0\|^2) + \sqrt{4(\sigma_\xi^2\alpha^2 - \sigma^2(1 - \|\Phi_0\|^2)^2 + 16\sigma_\xi^2\sigma^2\alpha^2}}}{4\sigma_\xi^2\alpha} \\ &= \frac{\sigma^2(1 - \|\Phi_0\|^2) - \alpha^2\sigma_\xi^2 + \sqrt{(\alpha^2\sigma_\xi^2 - \sigma^2(1 - \|\Phi_0\|^2)^2 + 4\alpha^2\sigma_\xi^2\sigma^2}}}{2\alpha\sigma_\xi^2},\end{aligned}\quad (\text{B.23})$$

where the second line multiplies by $(1/2)/(1/2) = 1$ and rearranges. Because $A = 2\sigma_\xi^2\alpha > 0$, we have that the numerator of (B.20) is a convex parabola with largest root ρ_\star , which means that it becomes negative for $\rho \in (0, \rho_\star)$ and positive for $\rho \in (\rho_\star, \infty)$. Combined with the fact that the denominator of (B.20) is always positive, we have that the bound is decreasing in ρ on the interval $(0, \rho_\star)$ and increasing on the interval (ρ_\star, ∞) . In sum, this means that the stationary point ρ_\star is indeed the global minimum. \square

B.4 Minimized MSE bound of ISD filter can be tight

Example 2 below illustrates a case in which the minimized asymptotic MSE bound for the ISD filter is tight, as it equals the steady-state variance of the Kalman filter. The optimal learning-rate selection reveals a connection with the Kalman gain.

Example 2 (Tight MSE bounds of ISD filter). *Consider an AR(1) model with additive observation noise, defined by the observation equation $y_t = \vartheta_t + \varepsilon_t$, where $\varepsilon_t \sim \text{i.i.d. } N(0, \sigma_\varepsilon^2)$ with $\sigma_\varepsilon > 0$, and linear first-order state dynamics $\vartheta_{t+1} = (1 - \phi_0)\omega_0 + \phi_0\vartheta_t + \xi_t$, where $\xi_t \sim \text{i.i.d. } N(0, \sigma_\xi^2)$ with $\sigma_\xi > 0$. Let the learning rate be positive and constant, $\mathbf{H}_t = \mathbf{P}_t^{-1} = \rho^{-1} = \eta > 0$, for all t . As in Kalman's classic setting, let Assumption 3 hold; that is, the observation density and parameters ω_0 and ϕ_0 are known to the researcher. Then, the asymptotic MSE bound*

$$\limsup_{t \rightarrow \infty} \text{MSE}_{t|t} \leq \frac{\eta^2\sigma_\varepsilon^2 + \sigma_\xi^2\sigma_\varepsilon^4}{2\eta\sigma_\varepsilon^2 + \eta^2 + (1 - \phi_0^2)\sigma_\varepsilon^4}, \quad (\text{B.24})$$

is minimized when the learning rate η is chosen as

$$\eta_* = \frac{\sigma_\xi^2 - \sigma_\varepsilon^2 (1 - \phi_0^2) + \sqrt{\sigma_\xi^4 + \sigma_\varepsilon^4 (1 - \phi_0^2)^2 + 2\sigma_\xi^2 \sigma_\varepsilon^2 (1 + \phi_0^2)}}{2}. \quad (\text{B.25})$$

For the local-level model, where $\phi_0 = 1$, the minimizer η_* simplifies to

$$\eta_* = \frac{\sigma_\xi^2 + \sqrt{\sigma_\xi^4 + 4\sigma_\xi^2 \sigma_\varepsilon^2}}{2} = \frac{\sigma_\varepsilon^2}{2} \left(\frac{\sigma_\xi^2}{\sigma_\varepsilon^2} + \sqrt{\frac{\sigma_\xi^4}{\sigma_\varepsilon^4} + 4\frac{\sigma_\xi^2}{\sigma_\varepsilon^2}} \right). \quad (\text{B.26})$$

As it turns out, η_* equals the steady-state variance of prediction errors in the Kalman filter, as given in Durbin and Koopman (2012, p. 37) and Harvey (1989, p. 175), where $\sigma_\xi^2/\sigma_\varepsilon^2$ is the signal-to-noise ratio. Substituting the minimizer η_* into the ISD update, we obtain the exact form of Kalman's level update with the (optimal) Kalman gain. Since the Kalman filter is optimal for this model, our minimized MSE bound is tight.

Proof. For readability, we omit all superscripts im. Under Assumptions 1–3, the asymptotic (Euclidean) MSE bound for the ISD filter is obtained by substituting $a = \left(\frac{\rho}{\rho+\alpha}\right)^2$, $b = a\rho^{-1}\sigma^2$, $c = \|\Phi_0\|^2$, and $d = \rho\sigma_\xi^2$ in equation (13), and multiplying by η to obtain

$$\limsup_{t \rightarrow \infty} \text{MSE}_{t|t} \leq \frac{\sigma^2 + \sigma_\xi^2 \rho^2}{\alpha^2 + 2\alpha\rho + (1 - \|\Phi_0\|^2)\rho^2} = \frac{\sigma\eta^2 + \sigma_\xi^2}{\alpha^2\eta^2 + 2\alpha\eta + (1 - \|\Phi_0\|^2)}, \quad (\text{B.27})$$

where $\eta := 1/\rho$. In the context of Example 2, $\Phi_0 = \phi_0$, $\alpha = -\nabla^2(y_t|\theta_{t|t-1}) = 1/\sigma_\varepsilon^2$ and $\sigma^2 = \sup_t \mathbb{E}(\|\nabla(y_t|\vartheta_t)\|^2) = 1/\sigma_\varepsilon^2$. The postulated log-likelihood function is

$$\log p(y_t|\theta_{t|t-1}) = -\frac{1}{2} \log(2\pi\sigma_\varepsilon^2) - \frac{(y_t - \theta_{t|t-1})^2}{2\sigma_\varepsilon^2}. \quad (\text{B.28})$$

Taking the first derivative with respect to $\theta_{t|t-1}$, the score is

$$\nabla \log p(y_t|\theta_{t|t-1}) = \frac{y_t - \theta_{t|t-1}}{\sigma_\varepsilon^2}. \quad (\text{B.29})$$

The second derivative with respect to $\theta_{t|t-1}$ is

$$\nabla^2 \log p(y_t | \theta_{t|t-1}) = -\frac{1}{\sigma_\varepsilon^2}. \quad (\text{B.30})$$

Thus, $\alpha = 1/\sigma_\varepsilon^2$. Now, for $y_t \sim N(\vartheta_t, \sigma_\varepsilon^2)$, the score evaluated at the true parameter is

$$\nabla \log p(y_t | \vartheta_t) = \frac{y_t - \vartheta_t}{\sigma_\varepsilon^2}, \quad (\text{B.31})$$

and taking the squared norm, we obtain

$$\|\nabla \log p(y_t | \vartheta_t)\|^2 = \frac{(y_t - \vartheta_t)^2}{\sigma_\varepsilon^4}. \quad (\text{B.32})$$

Taking the expectation with respect to y_t , we get:

$$\mathbb{E}_{y_t} (\|\nabla \log p(y_t | \vartheta_t)\|^2) = \frac{\mathbb{E}[(y_t - \vartheta_t)^2]}{\sigma_\varepsilon^4} = \frac{\sigma_\varepsilon^2}{\sigma_\varepsilon^4} = \frac{1}{\sigma_\varepsilon^2}. \quad (\text{B.33})$$

Thus, $\sigma^2 = \frac{1}{\sigma_\varepsilon^2}$. Next, we substitute $\Phi_0 = \phi_0$, $\alpha = 1/\sigma_\varepsilon^2$ and $\sigma^2 = 1/\sigma_\varepsilon^2$ in equation (B.27),

and subsequently multiply the numerator and denominator by $\sigma_\varepsilon^4 > 0$, to obtain

$$\limsup_{t \rightarrow \infty} \text{MSE}_{t|t} \leq \frac{\sigma_\varepsilon^2 \eta^2 + \sigma_\xi^2 \sigma_\varepsilon^4}{\eta^2 + 2\sigma_\varepsilon^2 \eta + (1 - \phi_0^2) \sigma_\varepsilon^4}. \quad (\text{B.34})$$

If $\eta = 0$, we obtain an upper bound equal to $\sigma_\xi^2 / (1 - \phi_0^2)$, which is the unconditional variance of the true state, ϑ_t . If $\eta = \infty$, we obtain an upper bound equal to σ_ε^2 , which is the conditional variance of the observations. We hope to find an (optimal) learning rate $\eta > 0$ that minimizes the upper bound, yielding a lower value than either $\eta = 0$ or $\eta = \infty$.

To this end, we compute the derivative (with respect to η) of the bound (B.34) and

equate to zero:

$$\frac{[2\sigma_\varepsilon^2\eta][2\sigma_\varepsilon^2\eta + \eta^2 + (1 - \phi_0^2)\sigma_\varepsilon^4] - [\sigma_\varepsilon^2\eta^2 + \sigma_\xi^2\sigma_\varepsilon^4][2\sigma_\varepsilon^2 + 2\eta]}{(\eta^2 + 2\sigma_\varepsilon^2\eta + (1 - \phi_0^2)\sigma_\varepsilon^4)^2} = 0. \quad (\text{B.35})$$

We will find that there exists a unique value of $\eta > 0$ that solves this equation. Moreover, this unique value $\eta > 0$ will turn out to deliver a lower MSE bound than either $\eta = 0$ or $\eta = \infty$. Because the bound is continuously differentiable in $\eta \geq 0$, this means that we will have found the global minimum.

Given that the denominator above is positive, finding the stationary point is equivalent to solving

$$4\sigma_\varepsilon^4\eta^2 + 2\sigma_\varepsilon^2\eta^3 + 2\sigma_\varepsilon^6\eta(1 - \phi_0^2) - (2\sigma_\varepsilon^4\eta^2 + 2\sigma_\varepsilon^2\eta^3 + 2\sigma_\xi^2\sigma_\varepsilon^6 + 2\sigma_\xi^2\sigma_\varepsilon^4\eta) = 0. \quad (\text{B.36})$$

Canceling out $2\sigma_\varepsilon^2\eta^3$, using that $4\sigma_\varepsilon^4\eta^2 - 2\sigma_\varepsilon^4\eta^2 = 2\sigma_\varepsilon^4\eta^2$, and that $2\sigma_\varepsilon^6\eta(1 - \phi_0^2) - 2\sigma_\xi^2\sigma_\varepsilon^4\eta = \eta(2\sigma_\varepsilon^6\eta(1 - \phi_0^2) - 2\sigma_\xi^2\sigma_\varepsilon^4)$, combining the terms we get a quadratic equation in η

$$2\sigma_\varepsilon^4\eta^2 + \eta(2\sigma_\varepsilon^6(1 - \phi_0^2) - 2\sigma_\xi^2\sigma_\varepsilon^4) - 2\sigma_\xi^2\sigma_\varepsilon^6 = 0. \quad (\text{B.37})$$

Dividing each term by $2\sigma_\varepsilon^4 > 0$ leads to

$$\eta^2 + \eta(\sigma_\varepsilon^2(1 - \phi_0^2) - \sigma_\xi^2) - \sigma_\xi^2\sigma_\varepsilon^2 = 0. \quad (\text{B.38})$$

Solving for η_* using the quadratic formula, we obtain

$$\eta_\pm = \frac{\sigma_\xi^2 - \sigma_\varepsilon^2(1 - \phi_0^2) \pm \sqrt{D}}{2}, \quad (\text{B.39})$$

where $D = (\sigma_\varepsilon^2(1 - \phi_0^2) - \sigma_\xi^2)^2 + 4\sigma_\xi^2\sigma_\varepsilon^2 = \sigma_\xi^4 + \sigma_\varepsilon^4(1 - \phi_0^2)^2 + 2\sigma_\xi^2\sigma_\varepsilon^2(1 + \phi_0^2)$. Because $\sqrt{D} > \sigma_\xi^2 - \sigma_\varepsilon^2(1 - \phi_0^2)$, we have $\eta_+ > 0$ and $\eta_- < 0$. Only the positive solution is of

interest. Specifically, we have

$$\eta_\star = \eta_+ = \frac{\sigma_\xi^2 - \sigma_\varepsilon^2 (1 - \phi_0^2) + \sqrt{\sigma_\xi^4 + \sigma_\varepsilon^4 (1 - \phi_0^2)^2 + 2\sigma_\xi^2 \sigma_\varepsilon^2 (1 + \phi_0^2)}}{2}. \quad (\text{B.40})$$

In the case of a local-level model (i.e., $\phi_0 = 1$), we have $a \times c = a \times \phi_0 = \left(\frac{\rho}{\rho+\alpha}\right)^2 < 1$ as $\alpha = 1/\sigma_\varepsilon^2$. Thus, the optimal learning rate reduces to

$$\eta_\star = \frac{\sigma_\xi^2 + \sqrt{\sigma_\xi^4 + 4\sigma_\xi^2 \sigma_\varepsilon^2}}{2} = \frac{\sigma_\varepsilon^2}{2} \left(\frac{\sigma_\xi^2}{\sigma_\varepsilon^2} + \sqrt{\frac{\sigma_\xi^4}{\sigma_\varepsilon^4} + 4\frac{\sigma_\xi^2}{\sigma_\varepsilon^2}} \right), \quad (\text{B.41})$$

which is the steady-state covariance associated with predictions in the Kalman filter, where $\sigma_\xi^2/\sigma_\varepsilon^2$ is the signal-to-noise ratio.

Substituting η_\star from equation (B.41) back into the bound (B.34), which was to be minimized, we can confirm (after some algebra) that the unique stationary point yields a value that does not exceed the value at either endpoint (i.e., at $\eta = 0$ or $\eta = \infty$). By continuous differentiability of the MSE bound in $\eta \geq 0$, the stationary point yields the global minimum as desired. \square

C Detailed discussion and further numerical results

C.1 Detailed discussion of ISD and ESD updates (4)–(5)

In optimization (4), the optimal value of the objective function (i.e., when evaluated at the argmax) must exceed the (suboptimal) value at any other point (e.g., at the predicted parameter). This fact yields $\ell(\mathbf{y}_t | \boldsymbol{\theta}_{t|t}^{\text{im}}) - \frac{1}{2} \|\boldsymbol{\theta}_{t|t}^{\text{im}} - \boldsymbol{\theta}_{t|t-1}^{\text{im}}\|_{\mathbf{P}_t}^2 \geq \ell(\mathbf{y}_t | \boldsymbol{\theta}_{t|t-1}^{\text{im}})$, where the left-hand side is the optimized value. After rearrangement, this implies

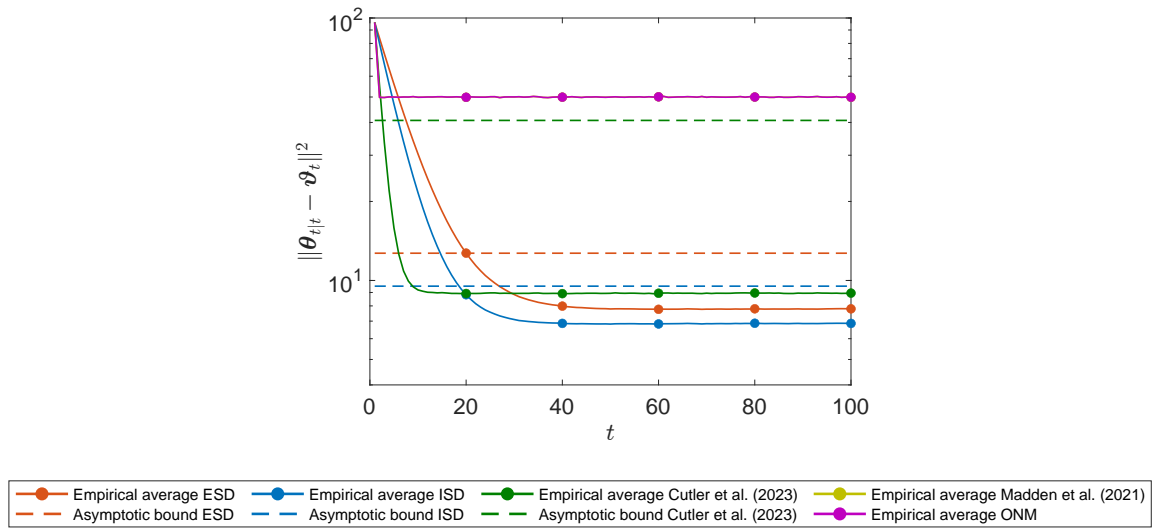
$$\ell(\mathbf{y}_t | \boldsymbol{\theta}_{t|t}^{\text{im}}) - \ell(\mathbf{y}_t | \boldsymbol{\theta}_{t|t-1}^{\text{im}}) \geq 1/2 \|\boldsymbol{\theta}_{t|t}^{\text{im}} - \boldsymbol{\theta}_{t|t-1}^{\text{im}}\|_{\mathbf{P}_t}^2 \geq 0,$$

which yields two desirable consequences: (i) the fit is improved at every time step, i.e., $\ell(\mathbf{y}_t|\boldsymbol{\theta}_{t|t}^{\text{im}}) - \ell(\mathbf{y}_t|\boldsymbol{\theta}_{t|t-1}^{\text{im}}) \geq 0$, and (ii) the stepsize is bounded, i.e., $\|\boldsymbol{\theta}_{t|t}^{\text{im}} - \boldsymbol{\theta}_{t|t-1}^{\text{im}}\|_{\mathbf{P}_t} < \infty$, as long as $\boldsymbol{\theta} \mapsto \ell(\mathbf{y}_t|\boldsymbol{\theta})$ is upper bounded, almost surely in \mathbf{y}_t . Hence the boundedness of the implicit update derives *not* from the boundedness of the gradient, but from the upper boundedness of the objective function itself.

In contrast, the solution (2) to the linearized update (5) may be prone to “overshooting”; i.e., unless the learning rate is very small, the undesirable situation $\ell(\mathbf{y}_t|\boldsymbol{\theta}_{t|t}^{\text{ex}}) < \ell(\mathbf{y}_t|\boldsymbol{\theta}_{t|t-1}^{\text{ex}})$ may regularly occur. In Section 4 we find that for the explicit method to asymptotically achieve bounded filtering errors over time, we require that, almost surely in \mathbf{y}_t , the driving mechanism $\mathbf{H}_t \nabla \ell(\mathbf{y}_t|\boldsymbol{\theta}_{t|t-1}^{\text{ex}})$ is Lipschitz in $\boldsymbol{\theta}_{t|t-1}^{\text{ex}}$. This additional condition, which is not needed for the implicit method, is required to avoid the explicit method from repeatedly overshooting and, possibly, diverging.

C.2 Details for Section 5.1

Figure C.1 presents the MSE performance of the ISD and ESD filters alongside three recent competitors in the setting of Section 5.1. In this case, however, we follow Cutler et al. (2023) by setting $\alpha = \beta = 1$. As a result, the “momentum” term in the ONM algorithm vanishes, reducing it to the stochastic gradient descent method from Madden et al. (2021). As opposed to when $\alpha = 1, \beta = 40$, the learning rate in the Cutler et al. (2023) algorithm no longer remains fixed at its cap, $1/(2\beta)$. While Cutler et al.’s (2023) algorithm performs well for small t , the ISD and ESD filters perform empirically better (and have better performance guarantees) for large t .



C.3 Details for Section 5.2

Table C.1: Overview of data-generating processes in simulation studies.

DGP		Link function		Density $p(y_t \theta_t)$		Score $\nabla \ell(y_t \theta_t)$		Negative Hessian $-\nabla^2 \ell(y_t \theta_t)$		Information	
Type	Distribution										
Count	Poisson	$\lambda_t = \exp(\theta_t)$		$\frac{\lambda_t^{y_t} \exp(-\lambda_t)/y_t!}{\Gamma(\kappa + y_t) \left(\frac{\kappa}{\kappa + \lambda_t}\right)^\kappa \left(\frac{\lambda_t}{\kappa + \lambda_t}\right)^{y_t}}$		$y_t - \lambda_t$		λ_t		$\frac{\kappa \lambda_t (\kappa + y_t)}{\kappa + \lambda_t}$	λ_t
Count	Negative bin.	$\lambda_t = \exp(\theta_t)$		$\frac{\Gamma(\kappa) \Gamma(y_t + 1)}{y_t^{\kappa - 1} \exp(-y_t/\beta_t)} \frac{\lambda_t^{\kappa} \Gamma(y_t + 1)}{\lambda_t \exp(-\lambda_t y_t)}$		$y_t - \frac{\lambda_t (\kappa + y_t)}{1 - \lambda_t y_t}$		$\frac{(\kappa + \lambda_t)^2}{y_t \lambda_t}$		$\frac{1}{\kappa + \lambda_t}$	$\frac{\kappa \lambda_t}{\kappa + \lambda_t}$
Intensity	Exponential	$\lambda_t = \exp(\theta_t)$		$\frac{\beta_t}{\kappa (y_t/\beta_t)^{\kappa - 1}}$		$y_t - \frac{\kappa}{\beta_t - \kappa}$		$\frac{y_t}{\beta_t}$		κ	κ
Duration	Gamma	$\beta_t = \exp(\theta_t)$		$\frac{\Gamma(\kappa) \beta_t^\kappa}{\beta_t \exp\{y_t/\beta_t\} \exp\{-y_t/\beta_t\}} \frac{\kappa (y_t/\beta_t)^\kappa}{\exp\{-y_t/\beta_t\} (2\sigma_t^2)}$		$\kappa \left(\frac{y_t}{\beta_t}\right)^\kappa - \kappa$		$\kappa^2 \left(\frac{y_t}{\beta_t}\right)$		κ^2	κ^2
Duration	Weibull	$\beta_t = \exp(\theta_t)$		$\frac{\Gamma(\nu + 1)}{\{2\pi\sigma_t^2\}^{1/2}} \left(1 + \frac{y_t^2}{(\nu - 2)\sigma_t^2}\right)^{-\frac{\nu + 1}{2}}$		$\frac{\omega_t y_t^2}{2\sigma_t^2} - \frac{1}{2}$		$\frac{1}{2\sigma_t^2}$		$\frac{1}{2}$	$\frac{1}{2}$
Volatility	Gaussian	$\sigma_t^2 = \exp(\theta_t)$		$\frac{\Gamma(\frac{\nu + 1}{2})}{\sqrt{(\nu - 2)\pi\Gamma(\nu/2)}\sigma_t} \left(1 + \frac{y_t^2}{(\nu - 2)\sigma_t^2}\right)^{-\frac{\nu + 1}{2}}$		$\frac{\omega_t y_t^2}{2\sigma_t^2} - \frac{1}{2}$		$\frac{\nu - 2}{\nu + 1} \frac{\omega_t^2 y_t^2}{2\sigma_t^2}$		$\frac{\nu}{2\nu + 6}$	$\frac{\nu}{2\nu + 6}$
Volatility	Student's t	$\sigma_t^2 = \exp(\theta_t)$		$\omega_t := \frac{\nu - 2 + y_t^2/\sigma_t^2}{\nu + 1}$		$\omega_t := \frac{\nu - 2 + y_t^2/\sigma_t^2}{\nu + 1}$		$\omega_t := \frac{\nu - 2 + y_t^2/\sigma_t^2}{\nu + 1}$		$\frac{1 + \rho_t^2}{4}$	$\frac{1 + \rho_t^2}{4}$
Dependence	Gaussian	$\rho_t = \frac{1 - \exp(-\theta_t)}{1 + \exp(-\theta_t)}$		$\exp\left\{-\frac{y_{1t}^2 + y_{2t}^2 - 2\rho_t y_{1t} y_{2t}}{2(1 - \rho_t^2)}\right\}$		$\frac{\rho_t}{2} + \frac{1}{2} \frac{z_{1t} z_{2t}}{1 - \rho_t^2}$		$0 \neq \frac{1}{4} \frac{z_{1t}^2 + z_{2t}^2}{1 - \rho_t^2} - \frac{1 - \rho_t^2}{4}$		$\frac{1 + \rho_t^2}{4}$	$\frac{1 + \rho_t^2}{4}$
Dependence	Student's t	$\rho_t = \frac{1 - \exp(-\theta_t)}{1 + \exp(-\theta_t)}$		$\frac{\nu \left(1 + \frac{y_{1t}^2 + y_{2t}^2 - 2\rho_t y_{1t} y_{2t}}{(\nu - 2)(1 - \rho_t^2)}\right)^{-\frac{\nu + 2}{2}}}{2\pi(\nu - 2)\sqrt{1 - \rho_t^2}}$		$z_{1t} := y_{1t} - \rho_t y_{2t}$ $z_{2t} := y_{2t} - \rho_t y_{1t}$		$0 \neq \frac{\omega_t}{4} \frac{z_{1t}^2 + z_{2t}^2}{1 - \rho_t^2} - \frac{1 - \rho_t^2}{4} - \frac{1}{2} \frac{\omega_t^2}{\nu + 2} \frac{z_{1t}^2 z_{2t}^2}{(1 - \rho_t^2)^2} - \frac{2 + \nu(1 + \rho_t^2)}{4(\nu + 4)}$		$\frac{\nu + 2}{2}$	$\frac{\nu + 2}{2}$
				$z_{1t} := y_{1t} - \rho_t y_{2t}$ $z_{2t} := y_{2t} - \rho_t y_{1t}$							

Note: The table contains nine distributions and link functions taken from Koopman et al. (2016). To aid the comparison (but at the expense of some consistency), we retain most of their parameter notation, even though some symbols are also used in the main text for different quantities. We assume that the observation density is known, i.e. $p^0(\cdot|\vartheta_t) = p(\cdot|\theta_t)$ (hence, $\vartheta_t = \theta_t$). In each case, the state-transition equation is $\vartheta_t = (1 - \phi_0)\vartheta_0 + \phi_0\vartheta_{t-1} + \xi_t$ where $\xi_t \sim \text{i.i.d.}(0, \sigma_\xi^2)$ being distributed either as a Gaussian or Student's t variate.

Table C.2: Static (hyper-)parameters for DGPs in Table C.1 in the low-volatility setting

Type	Distribution	ω_0	ϕ_0	σ_ξ	Shape
Count	Poisson	0.00	0.97	0.15	
Count	Negative binomial	0.00	0.97	0.15	$\kappa = 4$
Intensity	Exponential	0.00	0.97	0.15	
Duration	Gamma	0.00	0.97	0.15	$\kappa = 1.5$
Duration	Weibull	0.00	0.97	0.15	$\kappa = 1.2$
Volatility	Gaussian	0.00	0.97	0.15	
Volatility	Student's t	0.00	0.97	0.15	$\nu = 6$
Dependence	Gaussian	0.00	0.97	0.15	
Dependence	Student's t	0.00	0.97	0.15	$\nu = 6$

Table C.3: Out-of-sample MSE of $\{\theta_{t|t-1}^j\}$ for $j \in \{\text{im, ex}\}$ relative to true states $\{\vartheta_t\}$ under Gaussian state increments.

DGP		Assum. 1		MSE bound?		Low vol. ($\sigma_\xi = 0.15$)		Med. vol ($\sigma_\xi = 0.30$)		High vol. ($\sigma_\xi = 0.60$)	
Type	Distribution	α	β	ISD	ESD	ISD	ESD	ISD	ESD	ISD	ESD
Count	Poisson	0	∞	✓	✗	0.146	0.148	0.405	∞	1.64	∞
Count	Neg. Binomial	0	∞	✓	✗	0.158	0.160	0.430	0.452	1.64	1.85
Intensity	Exponential	0	∞	✓	✗	0.146	0.150	0.368	0.423	1.03	2.24
Duration	Gamma	0	∞	✓	✗	0.157	0.163	0.473	0.546	1.29	2.24
Duration	Weibull	0	∞	✓	✗	0.125	0.128	0.306	0.329	0.80	0.96
Volatility	Gaussian	0	∞	✓	✗	0.192	0.198	0.503	0.609	1.46	4.68
Volatility	Student's t	0	$\frac{\nu+1}{8}$	✓	✓	0.226	0.227	0.610	0.617	1.55	1.60
Dependence	Gaussian	$-\frac{1}{4}$	∞	✓	✗	0.239	0.231 [†]	0.596	∞	1.56	∞
Dependence	Student's t	$-\frac{1}{4}$	$\frac{\nu+1}{4}$	✓	✓	0.251	0.252	0.620	0.625	1.50	1.53

Note: MSE = mean squared error. ISD = implicit score driven. ESD = explicit score driven. \dagger = For the Gaussian dependence model, the ESD filtered path diverged for a single (out-of-sample) path in the low-volatility setting. For simplicity, we ignore this path and report a finite MSE.

C.4 Computing the ISD update

Standard Newton-Raphson iterates for solving the ISD update (4) with $\mathbf{P}_t = \mathbf{P}$ read

$$\boldsymbol{\theta}_{t|t}^{\text{im}} \leftarrow \boldsymbol{\theta}_{t|t}^{\text{im}} + [\mathbf{P} - \nabla^2 \ell(\mathbf{y}_t | \boldsymbol{\theta}_{t|t}^{\text{im}})]^{-1} [\nabla \ell(\mathbf{y}_t | \boldsymbol{\theta}_{t|t}^{\text{im}}) - \mathbf{P}(\boldsymbol{\theta}_{t|t}^{\text{im}} - \boldsymbol{\theta}_{t|t-1}^{\text{im}})], \quad (\text{C.1})$$

where $\nabla^2 := \nabla \nabla' = (\text{d}/\text{d}\boldsymbol{\theta})(\text{d}/\text{d}\boldsymbol{\theta})'$ denotes the Hessian operator. The algorithm may be initialized with $\boldsymbol{\theta}_{t|t}^{\text{im}} \leftarrow \boldsymbol{\theta}_{t|t-1}^{\text{im}}$. The inverse exists as $\mathbf{P} - \nabla^2 \ell(\mathbf{y}_t | \boldsymbol{\theta}_{t|t}^{\text{im}})$ is positive definite because of Assumption 1(b). Adding a standard line search is typically helpful.

For high-dimensional problems, it may be beneficial to employ an algorithm that avoids large-matrix inversions, such as the Broyden–Fletcher–Goldfarb–Shanno (BFGS) algorithm (e.g., Liu and Nocedal, 1989). When computational efficiency is critical, algorithm (C.1) may be terminated after a single NR iteration, in which case the output (after one iteration) reads $\boldsymbol{\theta}_{t|t-1}^{\text{im}} + [\mathbf{P} - \nabla^2 \ell(\mathbf{y}_t | \boldsymbol{\theta}_{t|t-1}^{\text{im}})]^{-1} \nabla \ell(\mathbf{y}_t | \boldsymbol{\theta}_{t|t-1}^{\text{im}})$. This “1NR” version is similar to the *explicit* update (2) in being computationally inexpensive; however, it is based on a quadratic (rather than linear) approximation of $\ell(\mathbf{y}_t | \boldsymbol{\theta})$ around the prediction, which is advantageous when $\boldsymbol{\theta} \mapsto \ell(\mathbf{y}_t | \boldsymbol{\theta})$ exhibits strong curvature. On the other hand, additional iterations typically provide additional precision; hence, depending on the available computer power, researchers may decide to execute more or fewer iterations of algorithm (C.1).

C.5 Details for Section 5.3

Here, we provide additional implementation details for the ESD and ISD filters, as well as the MSE bounds for the latter from Section 5.3.

ESD filter. For the ESD filters with *exponential* link functions, $\mu_{t|t}^{\text{ex}} = \exp(\theta_{t|t}^{\text{ex}})$, we define the learning rates as $\mathbf{H}_t^{\text{ex}} = \eta^{\text{ex}} \mathcal{I}(\theta_{t|t-1}^{\text{ex}})^{-\zeta}$, where $\mathcal{I}(\theta) = \exp(\theta)$ represents the Fisher information and $\zeta \in \{0, 1/2, 1\}$ determines the scaling of the score function. The ESD update becomes

$$\theta_{t|t}^{\text{ex}} = \theta_{t|t-1}^{\text{ex}} + \eta^{\text{ex}} \exp(-\zeta \theta_{t|t-1}^{\text{ex}})(y_t - \exp(\theta_{t|t-1}^{\text{ex}})). \quad (\text{C.2})$$

Combined with the prediction step (3), this leads to the standard score-driven prediction-to-prediction recursion (e.g., Creal et al., 2013, p. 779).

ISD filter. The ISD filter with *exponential* link function, $\mu_{t|t}^{\text{im}} = \exp(\theta_{t|t}^{\text{im}})$, and static

learning rate, $\mathbf{H}_t^{\text{im}} = \eta^{\text{im}}$ for all t , has update

$$\begin{aligned}\theta_{t|t}^{\text{im}} &= \underset{\theta \in \Theta}{\text{argmax}} \left\{ \ell(y_t | \theta) - \frac{1}{2\eta^{\text{im}}} (\theta - \theta_{t|t-1}^{\text{im}})^2 \right\} \\ &= \underset{\theta \in \Theta}{\text{argmax}} \left\{ y_t \theta - \exp(\theta) - \log(y_t!) - \frac{1}{2\eta^{\text{im}}} (\theta - \theta_{t|t-1}^{\text{im}})^2 \right\},\end{aligned}\quad (\text{C.3})$$

which is solved numerically using a standard Newton-Raphson algorithm (see Appendix C.4).

The ISD filter with *quadratic* link function, $\mu_{t|t}^{\text{im}} = (\theta_{t|t}^{\text{im}})^2$, and static learning rate, has an implicit update that can be solved analytically as

$$\begin{aligned}\theta_{t|t}^{\text{im}} &= \underset{\theta \in \Theta}{\text{argmax}} \left\{ \ell(y_t | \theta) - \frac{1}{2\eta^{\text{im}}} (\theta - \theta_{t|t-1}^{\text{im}})^2 \right\}, \\ &= \underset{\theta \in \Theta}{\text{argmax}} \left\{ y_t \log(\theta^2) - \theta^2 - \log(y_t!) - \frac{1}{2\eta^{\text{im}}} (\theta - \theta_{t|t-1}^{\text{im}})^2 \right\}.\end{aligned}\quad (\text{C.4})$$

Taking first-order conditions with respect to θ , and evaluating in $\theta = \theta_{t|t}^{\text{im}}$, yields

$$\frac{2y_t}{\theta_{t|t}^{\text{im}}} - 2\theta_{t|t}^{\text{im}} - \frac{1}{\eta^{\text{im}}} (\theta_{t|t}^{\text{im}} - \theta_{t|t-1}^{\text{im}}) = 0. \quad (\text{C.5})$$

Next we assume $\theta_{t|t}^{\text{im}} > 0$, which is without loss of generality, as the case $\theta_{t|t}^{\text{im}} = 0$ (which occurs when $y_t = \theta_{t|t-1}^{\text{im}} = 0$) will be automatically covered below. As $\eta^{\text{im}} > 0$, we can then multiply both sides by $\eta^{\text{im}}\theta_{t|t}^{\text{im}} > 0$ to obtain a quadratic equation in $\theta_{t|t}^{\text{im}}$ as follows:

$$-(1 + 2\eta^{\text{im}})(\theta_{t|t}^{\text{im}})^2 + \theta_{t|t-1}^{\text{im}}\theta_{t|t}^{\text{im}} + 2\eta^{\text{im}}y_t = 0. \quad (\text{C.6})$$

Solving for $\theta_{t|t}^{\text{im}}$ by the usual formula yields two potential solutions:

$$\theta_{t|t}^{\text{im}} = \frac{-\theta_{t|t-1}^{\text{im}} \pm \sqrt{(\theta_{t|t-1}^{\text{im}})^2 + 8(1 + 2\eta^{\text{im}})\eta^{\text{im}}y_t}}{-2(1 + 2\eta^{\text{im}})}. \quad (\text{C.7})$$

Multiplying the numerator and denominator by -1 and taking only the nonnegative solu-

tion, we obtain the ISD update

$$\theta_{t|t}^{\text{im}} = \frac{\theta_{t|t-1}^{\text{im}} + \sqrt{(\theta_{t|t-1}^{\text{im}})^2 + 8\eta^{\text{im}}(1+2\eta^{\text{im}})y_t}}{2(1+2\eta^{\text{im}})} \geq 0. \quad (\text{C.8})$$

This solution yields $\theta_{t|t}^{\text{im}} = 0$ if and only if $\theta_{t|t-1}^{\text{im}} = y_t = 0$, such that the limiting case is correctly covered.

MSE bounds. The gradient noise (in Assumption 2) of the ISD filter with quadratic link can be computed as

$$\begin{aligned} \sigma^2 &= \sup_t \mathbb{E} \left[\left(\frac{d\ell(y_t|\theta_t)}{d\theta_t} \right)^2 \mid_{\theta_t=\theta_t^*} \right] \\ &= \sup_t \mathbb{E} \left[\left(\frac{2y_t}{\theta_t} - 2\theta_t \right)^2 \mid_{\theta_t=\theta_t^*} \right] \\ &= \sup_t \mathbb{E} \left[\left(\frac{4y_t^2}{\theta_t^2} - 8y_t + 4\theta_t^2 \right) \mid_{\theta_t=\theta_t^*} \right] \\ &= \sup_t \mathbb{E} \left[\frac{4y_t^2}{\mu_t} - 8y_t + 4\mu_t \right] \\ &= \sup_t \mathbb{E} [4(\mu_t + 1) - 8\mu_t + 4\mu_t] \\ &= 4, \end{aligned} \quad (\text{C.9})$$

where in the first line we used that $\ell(y_t|\theta_t) = y_t \log(\mu_t) - \mu_t - \log(y_t!) = y_t \log(\theta_t^2) - \theta_t^2 - \log(y_t!)$, using $\mu_t = \theta_t^2$, hence $d\ell(y_t|\theta_t)/d\theta_t = 2y_t\theta_t/\theta_t^2 - 2\theta_t = 2y_t/\theta_t - 2\theta_t$. In the fourth line we used that the pseudo-true state is identified as $\theta_t^* = \sqrt{\mu_t} = \exp(\vartheta_t/2) \in (0, \infty)$ for all t , and thus $\theta_t^{*2} = \exp(\vartheta_t) = \mu_t$. In the fifth line, we used that $\mathbb{E}[y_t^2/\mu_t] = \mathbb{E}_{y_t}[\mathbb{E}[y_t^2]/\mu_t] = \mathbb{E}[(\mu_t^2 + \mu_t)/\mu_t] = \mathbb{E}[\mu_t + 1]$ and $\mathbb{E}[y_t] = \mathbb{E}_{y_t}[\mathbb{E}[y_t]] = \mathbb{E}[\mu_t]$, both using the tower property.

The MSE bound of the ISD filter with quadratic link function additionally depends on $q^2 = \sup_t \mathbb{E}[\|\theta_t^* - \theta_{t-1}^*\|^2] < \infty$ and $s_\omega^2 = \sup_t \mathbb{E}[\|\theta_t^* - \omega\|^2] < \infty$, which are assumed to be given. Here, we compute these quantities analytically assuming $\omega_0, |\phi_0| < 1$ and σ_ξ are

known.

$$\begin{aligned}
q^2 &= \sup_t \mathbb{E} \left[(\theta_t^* - \theta_{t-1}^*)^2 \right] \\
&= \sup_t \mathbb{E} \left[(\sqrt{\mu_t} - \sqrt{\mu_{t-1}})^2 \right] \\
&= \sup_t \mathbb{E} \left[\mu_t + \mu_{t-1} - 2\sqrt{\exp(\vartheta_t + \vartheta_{t-1})} \right] \\
&= \sup_t \left(2 \exp \left(\omega_0 + \frac{\sigma_\xi^2}{2(1 - \phi_0^2)} \right) - 2\mathbb{E} \left[\sqrt{\exp(\vartheta_t + \vartheta_{t-1})} \right] \right) \\
&= 2 \exp \left(\omega_0 + \frac{\sigma_\xi^2}{2(1 - \phi_0^2)} \right) - 2 \exp \left(\omega_0 + \frac{(1 + \phi_0)\sigma_\xi^2}{4(1 - \phi_0^2)} \right) \\
&= 2 \exp \left(\omega_0 + \frac{\sigma_\xi^2}{2(1 - \phi_0^2)} \right) - 2 \exp \left(\omega_0 + \frac{\sigma_\xi^2}{4(1 - \phi_0)} \right). \tag{C.10}
\end{aligned}$$

$$\begin{aligned}
s_\omega^2 &= \sup_t \mathbb{E} \left[\|\theta_t^* - \omega\|^2 \right] \\
&= \sup_t \mathbb{E} \left[\mu_t + \omega^2 - 2\omega\sqrt{\mu_t} \right] \\
&= \sup_t \mathbb{E} \left[\mu_t - 2\omega\sqrt{\mu_t} \right] + \omega^2 \\
&= \exp \left(\omega_0 + \frac{\sigma_\xi^2}{2(1 - \phi_0^2)} \right) + \omega^2 - 2\omega \exp \left(\frac{\omega_0}{2} + \frac{\sigma_\xi^2}{8(1 - \phi_0^2)} \right). \tag{C.11}
\end{aligned}$$

As $\{\vartheta_t\}$ follows stationary AR(1) dynamics $\vartheta_t = \omega_0(1 - \phi_0) + \phi_0\vartheta_{t-1} + \xi_t$, where $\xi_t \sim N(0, \sigma_\xi^2)$, the unconditional distribution of ϑ_t is $N(\omega_0, \sigma_\xi^2/(1 - \phi_0^2))$. Moreover, X being normally distributed implies that $\mathbb{E}[\exp(X)] = \exp(\mathbb{E}(X) + \mathbb{V}(X)/2)$, where $\mathbb{V}(X)$ denotes the variance of X . Taken together, this yields the following three identities:

$$\mathbb{E}[\exp(\vartheta_t)] = \exp \left(\omega_0 + \frac{\sigma_\xi^2}{2(1 - \phi_0^2)} \right), \tag{C.12}$$

$$\mathbb{E}[\sqrt{\exp(\vartheta_t)}] = \exp \left(\frac{\omega_0}{2} + \frac{\sigma_\xi^2}{8(1 - \phi_0^2)} \right), \tag{C.13}$$

$$\mathbb{E}[\sqrt{\exp(\vartheta_t + \vartheta_{t-1})}] = \exp \left(\omega_0 + \frac{(1 + \phi_0)\sigma_\xi^2}{4(1 - \phi_0^2)} \right). \tag{C.14}$$

To derive equation (C.14), we write $\sqrt{\exp(\vartheta_t + \vartheta_{t-1})} = \exp(S)$, where $S := (\vartheta_t + \vartheta_{t-1})/2$

is (unconditionally) Gaussian. By (weak) stationarity, its mean is

$$\mathbb{E}[S] = \frac{1}{2}(\mathbb{E}[\vartheta_t] + \mathbb{E}[\vartheta_{t-1}]) = \omega_0, \quad (\text{C.15})$$

while its variance is given by

$$\mathbb{V}(S) = \frac{1}{4} \mathbb{V}(\vartheta_t + \vartheta_{t-1}) = \frac{1}{4} (2 \mathbb{V}(\vartheta_t) + 2 \text{Cov}(\vartheta_t, \vartheta_{t-1})), \quad (\text{C.16})$$

where $\text{Cov}(\vartheta_t, \vartheta_{t-1}) = \phi_0 \mathbb{V}(\vartheta_t) = \phi_0 \sigma_\xi^2 / (1 - \phi_0^2)$. Hence,

$$\mathbb{V}(S) = \frac{1}{4} (2 + 2\phi_0) \frac{\sigma_\xi^2}{1 - \phi_0^2} = \frac{(1 + \phi_0)\sigma_\xi^2}{2(1 - \phi_0^2)}. \quad (\text{C.17})$$

Using $\mathbb{E}[\exp(S)] = \exp(\mathbb{E}(S) + \mathbb{V}(S)/2)$ yields equation (C.14).

The gradient noise in Assumption 2 for the ISD filter with an exponential link function follows from $\nabla \ell(y_t \mid \theta_t^*) = y_t - \exp(\theta_t^*) = y_t - \mu_t$, which uses the fact that $\theta_t^* = \vartheta_t$. Since $y_t \mid \mu_t \sim \text{Poisson}(\mu_t)$, and noting that $\mathbb{E}[(y_t - \mu_t)^2]$ is the centralized second moment, i.e., the unconditional variance of y_t , we have

$$\sigma^2 = \sup_t \mathbb{E}[(y_t - \mu_t)^2] = \sup_t \mathbb{E}[\mu_t] = \sup_t \mathbb{E}[\exp(\vartheta_t)] = \exp\left(\omega_0 + \frac{\sigma_\xi^2}{2(1 - \phi_0^2)}\right),$$

where the last equality follows from equation (C.12).

Figure C.2 plots the maximum likelihood-estimated learning rates of the ISD and ESD filters. The learning rates of the ISD filters both increase monotonically with the state variation, which is intuitive, as more sensitivity of the filter is needed to track more volatile states. The learning rates of the ESD filters, on the other hand, peak before declining, likely as an attempt to prevent divergence of the filter when the true states are volatile.

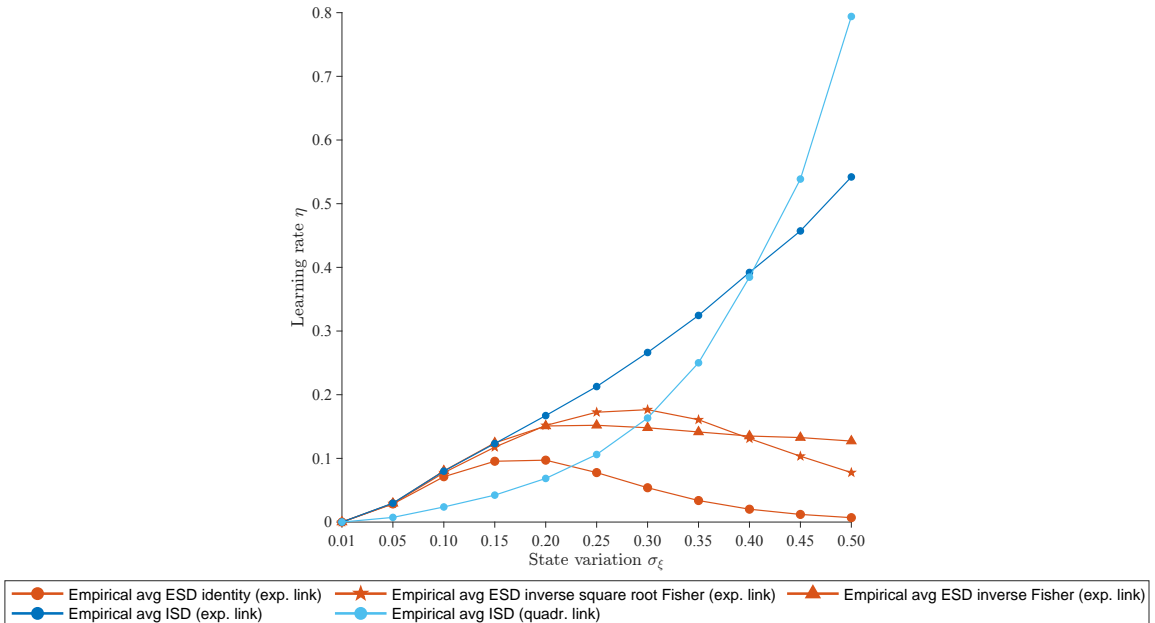


Figure C.2: Plot of the maximum likelihood-estimated learning rates for the ESD filter with identity scaling ($\zeta = 0$), inverse square root Fisher scaling ($\zeta = 1/2$), and inverse Fisher scaling ($\zeta = 1$), and the ISD filter, all using exponential link functions, along with the ISD filter using a quadratic link function.

References

Creal, D., S. J. Koopman, and A. Lucas (2013). Generalized autoregressive score models with applications. *Journal of Applied Econometrics* 28(5), 777–795.

Cutler, J., D. Drusvyatskiy, and Z. Harchaoui (2023). Stochastic optimization under distributional drift. *Journal of Machine Learning Research* 24(147), 1–56.

Durbin, J. and S. J. Koopman (2012). *Time Series Analysis by State Space Methods*. OUP.

Fahrmeir, L. (1992). Posterior mode estimation by extended Kalman filtering for multivariate dynamic generalized linear models. *Journal of the American Statistical Association* 87(418), 501–509.

Harvey, A. C. (1989). *Forecasting, Structural Time Series Models and the Kalman Filter*. CUP.

Henderson, H. V. and S. R. Searle (1981). On deriving the inverse of a sum of matrices.

SIAM Review 23(1), 53–60.

Horn, R. A. and C. R. Johnson (2012). *Matrix Analysis*. CUP.

Kalman, R. E. (1960). A new approach to linear filtering and prediction problems. *Journal of Basic Engineering* 82(1), 35–45.

Koopman, S. J., A. Lucas, and M. Scharth (2016). Predicting time-varying parameters with parameter-driven and observation-driven models. *Review of Economics and Statistics* 98(1), 97–110.

Lambert, M., S. Bonnabel, and F. Bach (2022). The recursive variational Gaussian approximation (R-VGA). *Statistics and Computing* 32(10), 1–24.

Lange, R.-J. (2024a). Bellman filtering and smoothing for state–space models. *Journal of Econometrics* 238(2), 105632.

Lange, R.-J. (2024b). Short and simple introduction to Bellman filtering and smoothing. *Preprint*. <https://arxiv.org/pdf/2405.12668.pdf>.

Lange, R.-J., B. van Os, and D. J. van Dijk (2024). Implicit score-driven filters for time-varying parameter models. *Preprint*. <https://ssrn.com/abstract=4227958>.

Liu, D. C. and J. Nocedal (1989). On the limited memory BFGS method for large scale optimization. *Mathematical Programming* 45(1), 503–528.

Madden, L., S. Becker, and E. Dall’Anese (2021). Bounds for the tracking error of first-order online optimization methods. *Journal of Optimization Theory and Applications* 189, 437–457.

Ollivier, Y. (2018). Online natural gradient as a Kalman filter. *Electronic Journal of Statistics* 12, 2930–2961.

Sherman, J. and W. J. Morrison (1950). Adjustment of an inverse matrix corresponding to a change in one element of a given matrix. *The Annals of Mathematical Statistics* 21(1), 124–127.